Uncatalyzed hydrogen transfer during 100-250 °C conversion of asphaltenes

by

Nazim Naghizada

A thesis submitted in partial fulfillment of the requirements for the degree of

Master of Science

in

Chemical Engineering

Department of Chemical and Materials Engineering
University of Alberta

ABSTRACT

Asphaltene is the most difficult fraction of bitumen and heavy oil to upgrade, as it has low H/C, high molecular weight and metal content. Asphaltenes are insoluble in paraffinic solvents, and undergo aggregation and coke formation during refining and cracking processes. No attention is usually paid to reaction chemistry of asphaltenes during low temperature processing, which assumes that asphaltenes remain unreactive upon exposure to mild heating. However, asphaltenes have ‘stable’ free radicals in their natural state. The free radical chemistry of asphaltenes might have relevance to its storage, processing, and transport in industry where exposure to heating is inevitable. The work employed industrially *n*-pentane precipitated asphaltenes from Athabasca oil sands bitumen. Free radical-radical reactions, hydrogen disproportionation and hydrogen donor/acceptor properties were investigated over the temperature range 100 to 250 °C. The objective was to observe any changes in terms of yield of each soluble or insoluble fraction, gas product, aromatic hydrogen content and free radical content. The potential effect of the metal wall of the reactor was tested on control reactions and subsequent work took this into account (Chapter 3). When heating asphaltenes on their own, it was found that the yield of the *n*-heptane insoluble fraction of the asphaltenes feed increased from 67 to 75 % as the temperature was increased to 150 °C (Chapter 4). The *n*-heptane insoluble fraction also gained more aromaticity upon heating. These observed changes were ascribed to hydrogen transfer and addition-combination reactions, which eventually lead to formation of more condensed and aromatic products. It appeared that addition products became less soluble in paraffinic solvents. It was also considered that mild heating might have enabled free-radical reactions by improving molecular mobility and disruption of aggregation, which provided “caging” effect role for free radicals, as suggested in the literature. Direct evidence for hydrogen transfer was found by using reactions of mixtures of asphaltenes with model compounds α-methylstyrene, cumene, 9,10-dihydroanthracene, and anthracene as probe molecules to facilitate analysis at species level (Chapter 5). The amount of the hydrogen transfer from asphaltenes to α-methylstyrene was evaluated and was of the order 1.8 mg H/ g asphaltenes in 1 h at 250 °C. Evidence for the reverse reaction was not found, indicating asphaltene free radicals are incapable of forming bonds which could be stronger than the weakest C–H bond in tertiary carbon atom of cumene (353 kJ/mol). Asphaltenes also donated hydrogen to anthracene at 250 °C, indicating the presence of transferrable hydrogens with bond strength less than 315 kJ/mol which is the bond strength of the C–H at 9- and 10-positions of 9,10-dihydroanthracene. The presence of free radicals in the asphaltenes feed was confirmed, and a minor decrease was observed in the free radical concentration due to heating alone, which indirectly supported the possibility of hydrogen transfer and free radical combination reactions. It was shown that some free radical fragments are sterically hindered with respect to each other, which were stabilized significantly by addition of 9,10-dihydroanthracene. The results suggested that asphaltenes can act both as hydrogen acceptor and hydrogen donor. Indirect evidence for the formation of combination or addition products was also shown with the model compounds through reactions that were induced by asphaltenes. In conclusion, asphaltenes were reactive over the temperature range studied.

Keywords: asphaltenes, hydrogen transfer, free radicals.

DEDICATION

To my grandpa

ACKNOWLEDGEMENTS

Firstly, I would like to express my sincere gratitude to my supervisor Prof. Arno De Klerk for his continuous support, patience, motivation during my MSc. His guidance helped me in all time of my research and he consistently allowed this work to be my own work, but always showed me the right direction whenever I needed it. I would also like to thank Dr. Glaucia for her guidance, she was always available whenever I had a question about my research or writing.

I would also like to express our gratitude to Dr. Arno Siraki (University of Alberta) for performing ESR analyses on selected samples.

I want to thank to my labmates for their help and company, especially to Yuan, his advices on chemistry and friendship have been invaluable. It was great sharing laboratory with all of you during last 2 years. Special thanks to all my friends in Edmonton, specially Shahin, Ozgur, Dilqam, Osman, Amir for their moral support and making me feel at home. I am also grateful to all members of UofA judo club for the amazing experience, specially to Amin, sensei Kelly and Gordon.

And, I want to thank to Leila, for being always there, every time that I have needed support or bored.

Last but not the least, I would like to thank my family: my parents, my sisters and my brother for their support throughout their life. They were always keen to know what I was doing and how I was proceeding with my research.

Finally, I want to acknowledge that this work was funded through the NSERC/Nexen-CNOOC Ltd. Industrial Research Chair program in Field Upgrading and Asphaltenes Processing.

Table of Contents

List of Figures

List of Tables

1. INTRODUCTION TO THE REACTIVITY OF ASPHALTENES AT LOW TEMPERATURES

1.1 Background

Asphaltenes are considered a significant constituent of oil sand derived bitumen. Compared to other fractions of petroleum oil, they are defined as solubility class, rather than a chemical or a distillation class. This makes it very hard to study or predict due to complex nature of mixture. Recent advances in the science of asphaltenes revealed much about the architecture of asphaltenes,[1-3] but the conversion chemistry of asphaltenes remains an area where much is still to be learned.

Asphaltenes are considered as potential challenge for oil field, both in downstream and upstream (reservoir) processes. Asphaltenes have tendency to precipitate in production systems and might lead to deposits and flow assurance problems in pipelines. Removal of the asphaltene deposits is usually done manually, which is costly and may even require shut downs in the process and use of a large amount of chemical solvents.[4] Despite some practical uses of asphaltenes, such as road paving material, or waterproofing for roofing,[5] asphaltenes are considered as a problematic fraction in refinery processes.

The presence of the asphaltenes in the oil feed affect refining of crude oil, and might require special design considerations to deal with asphaltenes in processes. In the processing of asphaltenes rich heavy oil, one strategy is to remove asphaltenes to prevent them from entering the rest of the process. A solvent deasphalting process can remove the asphaltenes to produce asphaltenes free deasphalted oil.[6]

Focus has been directed towards two main issues with asphaltenes. First, asphaltenes instability in crude oil (precipitation, deposition) and second, conversion of asphaltenes.[7,8] Due to the large number of aromatic rings in typical asphaltenes molecules, asphaltenes conversion to light valuable products are hindered, and it even seems impossible with conventional refinery methods. Hydroprocessing to yield lighter products is one approach to the problem, but it requires a large amount of hydrogen (H_2).[9] Preferably a different strategy has to be developed.

There are two aspects of the behavior of asphaltenes that are of interest in this study. The first is the ability to transfer hydrogen by hydrogen disproportionation, i.e. not hydrogen as H_2. The second is the low temperature behavior of asphaltenes and particularly the ability of asphaltenes to perform hydrogen disproportionation at temperatures well below thermal cracking temperatures and ideally below 250 °C.

Hydrogen disproportionation. Asphaltenes are known as the main coke precursors during thermal processing.[10] Recently it was reported that asphaltenes exhibited high degree of hydrogen donor capability, partially contradicting phase separation model of coke formation mechanism which claims asphaltenes fraction has little or no donor hydrogen.[9] Due to high reactivity of asphaltenes donors, fast depletion of hydrogen is likely to cause higher molecular weight coke. Hydrogen transfer has become very critical phenomenon in controlling coke formation and lots of applications have been suggested to increase conversion of asphaltenes by providing hydrogen in a similar way to hydroprocessing, but without resorting to the use of H_2.

It is generally accepted that asphaltenes core structures possess significant amount of naphthenic rings fused to aromatics.[8] Benzylic C–H bond dissociation energy is lower than found in typical aliphatic C–H bonds and hydrogen transfer reactions are expected to take place at lower temperatures. Nevertheless, these are still strong bonds, and on its own, benzylic C–H bonds cannot explain hydrogen disproportionation at low temperature. It was suspected that the natural free radical content of the asphaltenes would play a role.

Low temperature behavior. Asphaltenes might be stored and processed in different conditions (T, P) which can induce flocculation properties. Temperature effects on the asphaltenes precipitation and aggregation has been investigated in detail, which gave a clear picture of formation of clusters from asphaltenes nanoparticles.[7] As the temperature increases from room temperature to reservoir conditions, it causes the asphaltenes aggregates to dissociate in crude oil.[11] It is questionable that association of asphaltenes is merely a result of interaction of polar groups, donor-acceptors and π- π stacking of condensed aromatic rings which is a "common wisdom" for aggregation.[8,12,13] While the focus is mainly on the aggregation properties of asphaltenes, it needs to be questioned what happens to individual molecules of asphaltenes in this temperature range. The reactivity of asphaltenes is largely unknown at low temperatures, which might play an important role in asphaltenes self-association as well as in fouling. This material has the highest concentration of stable free radicals in the bitumen, so changes might likely occur below cracking temperatures.[14,15] Free radicals are reactive species, and their persistence at ambient temperature was explained by "caging" effect which protects them against free radical-radical or hydrogen transfer reactions.[16] It could be hypothesized that with increasing temperature the "caging" effect would decrease due to dissociation of aggregates, or that mobility would improve, and thus free radical type reactions would be enabled. When industrially obtained asphaltenes were heated over the temperature range 60–250 °C, the *n*-pentane soluble fraction of product changed with temperature.[17] Moreover it has been proposed that components of residue fraction can change their solubility class by changing its hydrogen content and molecular weight.[18]

From the standpoint of industry, solvent deasphalting is a process that is assumed to be only a physical separation process. The phase separation is caused by the insolubility of asphaltenes in paraffinic solvents, and free radical chemistry is not considered as a contributor to the overall process. However, at the operating conditions for solvent deasphalting, which is typically in the range 170–210 °C for *n*-pentane solvent deasphalting,[19] it is not clear that free radical reactions can be discounted.

1.2 Objectives

The objective of this study is to investigate changes that take place in asphaltenes in the temperature range 100–250 °C with the emphasis on hydrogen transfer reactions. The working hypothesis is that asphaltenes may undergo free radical type reactions in this temperature range, including hydrogen transfer reactions.

Specific objectives include:

(a) Study chemical changes of asphaltenes due to their intermolecular and intramolecular hydrogen transfer ability in the low temperature range (100–250 °C).

(b) Study hydrogen disproportionation reaction as the reaction mechanism responsible for hydrogen transfer ability of asphaltenes at low temperature.

1.3 Scope of work

I. Chapter 2 presents the literature review regarding the asphaltenes and thermal hydrogen atom transfer.

II. Chapter 3 presents a study to define a strategy for the asphaltenes conversion due to inhomogeneity in the reaction mixture.

III. Chapter 4 presents the thermal conversion results of asphaltenes at lower temperature range as stated by the hypothesis.

IV. Chapter 5 presents asphaltenes - model compound study to investigate hydrogen donor capability of asphaltenes as well as hydrogen transfer reactions. This study evolved from the observations made from Chapter 4.

References

1. Schuler, B.; Meyer, G.; Pena, D.; Mullins, O. C.; Gross, L. Unraveling the molecular structures of asphaltenes by atomic force microscopy. *J. Am. Chem. Soc.* **2015***, 137*, 9870-9876.

2. Mullins, O. C. The asphaltenes. *Annual Review of Analytical Chemistry* **2011***, 4*, 393-418.

3. Dutta Majumdar, R.; Gerken, M.; Hazendonk, P. Solid-State 1H and 13C Nuclear Magnetic Resonance Spectroscopy of Athabasca Oil Sands Asphaltenes: Evidence for Interlocking π-Stacked Nanoaggregates with Intercalated Alkyl Side Chains. *Energy Fuels* **2015***, 29*, 2790-2800.

4. Thawer, R.; Nicoll, D. C.; Dick, G. Asphaltene deposition in production facilities. *Spe production engineering* **1990***, 5*, 475-480.

5. Lian, H.; Lin, J.; Yen, T. F. Peptization studies of asphaltene and solubility parameter spectra. *Fuel* **1994***, 73*, 423-428.

6. Strausz, O.; Lown, E. *The Chemistry of Alberta Oil Sands, Bitumens and Heavy Oils.* Alberta Energy Research Institute (AERI): Calgary, Alberta, 2003.

7. Akbarzadeh, K.; Hammami, A.; Kharrat, A.; Zhang, D.; Allenson, S.; Creek, J.; Kabir, S.; Jamaluddin, A.; Marshall, A. G.; Rodgers, R. P. Asphaltenes—problematic but rich in potential. *Oilfield Review* **2007***, 19*, 22-43.

8. Wiehe, I. A. *Process chemistry of petroleum macromolecules.* CRC press: Boca Raton, FL, 2008.

9. Gould, K. A.; Wiehe, I. A. Natural hydrogen donors in petroleum resids. *Energy Fuels* **2007***, 21*, 1199-1204.

10. Wiehe, I. A. A phase-separation kinetic model for coke formation. *Ind Eng Chem Res* **1993***, 32*.

11. Espinat, D.; Fenistein, D.; Barre, L.; Frot, D.; Briolant, Y. Effects of temperature and pressure on asphaltenes agglomeration in toluene. A light, X-ray, and neutron scattering investigation. *Energy Fuels* **2004***, 18*, 1243-1249.

12. da Costa, L. M.; Stoyanov, S. R.; Gusarov, S.; Tan, X.; Gray, M. R.; Stryker, J. M.; Tykwinski, R.; de M. Carneiro, J Walkimar; Seidl, P. R.; Kovalenko, A. Density functional theory investigation of the contributions of π- π stacking and hydrogen-bonding interactions to the aggregation of model asphaltene compounds. *Energy Fuels* **2012***, 26*, 2727-2735.

13. Tan, X.; Fenniri, H.; Gray, M. R. Water enhances the aggregation of model asphaltenes in solution via hydrogen bonding. *Energy Fuels* **2009***, 23*, 3687-3693.

14. Moschopedis, S. E.; Parkash, S.; Speight, J. G. Thermal decomposition of asphaltenes. *Fuel* **1978***, 57*, 431-434.

15. Jha, K.; Montgomery, D.; Strausz, O.; Strausz, O.; Lown, E. Chemical composition of gases in Alberta bitumens and in low-temperature thermolysis of oil sand asphaltenes and maltenes. In *Oil sand and oil shale chemistry*; Strausz, O. P., Lown, E. M., Eds.; Verlag Chemie: New York, 1978; pp 33-54.

16. Mujica, V.; Nieto, P.; Puerta, L.; Acevedo, S. Caging of molecules by asphaltenes. A model for free radical preservation in crude oils. *Energy Fuels* **2000***, 14*, 632-639.

17. Styles, Y.; de Klerk, A. Sodium Conversion of Oilsands Bitumen-Derived Asphaltenes. *Energy Fuels* **2016***, 30 (7)*, 5214-5222.

18. Wiehe, I. A. A solvent-resid phase diagram for tracking resid conversion. *Ind Eng Chem Res* **1992***, 31*, 530-536.

19. Le Page, J.; Chatila, S. G.; Davidson, M. *Resid and heavy oil processing;* Editions Technip: Paris, 1992.

2. LITERATURE REVIEW

2.1 Asphaltenes

Asphaltenes are the lowest value fraction of crude oil and they are defined in terms of its solubility, i.e., they are insoluble in paraffinic solvents and soluble in aromatic solvents. Asphaltenes contain high content of heteroatoms, metals, and polycyclic aromatic compounds and has high tendency to aggregate.[1] However, their molecular structure and aggregation mechanism are not fully known and there is debate in the literature to describe asphaltenes molecular structure and aggregation mechanism.[2-4] Understanding the chemical reactivity, behavior and architecture of the asphaltene molecules are one of the main problems in the petroleum industry. Considering the large oilsand reserves of Canada, asphaltenes have immense economic importance for the petroleum industry of the country. It is not only that conversion of those complex molecules will contribute to overall petroleum production, it also potentially hinders normal production.

In this chapter the characterization of asphaltenes in terms of solubility, molecular weight and architecture is reviewed. By providing some recent advances in molecular structural characterization of asphaltenes, a clearer picture of asphaltenes can be presented. Owing to their indigenous higher free radical contents, asphaltenes are expected to be reactive. Since this study of asphaltenes is mainly concerned with structural changes, which was speculated to take place at low temperature, more detailed information will be provided on free radical and hydrogen transfer reactions in this section based on the existing literature.

Since asphaltenes are defined as a solubility class, the solubility of asphaltenes has a particular interest in almost all stages of petroleum industry, where precipitation can cause trouble in operation. In solubility models of asphaltenes, there are generally two approaches. In the first approach, asphaltenes precipitation occurs by means of formation of micelles due to resin-asphaltenes interactions, subsequently leading to formation of aggregates and flocculation. From molecular weight studies, there is sufficient evidence to indicate that aggregation plays a role.[5] Another approach assumes that asphaltenes precipitates as free molecules where aggregation is not considered as a significant factor to effect solubility and therefore modeled as non-associated molecules.[6]

The molecular weight of asphaltenes has been determined by different techniques such as vapor pressure osmometry (VPO) and gel permeation chromatography (GPC).[7-12] The molecular weight of asphaltenes were reported to range from 400 to 10000 Da, depending on the technique used. The discrepancy in molecular weight values for the different techniques is due to the asphaltenes behaviour such as aggregation and insolubility in some solvents.

Despite of the highly complex nature of the asphaltenes, a large amount of work has been accomplished recently which has given us some knowledge to understand asphaltene science.[13-15] Number of possible structure has been proposed over the years, but there are predominantly two motifs: Archipelago model and Yen-Mullins model or island model. The archipelago model proposes multiple linearly condensed polyaromatic hydrocarbon units are interconnected each other with aliphatic thioethers and alkyl groups. Presence of those bridges between pendant groups, which is another controversy in asphaltenes science, has been confirmed with different studies.[16-19] The island model proposes that asphaltenes molecules consist of large polycyclic aromatic cores with aliphatic side chains. Problems affecting the molecular weight measurements, such aggregation and fragmentation associated with mass spectrometric techniques have persisted for decades.

The time-resolved fluorescence depolarization (TRFD) was employed first time for the molecular diffusion studies of asphaltenes to avoid above-mentioned problems.[20] TRFD employs polarized light, which excite polycyclic aromatic ensembles and the molecules undergo a rotational random walk, which is called rotational diffusion. The rotational correlation time (τ_r) was measured, which corresponds to reorientation of the molecule on the order of 1 rad and depends upon the shape and size of molecules. The τ_r presented for the asphaltenes was comparable to τ_r of two standard molecules, octaethyl porphyrin (OEP) with molecular weight of 534 g/mol and solar dye (SD) with molecular weight of 754 g/mol, which are molecules of the predicted island-type structure. This similarity in τ_r implies that molecular size of asphaltene and model compounds are alike. The fluorescence emission spectra of the asphaltenes were found to be significant in the range of 400 to 650 nm, with a maximum at around 500 nm. The τ_r of the asphaltenes corresponds to that of SD at this excitation wavelength, which indicated molecular weight for asphaltenes of around 750 g/mol. More recently, atomic microscopy and STM was employed together for structural elucidation of both petroleum and coal asphaltenes.[21] By analyzing the images carefully, it was found that asphaltenes are dominant with the molecules which consist of single polycyclic aromatic hydrocarbons (PAH) core with peripheral aliphatic chains. Nevertheless, very few bridged PAH s which connected with single bonds were observed, which depicted the presence of Archipelago type molecules. Solid state ^{1}H and ^{13}C nuclear magnetic resonance spectroscopic studies on the Athabasca asphaltenes showed very strong evidence for the Island model over Archipelago model.[22] The size of the condensed aromatic rings was defined between 5 and 7 by calculating "aromatic condensation index" which is ratio of bridgehead carbons to aromaticity. Those findings supported the aromatic structures are very rigid and ruled out the possibility of much pendant groups attached to the aromatic core.

2.1.1 Free radicals in asphaltenes

An intriguing fact about the asphaltenes is the presence of the stable free radicals.[23-26] The electron spin resonance (ESR) spectra of asphaltenes exhibit at least two different kinds of absorption: one with hyperfine splitting which identifies as the naturally occurring vanadium radical ion in vanadyl porphyrin complexes (VO^{2+}-porphyrin)[26,27] and the other one consists of single absorption line without any hyperfine spectrum which has been attributed to asphaltenes organic radicals.[23,25] The concentration of the organic free radicals in the asphaltenes lie in the range of $0.8 – 20 \times 10^{18}$ spins /g asphaltenes.[1]

Despite of the potential reactivity of free radicals, they are shielded against the possible reactions such as hydrogen transfer by other polycyclic aromatic hydrocarbons in aggregates, which is known as the "cage effect".[28] Due to the tendency of asphaltenes to form aggregates this phenomenon is expected to occur, so reactive hydrogens cannot interact with free radicals. Another study revealed that there was significant reduction in spin density after refluxing asphaltenes in tetrahydrofuran (THF) for 24 h at 62 °C.[29] Therefore it was claimed that THF caused the disruption of aggregates which enabled the free radicals to be exposed hydrogen atoms of the solvent due to removal of the cage effect.

The initial hypothesis was that free radicals in the asphaltenes might enable some addition or hydrogen transfer reactions at low temperature ranges. Therefore ESR could provide indirect evidence for combination and addition reactions of free radicals if these so called reactions take place when asphaltenes are heated at low temperatures. It was expected that the "caging effect" would reduce with heating of asphaltenes due to increased mobility of molecules and favor the hydrogen transfer reactions.

2.1.2 Natural hydrogen donors in asphaltenes

Asphaltenes are often regarded as hydrogen deficient compounds. Nevertheless, measurements of donor hydrogen concentration in asphaltenes changed the perception about the hydrogen availability in asphaltenes radically. And potential use of hydrogen from asphaltenes for petroleum upgrading has been pointed out.[30]

A commonly used chemical dehydrogenation agent, 2-3-dichloro-5,6-dicyano-p-benzoquinone (DDQ) was employed to abstract hydrogen from different model compounds and petroleum fractions (Figure 2.1).[31]

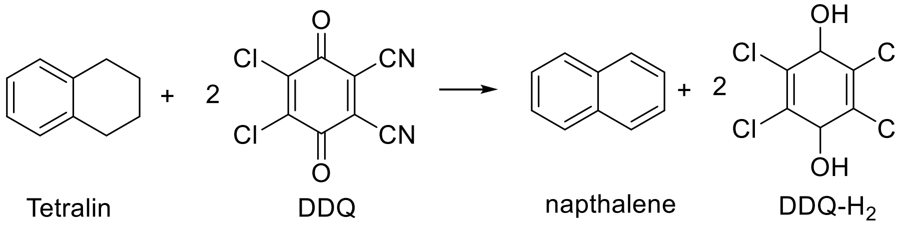

Figure 2.1. Abstraction of two hydrogens per molecule of tetralin.

The study[21] found that Arabian heavy asphaltenes (1.9 g H/100 g sample) have as high a concentration of donor hydrogen as the total Arabian heavy resid, and Hondo vacuum full resid fraction has only slightly higher concentration of donor hydrogen than its asphaltenes fraction (2.7 g H/100 g sample). Although completely saturated compounds such as decaline and cholestane did not donate hydrogen to DDQ, the saturate fraction of Arabian heavy still contains lower amount of donatable hydrogen (1.1 g H/ 100 g sample) than other fractions aromatics, resins (2.0 g H/ 100 sample) and asphaltenes. This could be due to separation of small ring aromatics (one-ring or two-ring aromatics with fused naphthenic rings) with the saturates-fraction, during separation of this class from aromatics in laboratory. Thus it was suggested that

25 % of the hydrogens in Arabian Heavy asphaltenes and 32 % of the hydrogen in Hondo asphaltenes belong to hydroaromatics which are saturates fused into aromatics.

Asphaltenes was found to have the highest hydrogen donor reactivity among the factions of Arabian heavy. When asphaltenes donated hydrogens, the number of rings of the aromatic cores in the asphaltenes increased, which was confirmed with percent aromatic carbon by ^{13}C NMR (13-Carbon Nuclear Magnetic Resonance Spectroscopy). The full resid of Arabian heavy was reacted at 400 °C at various times and asphaltenes were separated. The results showed that amount of transferred hydrogen (g H/ 100 g sample) of asphaltenes decreased from 1.89 to 1.51 while the percent aromatic carbon increased from 54 to 71 % upon heating of the resid for 90 min at 400 °C. Hydogen donor concentration of asphaltenes dropped very fast upon heating.

NMR spectroscopic analyses can be used as an analytical tool for structural characterization of petroleum asphaltenes and can be informative about average molecular parameters such as structure and compositions. A convenient method was developed to estimate transferrable hydrogen (hydroaromatics) in petroleum feedstocks based on the ^{1}H NMR spectroscopic technique. [32]

The ^{13}C NMR spectra of asphaltenes is similar to non-distillable fractions of oil sands which include a broad peak with some sharp absorption peaks in the 10-60 ppm region due to aliphatic carbons, and a broad hump in the range of 110-160 ppm due to aromatic carbons.[33] The sharp signals in aliphatic region were assigned to methylene groups relative to tetramethylsilane as follows: 23 ppm (methylene attached to terminal methyl in alkyl chain); 30 ppm (methylene in long alkyl chain, more than three carbons removed from the end); third carbon from end of chain, and β to aromatic system); 37 ppm (α to aromatic system). The proton spectra of asphaltenes were divided into following sections: methyl protons (0-1.0 ppm), methylene and methane protons (1.0-2.1 ppm), protons α to aromatics (2.1 – 5.0 ppm), and aromatic protons (6.0-9.0 ppm). [34] Various studies have been done on the analysis of hydrocarbon group type including transferrable hydrogen of the coal and pitch by using NMR.[32,35,36]

It was postulated that due to relatively higher reactivity of hydrogen donors in asphaltenes, which consists of napthenic rings fused into aromatics in asphaltenes, they can donate hydrogen at low temperature range (100-250 °C) without cracking the material appreciably. It has been hypothesized hydro-aromatics with relatively weaker bond dissociation energy can effectively donate hydrogen at temperature as low as 220 °C.[37] The catalytic activity of those polycyclic hydrocarbons depends on the C-H bond energy. This might have an implication to hydrogen donor capability of asphaltenes at low temperature. By using suitable hydrogen acceptor, hydrogen donor properties of asphaltenes could be evaluated at molecular level and their reactivity can be rationalized in comparison with donor molecules. The amount of transferrable hydrogen can also be measured at certain conditions if a suitable hydrogen probe is used.

2.2 Uncatalyzed hydrogen transfer

Central to this study, is the process of hydrogen transfer. An overview will be provided of the different ways in which hydrogen transfer from a donor compound to an unsaturated bond or a free radical can take place. Since hydroaromatics are prevalent and effective hydrogen donors in petroleum feedstocks, this section will mainly provide examples and information on hydrogen transfer from hydroaromatics.

2.2.1 General overview of free radical reactions

Due to presence of free radicals in asphaltenes, a general overview of the feasible reactions that involves free radicals will be presented in this section (Figure 2.4). It should also be noted that the an initiation step is not required, because the asphaltenes naturally contain free radicals.

Radicals undergo different type of reactions, so they can convert into a more stable form of radical or a non-radical species. A radical reaction became favorable when those bonds are being formed are stronger than those being broken. Since the energy is released in the formation of strong bonds, reactions results in a negative value of enthalpy ($\Delta H^{\Theta}<0$). Exothermic free radical reactions such as combination, disproportionation and etc. are able to proceed very fast, since the enthalpy of activation ($\Delta H^{\ddagger}$) for radicals is small or enthalpy of reaction is more negative.[38]

The reaction which converts a radical into a more stable radical are called propagation reactions (Figure 2.2). In all reactions, radicals simply form another radical by abstraction of a hydrogen atom from a non-radical which produce a more stable radical and much stronger σ bond or by addition to a non-radical molecule (bond) to form a new strong C-C bond at the expense of a weaker C-C π bond.[38] It is also worthwhile to mention intramolecular addition of radicals, which lead to formation of cyclic products.

As a termination reaction, radicals form non-radical species. This type of reactions involves recombination of two radicals, which produce dimerization products (reverse of homolysis), and also radicals can disproportionate each other to form a saturated (C-H σ bond) and an unsaturated non-radical product (C-C π).[38]

Fragmentation reactions of free radicals are driven by entropy, which is endothermic ($\Delta H^{\Theta} > 0$), result in positive change in entropy (ΔS^{Θ}).[38] High temperature required to increase the $T\Delta S^{\Theta}$ to obtain a negative value of Gibbs free energy (ΔG^{Θ}) based on the equation for Gibbs free energy ($\Delta G^{\Theta} = \Delta H^{\Theta} - T\Delta S^{\Theta}$), so the reaction will be favored. This is why they are not prevalent at low temperature range compared to exothermic reactions.

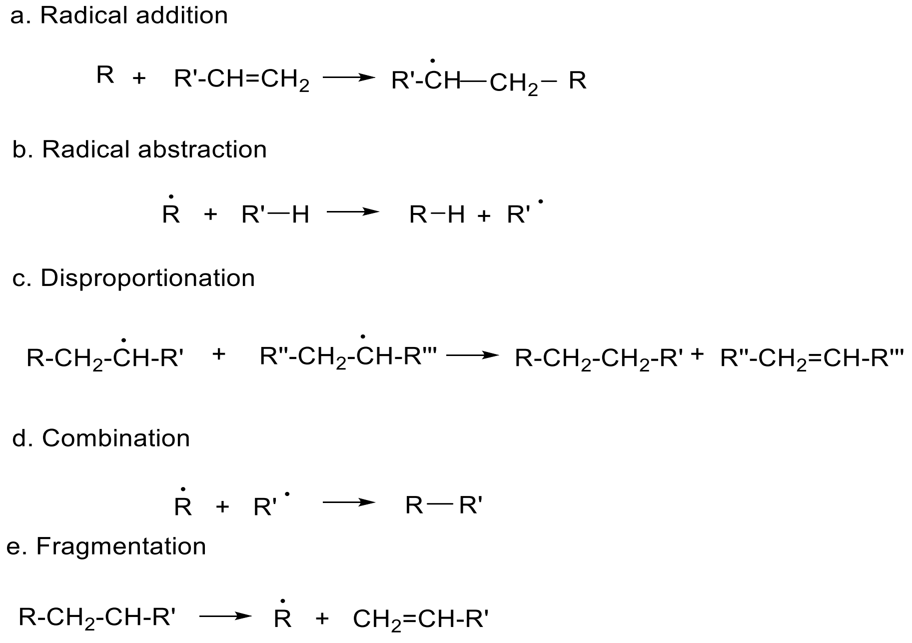

Figure 2.2. Free radical reactions.

2.2.2 Hydrogen disproportionation

“Molecular disproportionation” which is known as the reverse of radical disproportionation is a key radical-forming step in many polycyclic hydrocarbon systems as well as in coal chemistry. Since it forms stabilized radicals, this reaction pathway is held responsible for the high concentration of free radicals in PAH systems. Kinetic studies of hydrogen migration between 9, 10-dihydroanthracene (AnH_2) and 2-ethylanthracene ($EAnH_2$) conducted over the temperature range 250 – 375 °C revealed that transfers of benzylic H atoms follow a simple bimolecular step which forms two highly stabilized radical mechanisms.[39]

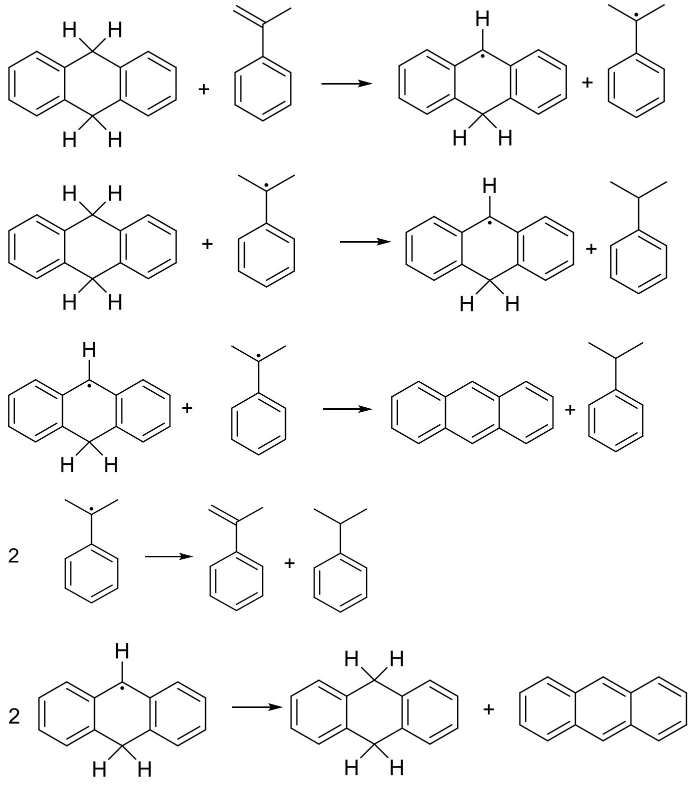

(1)

(2)

(3)

(4)

(5)

Figure 2.3. The reaction mechanism for hydrogenation of α-methylstyrene.

Molecular disproportionation has also been proposed for the reaction of 9,10-dihydroanthracene and α-methylstyrene as a initiating step shown by reaction (1) in Figure 2.3.[40] The observations have led to a conclusion that this step is the rate determining step and it is irreversible under the reaction conditions. This type of reaction has been suitable for mechanistic studies of hydrogen transfer which proceeds by radical formation. The reactions path is followed predominantly by a

H transfer from 9,10-dihydroanthracene to cumyl radical via reaction (2) and the rate of this step was found to be 10^3 times faster than radical-radical disproportionation steps: (3) and (4) (Figure 2.3).

Increasing concentration of donor compounds did not accelerate the rate constant and also rate constants remain unchanged upon addition of the initiators such as bifluorene. Thus possibility of chain reactions has been ruled out and a stoichiometric transfer hydrogenation was claimed.[40] Because of fast disproportionation reactions of their concentration was too low to detect by ESR. However, when xanthene was employed for as H-donor, a well resolved ESR spectra was observed indicating presence of xanthyl radicals, due to fact that those radicals cannot disproportionate further.[40]

2.2.3 Radical hydrogen transfer

The contribution of this type of reaction has been underestimated due to fact that it is often in competition with elimination, addition and disproportionation reactions which are thought to be main hydrogen pathway in coal liquefaction processes.[41] In coal liquefaction, it was suggested that radical hydrogen transfer does not merely serve to scavenge radical fragments which produced during pyrolysis but also induce bond scission (Figure 2.4).

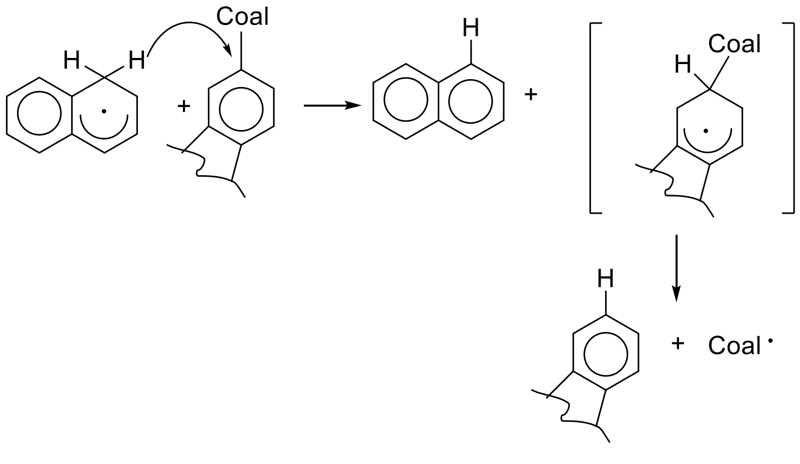

Figure 2.4. Radical hydrogen transfer from cyclohexadienyl radical to coal structure.[41]

Some kinetic studies (rate constants) were also produced for this proposed mechanism of hydrogen transfer from a radical to a molecule and are in agreement with each other.[39,42,43] Upon examination of proposed mechanism for the reaction of 9,10-dihydroanthracene and ethylanthracene, two more steps: reaction (5) and (6) were considered addition to molecular and radical-radical disproportionation reactions given in Figure 2.5.[39]

Mechanism of conversion of EAnH• radical to $EAnH_2$ is primarily by radical-radical disproportionation steps (reactions 3, 4) when concentrations of both reagents were the same.[39]The reaction (5) predominates with increased concentration of AnH_2. This is in well agreement with the reaction of 9,10-dihydroanthracene and α-methylstyrene where donor-acceptor concentration ratio was at least 10:1.[40] As mentioned earlier, H transfer from 9,10-dihydroanthracene to cumyl radicals was a dominant path of conversion of cumyl radicals to cumene after initiation step. Rate constants for H atom abstractions by diphenylmethyl radicals from various donors were measured.[44] The highest rate constant was recorded for H abstraction from 9,10-dihydroanthracene, which also showed the dependence of hydrogen transfer rates on donor structure.

$$\mathrm{AnH_2 + EAn \rightleftharpoons A\dot{n}H + EA\dot{n}H} \tag{1}$$

$$\mathrm{2A\dot{n}H \longrightarrow AnH_2 + An} \tag{2}$$

$$\mathrm{EA\dot{n}H + A\dot{n}H \longrightarrow EAnH_2 + An} \tag{3}$$

$$\mathrm{2EA\dot{n}H \longrightarrow EAnH_2 + EAn} \tag{4}$$

$$\mathrm{EA\dot{n}H + AnH_2 \longrightarrow EAnH_2 + A\dot{n}H} \tag{5}$$

$$\mathrm{A\dot{n}H + EAn \rightleftharpoons An + EA\dot{n}H} \tag{6}$$

AnH_2	9,10-dihydroanthracene
EAn	2-ethylanthracene
An	anthracene
$A\dot{n}H$	9-hydroanthryl radical
$EA\dot{n}H$	9,10-hydro-2-ethylanthryl radical
$EAnH_2$	2-ethyl-9,10-dihydroanthracene

Figure 2.5. Free radical hydrogen transfer mechanism between 9,10-dihydroanthracene and ethylanthracene.

At very low [AnH_2]/[EAn] ratios (<< 0.1), based on the increase in observed rate constant (k_{obsd}) it appeared that reaction step (6) given in Figure 2.5, which involves radical hydrogen transfer, predominates the overall reaction.[39] This reaction step was further supported by addition of anthracene (An) to the reaction medium, indicating a decrease in k_{obsd} with increasing An concentration. This was explained by the reverse of reaction (6) which favored with increasing An concentration (AnH• +EAn ↔ An + EAnH•).

The results also claimed C-H bond strength (180 kJ/mol) of the radical is too high for a free H atom transfer reaction (AnH• → An +H•; H• + EAn→ EAnH•; AnH• ≡ 9-hydroanthryl radical, An ≡ anthracene, EAn ≡ 2-ethylanthracene, EAnH• ≡ 9,10-hydro-2-ethylanthryl radical), indicating also H• is not a good leaving group. Because of its endothermic nature, it can be speculated free H atom transfer is unlikely at low temperature range. Thus this reaction can be shifted to the right at higher temperatures (AnH• → An +H•).

In a different study by same group, rate constants were determined from the proposed kinetic model of H transfer from 9,10-dihydrophenanthrene (Ph) to anthracene (An) at 300 °C.[43] The rate of H atom transfer from a 9-hydrophenanthryl radical (PhH•) to anthracene (7.5×10^3 $M^{-1}s^{-1}$) was found to be 62 times higher than that from 9,10-hydro-2-ethylanthryl radical to anthracene (120 $M^{-1}s^{-1}$), indicating relatively lower activation energy. Based on the kinetic model studies, the direct H-transfer from PhH• to An (An + PhH• → AnH• + Ph) were favored strongly rather than a two-step free H atom mechanism (PhH• → Ph +H•; H• + An→ AnH•). The single step H atom transfer involves a transition state which also favored by a different study.[45]

Another alternative path to single step H transfer was considered as possible pathways for radical hydrogen transfer. It consists in three steps :addition, isomerization, and dissociation) (Figure 2.6).[39]

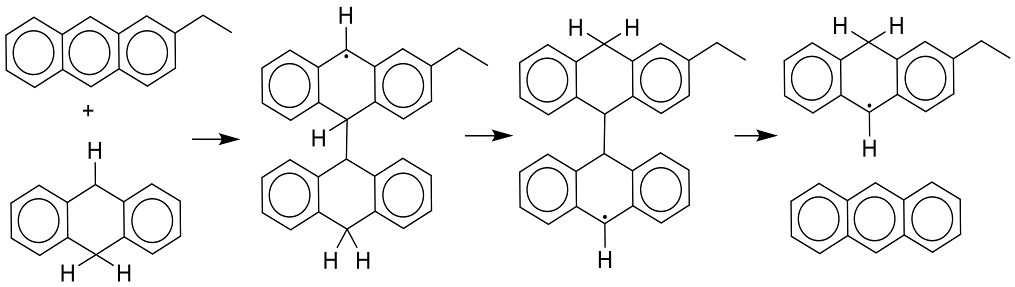

Figure 2.6. A three step radical hydrogen transfer.[39]

Recombination reactions are often in competition with radical-radical disproportionation as both reactions proceed with less activation energy. Those reactions have not been taken into consideration in kinetic model for above reactions. This was justified with fast homolysis of secondary C-C formed between radicals (AnH-AnH) which is about 87 kJ/mol weaker than primary C-C bond in diphenylethane ($PhCH_2$-CH_2PH).[43]

Lastly, another type of reaction which might be important to mention is free-radical aromatic substitution (addition to aromatics) (Figure 2.7).[45] Addition of a radical to aromatic system form another radical which stabilized by resonance. The hydrogen, which becomes weak upon addition, can be abstracted by another more stable radical. The strength of H bond in radical intermediate in reaction (1) can be approximated based on the enthalpy of H addition to various site in polyaromatics which change between 80-160 kJ/mol based on the available thermochemical data (An +H• → AnH•, $\Delta H = [\Delta H_r$ (An + $H_2 \rightarrow AnH_2$) + BDE (AnH-H) - 2 ΔH_f(H•)]; where An is anthracene, ΔH_r is enthalpy of hydrogenation, BDE is bond dissociation energy for C-H).[45] Addition enthalpy of R• to aromatics is less exothermic than H atom addition to same position.

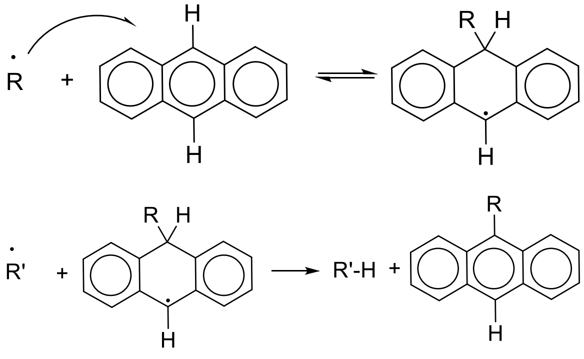

Figure 2.7. Free radical aromatic substitution reaction.

2.3 Summary

Since asphaltenes consists of complex molecules, spectroscopy becomes less informative about changes take place in molecular level. However, NMR studies can still provide quantitative changes regarding the chemical alteration.

ESR can provide indirect evidence combination, addition and H transfer reactions based on the changes in free radical concentration. Based on the discussion in Section 2.2.1, exothermic reactions such as addition, recombination or disproportionation reactions are likely to take place rather than cracking or fragmentation, which are not favored thermodynamically at low temperature because of their endothermicity ($\Delta H^{\Theta} > 0$). However, endothermic reactions cannot be ruled out completely.

It is difficult to analyze asphaltenes at molecular level and also less thermochemical data available for asphaltenes, because they are complex mixtures of species. However, by studying asphaltenes and model compound reactions, one can also predict the thermodynamic stability of free radicals relative to model compounds by using their available C-H bond energy.

A general overview of H-transfer reactions was also provided which can be relevant to asphaltenes – model compound study. In general hydrogen transfer reaction can be grouped as following: (1) H transfer from a molecule to a radical; (2) molecular disproportionation; (3) radical-radical disproportionation; (4) H transfer from a radical to a molecule. The relevance of these will become apparent when discussing the experimental work in Chapter 5.

References

1. Strausz, O.; Lown, E. *The Chemistry of Alberta Oil Sands, Bitumens and Heavy Oils.* Alberta Energy Research Institute (AERI): Calgary, Alberta, 2003.

2. Mullins, O. C. Review of the molecular structure and aggregation of asphaltenes and petroleomics. *Journal* **2008***, 13*, 48-57.

3. Gray, M. R.; Tykwinski, R. R.; Stryker, J. M.; Tan, X. Supramolecular assembly model for aggregation of petroleum asphaltenes. *Energy Fuels* **2011***, 25*, 3125-3134.

4. Strausz, O. P.; Mojelsky, T. W.; Lown, E. M. The molecular structure of asphaltene: an unfolding story. *Fuel* **1992***, 71*, 1355-1363.

5. Speight, J.; Wernick, D.; Gould, K.; Overfield, R.; Rao, B. Molecular weight and association of asphaltenes: a critical review. *Revue de l'Institut français du pétrole* **1985***, 40*, 51-61.

6. Mannistu, K.; Yarranton, H.; Masliyah, J. Solubility modeling of asphaltenes in organic solvents. *Energy Fuels* **1997***, 11*, 615-622.

7. Baltus, R. E.; Andersen, J. L. Comparison of gpc elution characteristics and diffusion coefficients of asphaltenes. *Fuel* **1984***, 63*, 530-535.

8. Hurtado, P.; Hortal, A. R.; Martínez-Haya, B. Matrix-assisted laser desorption/ionization detection of carbonaceous compounds in ionic liquid matrices. *Rapid Communications in Mass Spectrometry* **2007***, 21*, 3161-3164.

9. Martínez-Haya, B.; Hortal, A. R.; Hurtado, P.; Lobato, M. D.; Pedrosa, J. M. Laser desorption/ionization determination of molecular weight distributions of polyaromatic carbonaceous compounds and their aggregates. *Journal of mass spectrometry* **2007***, 42*, 701-713.

10. Hortal, A. R.; Martínez-Haya, B.; Lobato, M. D.; Pedrosa, J. M.; Lago, S. On the determination of molecular weight distributions of asphaltenes and their aggregates in laser desorption ionization experiments. *Journal of mass spectrometry* **2006***, 41*, 960-968.

11. Rodgers, R. P.; Marshall, A. G. Petroleomics: Advanced characterization of petroleum-derived materials by Fourier transform ion cyclotron resonance mass spectrometry (FT-ICR MS). In *Asphaltenes, Heavy Oils, and Petroleomics*Springer; Mullings, O. C., Sheu, E.Y., Hammami, A., Marshall, A.G., Eds.; Springer: New York, 2007; pp 63-93.

12. Acevedo, S.; Escobar, G.; Ranaudo, M. A.; Rizzo, A. Molecular weight properties of asphaltenes calculated from GPC data for octylated asphaltenes. *Fuel* **1998***, 77*, 853-858.

13. Mullins, O. C. The asphaltenes. *Annual Review of Analytical Chemistry* **2011***, 4*, 393-418.

14. Liao, Z.; Zhao, J.; Creux, P.; Yang, C. Discussion on the structural features of asphaltene molecules. *Energy Fuels* **2009***, 23*, 6272-6274.

15. Karimi, A.; Qian, K.; Olmstead, W. N.; Freund, H.; Yung, C.; Gray, M. R. Quantitative evidence for bridged structures in asphaltenes by thin film pyrolysis. *Energy Fuels* **2011***, 25*, 3581-3589.

16. Strausz, O. P.; Mojelsky, T. W.; Faraji, F.; Lown, E. M.; Peng, P. Additional structural details on Athabasca asphaltene and their ramifications. *Energy Fuels* **1999***, 13*, 207-227.

17. Ping'an, P.; Angelina, M. I.; Alan, H.; and Otto, P. S. Molecular Structure of Athabasca Asphaltene: Sulfide, Ether, and Ester Linkages. *Energy Fuels* **1997***, 11 (6)*, 1171–1187.

18. Ignasiak, T.; Kemp-Jones, A.; Strausz, O. The molecular structure of Athabasca asphaltene. Cleavage of the carbon-sulfur bonds by radical ion electron transfer reactions. *J. Org. Chem.* **1977***, 42*, 312-320.

19. Gray, M. R.; Le, T.; McCaffrey, W. C.; Berruti, F.; Soundararajan, S.; Chan, E.; Huq, I.; Thorne, C. Coupling of mass transfer and reaction in coking of thin films of an Athabasca vacuum residue. *Ind Eng Chem Res* **2001***, 40*, 3317-3324.

20. Groenzin, H.; Mullins, O. C. Asphaltene molecular size and structure. *The Journal of Physical Chemistry A* **1999***, 103*, 11237-11245.

21. Schuler, B.; Meyer, G.; Pena, D.; Mullins, O. C.; Gross, L. Unraveling the molecular structures of asphaltenes by atomic force microscopy. *J. Am. Chem. Soc.* **2015***, 137*, 9870-9876.

22. Dutta Majumdar, R.; Gerken, M.; Hazendonk, P. Solid-State 1H and 13C Nuclear Magnetic Resonance Spectroscopy of Athabasca Oil Sands Asphaltenes: Evidence for Interlocking π-Stacked Nanoaggregates with Intercalated Alkyl Side Chains. *Energy Fuels* **2015***, 29*, 2790-2800.

23. Niizuma, S.; Steele, C. T.; Gunning, H. E.; Strausz, O. P. Electron spin resonance study of free radicals in Athabasca asphaltene. *Fuel* **1977***, 56*, 249-256.

24. Schultz, K. F.; Selucky, M. L. Esr measurements on asphaltene and resin fractions from various separation methods. *Fuel* **1981***, 60*, 951-956.

25. Yen, T. F.; Erdman, J. G.; Saraceno, A. J. Investigation of the Nature of Free Radicals in Petroleum Asphaltenes and Related Substances by Electron Spin Resonance. *Anal. Chem.* **1962***, 34*, 694-700.

26. Malhotra, V. M.; Buckmaster, H. A. 34 GHz epr study of vanadyl complexes in various asphaltenes: Statistical correlative model of the coordinating ligands. *Fuel* **1985***, 64*, 335-341.

27. Saraceno, A.; Fanale, D.; Coggeshall, N. An electron paramagnetic resonance investigation of vanadium in petroleum oils. *Anal. Chem.* **1961***, 33*, 500-505.

28. Mujica, V.; Nieto, P.; Puerta, L.; Acevedo, S. Caging of molecules by asphaltenes. A model for free radical preservation in crude oils. *Energy Fuels* **2000***, 14*, 632-639.

29. Acevedo, S.; Escobar, G.; Ranaudo, M. A.; Pinate, J.; Amorín, A.; Díaz, M.; Silva, P. Observations about the structure and dispersion of petroleum asphaltenes aggregates obtained from dialysis fractionation and characterization. *Energy Fuels* **1997***, 11*, 774-778.

30. Alemán-Vázquez, L. O.; Torres-Mancera, P.; Ancheyta, J.; Ramírez-Salgado, J. Use of Hydrogen Donors for Partial Upgrading of Heavy Petroleum. *Energy Fuels* **2016***, 30*, 9050-9060.

31. Gould, K. A.; Wiehe, I. A. Natural hydrogen donors in petroleum resids. *Energy Fuels* **2007***, 21*, 1199-1204.

32. Bansal, V.; Kumar, R.; Krishna, G.; Patel, M.; Sarpal, A.; Basu, B. Transferable hydrogen by 1H nuclear magnetic resonance spectroscopy–Vital structural aspects of petroleum heavier ends (370–660° C) feed stocks. *Fuel* **2014***, 118*, 148-155.

33. Cyr, N.; McIntyre, D.; Toth, G.; Strausz, O. Hydrocarbon structural group analysis of Athabasca asphaltene and its gpc fractions by 13C nmr. *Fuel* **1987***, 66*, 1709-1714.

34. Cyr, N.; Selucky, M. L. Nuclear magnetic resonance studies of asphaltenes and coals. A new approach to obtaining asphaltene structural parameters with dipolar dephasing. *Liquid fuels technology* **1985***, 3*, 377-396.

35. Del Bianco, A.; Zaninelli, M.; Girardi, E. Determination of transferable hydrogen in coal liquefaction solvents by spectroscopic methods. *Fuel* **1986***, 65*, 1062-1066.

36. Guillén, M. D.; Díaz, C.; Blanco, C. G. Characterization of coal tar pitches with different softening points by 1H NMR: role of the different kinds of protons in the thermal process. *Fuel Process Technol* **1998***, 58*, 1-15.

37. Rüchardt, C.; Gerst, M.; Ebenhoch, J. Uncatalyzed Transfer Hydrogenation and Transfer Hydrogenolysis: Two Novel Types of Hydrogen-Transfer Reactions. *Angewandte Chemie International Edition in English* **1997***, 36*, 1406-1430.

38. Parsons, A. F. *An introduction to free radical chemistry;* Wiley-Blackwell: 2000.

39. Billmers, R.; Griffith, L.; Stein, S. Hydrogen transfer between anthracene structures. *J. Phys. Chem.* **1986***, 90*, 517-523.

40. Rüchardt, C.; Gerst, M.; Nölke, M. The Uncatalyzed Transfer Hydrogenation of α-Methylstyrene by Dihydroanthracene or Xanthene—a Radical Reaction. *Angewandte Chemie International Edition in English* **1992***, 31*, 1523-1525.

41. McMillen, D. F.; Malhotra, R.; Nigenda, S. E. The case for induced bond scission during coal pyrolysis. *Fuel* **1989***, 68*, 380-386.

42. McMillan, D. F.; Ogier, W. C.; Chang, S. J.; Fleming, R. H.; Ogier, W. C.; Nigenda, S. E. Mechanisms of hydrogen transfer and bond scission of strongly bonded coal structures in donor-solvent systems. *Fuel* **1987**, 66, 1611.

43. Billmers, R.; Brown, R.; Stein, S. Hydrogen transfer from 9, 10-dihydrophenanthrene to anthracene. *Int J Chem Kinet* **1989***, 21*, 375-386.

44. Manka, M.; Brown, R.; Stein, S. Rate constants for hydrogen abstraction by resonance stabilized radicals in high temperature liquids. *Int J Chem Kinet* **1987***, 19*, 943-957.

45. Stein, S. E. A fundamental chemical kinetics approach to coal conversion. In *New Approaches in Coal Chemistry,* ACS Symposium Series, 169; Blaustein, B.D; Bockrath, B.C; Friedman, S., Eds.; American Chemical Society; Washington, DC, 1981; pp 97-129.

3. SELECTION OF RECOVERY METHOD FOR CONVERTED ASPHALTENES

Abstract

Asphaltenes are converted at low temperatures and recovered manually and with solvent to select appropriate recovery method that fits to our research. It was found that due to possible heterogeneity in the mixture, whole products have to be analyzed to have meaningful results instead of taking sub-samples for analysis.

Keywords: asphaltenes, catalytic effect, heterogeneity

3.1 Introduction

Because of very diverse nature of molecules in petroleum products, it is more practical to separate them into boiling or solubility classes rather than separating them based on chemical structure. Most commonly, the heaviest fraction of petroleum heavy oils are separated into different classes based on their solubility properties in different solvents. Since this work will be dealing with asphaltenes, it is very important to give an appropriate definition of this solubility class.

Asphaltenes in this work are by definition a solubility class that is separated from crude oil by the addition of 40 volumes of the liquid hydrocarbon (*n*-pentane or *n*-heptane).[1] Various standard separation methods (IP 143, ASTM D4124 and etc.) in terms of solvent power, precipitation time and etc. can be encountered in the literature, which shows yields and quality can vary depending on the procedures.[2,3] Reproducibility is a real challenge for the separation processes, which can significantly affected by solvent type, solvent amount, settling time. Procedures should be followed very closely to have low variance in results.

From the standpoint of industrial recovery, the selection of solvent and the solvent to oil ratio, which are key variables, needs careful consideration. For industrial solvent deasphalting processes, the feed and the solvent are mixed together in solvent to feed ratios ranging from 3:1 up to 10:1.[4] Removal of asphaltenes improves the quality of the remaining oil in terms of density and composition (lower heteroatom content). Hydrogen content can be used as representative property of deasphalted oil, which increases with a decrease in asphaltene weight fraction remaining in the oil.[4]

The work in this thesis is concerned with asphaltenes conversion. Performing reactions with asphaltenes is difficult and an important first step in the investigation was to ensure that the experimental protocols were appropriate for the investigation.

In laboratory research, one of the most common solvents for recovery of converted oil from batch reactors after performing reactions is toluene.[5,6] It has been observed that the viscosity and density measurements of solvent-extracted oil are generally inaccurate.[7] This was because solvent was not completely removed prior to measurement, or that the process of solvent removal also removed volatile components in the bitumen, thus affecting the actual viscosity or density. Toluene removal from heavy oil is especially difficult and time consuming and there will always be residual toluene in the reaction product. Due to the residual solvent, measurement of other properties of solvent extracted material, such as hydrogen content, may not be accurate. To avoid or limit inaccuracy during product analysis, a simple and efficient way to recover and work-up the reaction product after reaction needed to be found.

In scientific studies conducted to investigate changes in the nature of compounds after thermal conversion, it is important to eliminate foreign substances (like solvent) without affecting the original material itself. Apart from solvent extraction or precipitation, other factors also need to be considered and eliminated for meaningful results. For example, before making a conclusion about the temperature effect on material, one must verify that there are no external factors, such as the metal surface of reactor, which caused or contributed to the observed change.

The possibility of catalytic effects of the reactor walls has been investigated experimentally and it was found that nature of the surface affected the rate of carbon formation.[8] Therefore it is preferable to heat the asphaltenes in a glass vial to avoid direct contact with the metal surface of the reactor, which might exhibit catalytic behavior. However, there are downsides to the use of a glass vial in a metal reactor. First, there is the additional insulation of reaction mixture, so that the heat up and cool down times of the reactor are prolonged. Second, solidification of the feed in the glass vial, which is fragile, limits the physical recovery of the materials from the reactor, because too much force will cause the vial to break and using a solvent has drawbacks, as was previously pointed out.

The purpose of this study is to define the most appropriate way of heating the asphaltenes feed (within vial or direct heating in microbatch reactor) and recovery of products after reaction (manually or with the aid of a solvent, toluene). After using different methodologies, quantitative comparison of results was made also to select a methodology. Study of impact of recovery method on hydrogen content of the samples will produce preliminary results for making decisions about an appropriate experimental protocol. This study was also undertaken to provide information on variation in properties of product (inhomogeneity) in different sections of reactor. In all instances the change in the aliphatic to aromatic hydrogen content as measured by proton nuclear magnetic resonance spectroscopy was used to track changes in the chemical nature of the products following on previous work.[9]

3.2 Experimental

3.2.1 Materials

The asphaltenes feed was obtained from the *n*-pentane based solvent deasphalting unit at Long Lake Upgrader of Nexen Energy ULC. The Long Lake upgrader is situated in the Athabasca oilsand region, and it upgrades bitumen recovered from subsurface oilsands deposits by steam assisted gravity drainage (SAGD).

Re-precipitation of the industrial asphaltenes from 40:1 *n*-heptane to asphaltene mixture at room temperature indicated that around 66.8 ± 1.7 % of the feed can be classified as *n*-heptane insoluble asphaltenes. Other characterization data of the feed material was obtained from previous work and the combined results are repeated here for ease of reference (Table 3.1).[9]

Table 3.1. Feed characterization of industrial asphaltenes from Nexen Energy ULC.

Description	Industrial asphaltenes feed[a]	
	x	s
C_7-asphaltenes (wt%)	66.8	1.7
Maltenes	32.5	1.5
Elemental analysis[b]		
carbon (wt%)	80.3	0.1
hydrogen (wt%)	8.0	0.1
nitrogen (wt%)	1.1	0.0
sulfur (wt%)	7.7	0.1
^1H NMR[b]		
aliphatic hydrogen	86.5	0.5
aromatic hydrogen	13.5	0.5
TGA[b]		
micro carbon residue (wt%)	36.0	

[a] average (x) and standard deviation (s) of triplicates

[b] extracted from Styles and De Klerk[9]

Table 3.2.Materials employed in this study.

Compound	Formula	CASRN [a]	Mass fraction purity [b]	Supplier
Materials used for precipitation				
Toluene	$C_6H_5CH_3$	108-88-3	0.99	Aldrich
Solvent for NMR				
Chloroform-*d*	$CDCl_3$	7727-37-9	0.99 [c]	Praxair

[a] CASRN = Chemical Abstracts Services Registry Number

[b] This is the purity of the material guaranteed by the supplier; material was not further purified.

[c] Mole fraction purity.

3.2.2 Equipment and procedure

The experiments with industrial asphaltenes for this investigation were conducted in microbatch reactors. The microbatch reactors were built from Swagelok 316 stainless-steel 0.5 in. tubing (with 12.7 mm outside and 10.2 inside diameter), approximately 80 mm in length. The inner and outer diameters of reactors were 2.7 and 3.3 cm respectively with a length equal at 8.7 cm. A schematic drawing of the reactor showing all the dimensions have been listed above is shown in Appendix A.

For each experiment, 4 ± 0.2 g of asphaltenes was loaded directly into the stainless steel reactors, or into a clear glass vial (7mL) that was placed in the stainless steel reactor. The reactors were purged with nitrogen, leak-tested and then pressurized with nitrogen. All reactions were performed under nitrogen atmosphere at approximately 4 MPa gauge pressure. The micro-batch reactors were placed in a preheated fluidized sand bath heater, Omega fluidized bath, to heat the reactors up to reaction temperature (Figure 3.1).

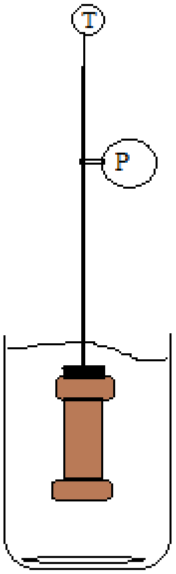

Figure 3.1 Batch reactor system used for thermal reactions.

The heat-up time to reach 150 °C was 8 minutes for reactors without glass vials and was not taken into account for the reaction time, which was measured as 1 h from the time that reactor internal temperature reached the set point. Although the heat-up time to reach set point for the reactors with glass vials was somewhat longer (measured and discussed in Chapter 5), for the present comparison the same heat-up period was allowed.

The micro-batch reactors were not equipped with any form of agitation. A thermocouple was placed in the reaction mixture inside the reactor to measure the temperature.

At the end of reactions, reactors were removed from the sand bath heater and cooled down to room temperature. No significant pressure build-up was observed and the nitrogen was released from the reaction system. Reactors and products were weighed at each step using a Mettler Toledo ML 3002 balance, which had a 3200 g capacity with 0.01 g readability. Material balance closure was generally within 98 to 102 wt %. All experiments were performed triplicate.

All reactions were performed at 150 °C for 1 hour. After each reaction, products were recovered by using the following procedures. Toluene was used as a solvent to when converted asphaltenes were recovered from the reactor. The recovery procedure can be described in following steps:

In total 6 reactions of asphaltenes were performed in the glass vial by placing it into micro-batch reactor. The reaction products of 3 of them were recovered manually to the greatest extent possible by scraping material out without the use of solvent and labelled as (b.1). Since the products became hardened solids, it was not possible to extract the product fully. The glass was fragile and was broken a couple of times during the manual recovery. The remaining 3 three vials were not scraped clean completely and only product from top section was recovered manually by scraping the material and labelled as (exp.2). Then the remainder portion of products in the vial was recovered with a known amount of solvent and concentration was estimated. The amount of product which recovered from top and bottom sections of the reactor were reported in Table A.2. These samples were labeled as (b.3) and weight was estimated based on the material balance. As little as possible solvent was used and the concentration of products was recorded. Then half of the manually collected material, i.e. (exp.2), was dissolved in the solvent to get the same concentration as obtained in (b.3), which recovered with solvent. This sample was labelled (b.2). The toluene in samples (b.2) and (b.3) was removed by using rotary evaporator at 55 °C under 60 mmHg over 24 h.

Another 3 reactions were performed directly in the micro-batch reactor, without a glass vial. The products were recovered from the micro-batch reactors manually by scraping the material out and these products were labelled as (b.4).

A summary of the samples and their sample designations are provided in Table 3.3. All of these samples were analysed by proton magnetic nuclear resonance spectroscopy and infrared spectrometry.

Table 3.3. Short description of samples.

Label	Description
(b.1)	Manually recovered product from vial.
(b.2)	Dissolved material that was manually recovered product from vial (Top section of vial).
(b.3)	Dissolved material that was recovered with solvent from vial (Bottom section of vial).
(b.4)	Manually recovered products directly heated in the reactors (no vial).

3.2.3 Analyses

3.2.3.1 Proton magnetic nuclear resonance spectroscopy

Proton magnetic nuclear resonance spectroscopy (^{1}H NMR) was performed with a Nanalysis 60 MHz spectrometer. Samples were diluted with $CDCl_3$ solvent in a ratio equal to 1:10 (mg/µL). The 60 MHz NMR spectrometer utilizes a processing software called MNova. Hydrogen shift values between 6 to 9 ppm and 0.5 to 4.5 ppm were considered aromatic and aliphatic respectively. It was assumed that the products were free of olefinic compounds. The following analysis parameters were used: range: 0-12 ppm; number of scans for sample: 32; 14.7 seconds was the average scan time and 4096 points were recorded per scan.

3.2.3.2 Fourier transform infrared spectrometry

Infrared analyses were performed by using an ABB MB 3000 Fourier transform infrared (FTIR) spectrometer with Horizon MB FTIR software. The spectrometer was equipped with a Pike MIRacle^{TM} Reflection attenuated total reflectance (ATR) diamond crystal plate. A small amount of sample was placed in the sample compartment, and the spectrum was collected over the wavenumber range 4000 to 500 cm^{-1} as the average 120 scans. The spectral resolution employed was 4 cm^{-1}, the acquisition mode was transmittance, and the detector gain was set at 243.

3.2.3.3 Paired Student t-test

Paired student t-test was used to determine the differences between (b.2) and (b.3), and (b.1) and (b.4). These tests were administered using IBM SPSS Statistics 21 (2012) Mac OS X.

3.3 Results

3.3.1 Material balance

Material balance closure for the experiments performed in micro-batch reactors was performed and it was found to be in the range of 98 to 102 wt%, which can be considered acceptable. All the experiments (9 in total) were conducted in triplicate and results were reported as an average with one sample standard deviation, this is shown in Table A.1.

3.3.2 ^{1}H NMR reaction product analyses

^{1}H NMR was employed as a main tool for comparison of samples listed in Table 3.3. The integrated intensities of the aromatic and aliphatic hydrogens whose resonance positions are aromatic range, H_{ar} (δ 6.0-9.0 ppm) and aliphatic range, H_{sat} (δ 0.5-4.5 ppm) were determined and were shown as ratio of aliphatic hydrogen to aromatic hydrogen. An example of the ^{1}H NMR spectrum of an asphaltenes samples is provided in Appendix A. All data and derived results of the reaction products and the asphaltenes feed are provided in Table 3.4.

Table 3.4. ^{1}H NMR results of the converted asphaltenes with different methods: (b.1) Manually recovered product from vial; (b.2) Dissolved material that was manually recovered product from vial; (b.3) Dissolved material that was recovered with solvent from vial, and (b.4) Manually recovered products directly heated in the reactor.

Samples	Ratio of aliphatic hydrogen to aromatic hydrogen			Average aromatic hydrogen [%]	Standard deviation
	1	2	3		
Feed	8.89	8.99	8.9	10.07	0.06
b.1	8.69	8.85	8.53	10.32	0.17
b.2	5.56	5.27	5.58	15.46	0.42
b.3	4.6	4.36	4.74	17.98	0.63
b.4	7.67	7.52	7.5	11.68	0.13

Table 3.5. T-test values for data from Table 3.4.

	t test value	degree of freedom.	two tailed p values (p-value < 0.5)
Pair 1: b2 - b3	25.957	2	0.001
Pair 2: b1 - b4	11.078	2	0.008

It was speculated that properties such as aromaticity of the reaction product might vary along the height of the reactor. In order to evaluate the homogeneity concerns related to reaction medium, the hydrogen distribution of aliphatic versus aromatic hydrogen content of material that was manually recovered from top section of the vial (b.2) and dissolved material that was recovered with solvent from bottom section of vial (b.3) was investigated. There was a clear difference (2-3 %) between (b.2) and (b.3) in average aromatic hydrogen content (Table 3.4).

Another point worth noting is the comparison of the experimental data based on the aromatic hydrogen content (derived from ratio of aliphatic versus aromatic) of the products recovered from vial and reactor (Table 3.4). The sample (b.4) which was obtained by heating of asphaltenes feed directly in the metal reactor has higher aromatic hydrogen content than that recovered from the vial (b.1).

3.3.3 FT-IR analysis

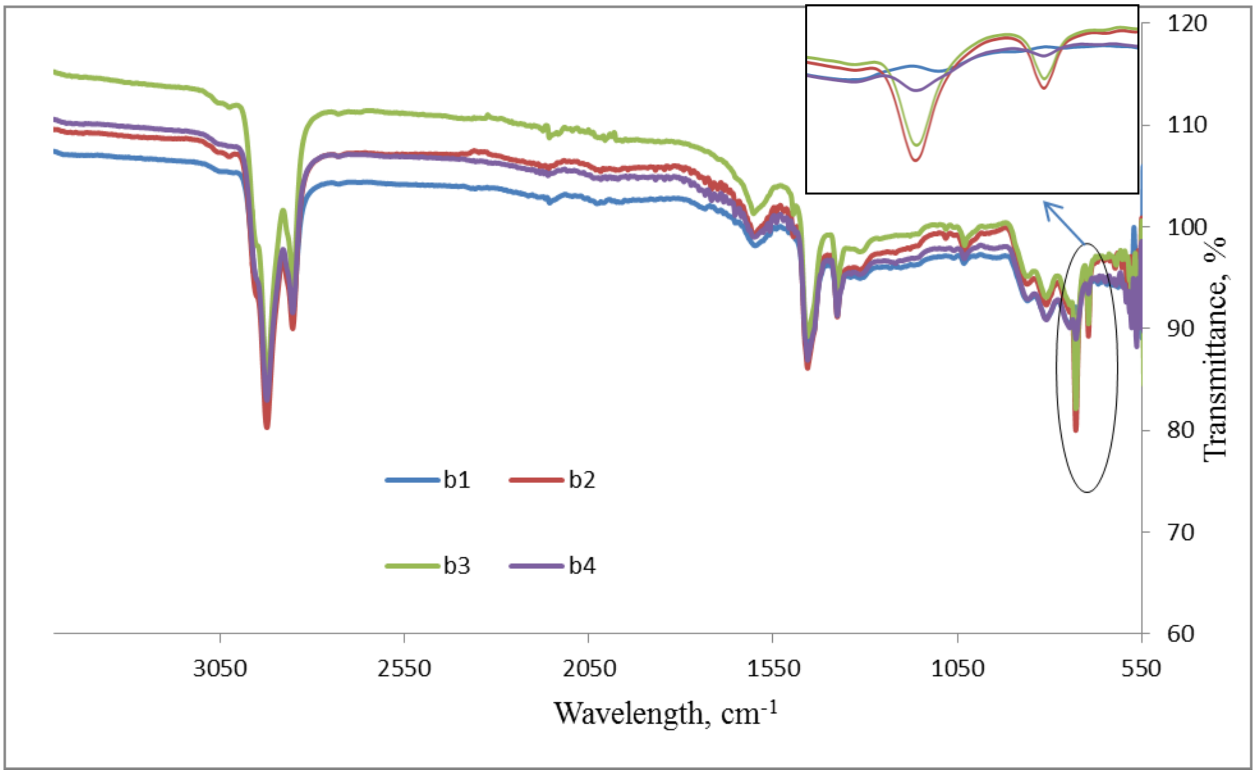

Figure 3.2 FT-IR spectra of the recovered asphaltenes after thermal heating at 150 °C.

FT-IR spectra (Figure 3.2) of the products which were recovered from reactor (b.4) and vial (b.1) do not visually exhibit a significance difference in terms of peak intensity or the wavenumbers of absorption bands.

However, two intense peaks were observed in the samples that had been recovered with solvent at around 703 cm^{-1} and relatively weaker band at 692 cm^{-1} (Figure 3.2). These were caused by residual toluene in these samples; the infrared spectrum of toluene can be found in Figure 3.3.

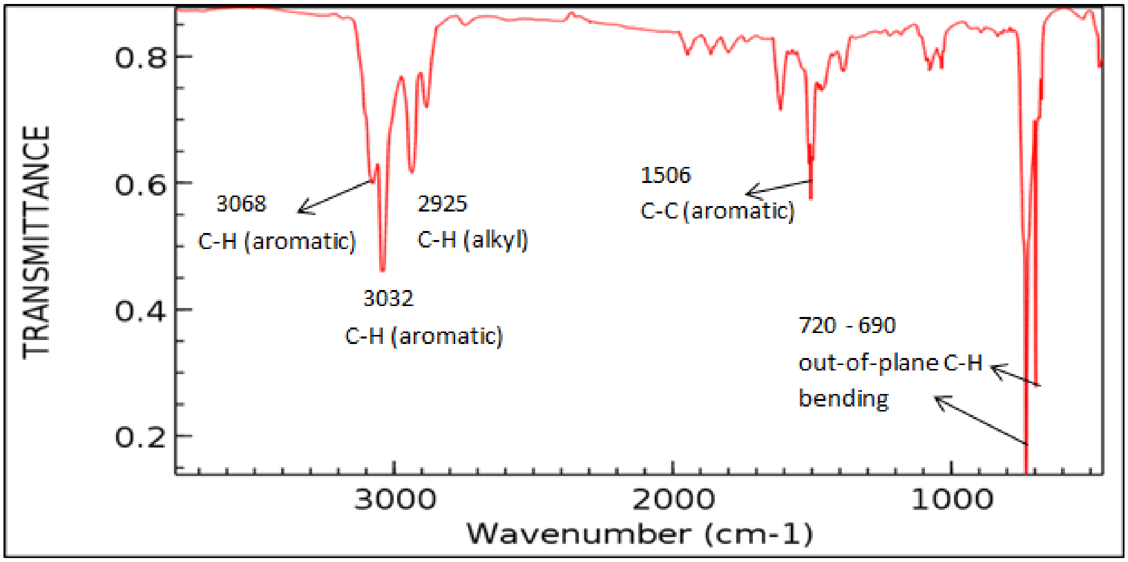

Figure 3.3. Infrared spectrum of toluene (Source: NIST Chemistry webbook

3.4 Discussion

3.4.1 Inhomogeneity in reaction products

Based on the data given in Table 3.7, it can be suggested that material extracted from bottom (b.3) of the vial is different than material that recovered from the top (b.2). The means of (b.2) and (b.3) were compared using a paired Student t-test and it was found that the means were statistically different at a 95 % confidence level. The data gives a good picture of variation with the depth of the vial.

This study suggests that reaction medium might exhibit heterogeneity, or it might be attributed to uneven temperature distribution due to absence of mixing, or it might be due to a difference in the amount of toluene remaining in the samples.

The high aromatic hydrogen contents (Table 3.4) of samples (b.2) and (b.3), which were recovered with solvent, can be attributed to the toluene. Evidence of residual toluene in the products was confirmed with FTIR. The appearance of 703 cm^{-1} and relatively weaker band at 692 cm^{-1} could be ascribed to out of plane bending of the ring C-H bonds (Figure 3.2).[10] Those strong absorption bands which are very characteristic for substituted benzene compounds frequently appear at low frequency range between 700-615 cm^{-1}. An infrared spectrum of toluene can be found in Appendix A. The amount of toluene was not quantified and even if it had been, the variance in analysis of the toluene content would have eroded the confidence interval with which (b.2) and (b.3) were found to be different.

There is consequently more uncertainty in the conclusion that the reaction products were inhomogenous than calculated based on the ^1H NMR data due to the possible difference in toluene content.

3.4.2 Use of solvent for recovery of reaction products

Based on the observations it was concluded that toluene is very unlikely to evaporate completely from the products after recovery. Vapor pressure of toluene (ideal solution) was calculated at 55 °C by using Antoine equation and found to be equal at 0.12 bar.

$$\log_{10} P = A - \frac{B}{(T + C)}$$

where temperature is in Kelvin and A = 4.08245, B = 1346 and C = - 53.508, which have been derived from experimental data at temperatures ranging from 30 to 70 °C, and can be found in NIST Standard Reference Database 69: *NIST Chemistry WebBook* .

Although the chosen vacuum condition (0.07 bar) for evaporation was sufficiently lower than the calculated vapor pressure of toluene, it was not possible to evaporate it completely. Thus it is therefore beneficial not to use solvent for product recovery after reaction.

3.4.3 Impact of reactor material on reaction products

To investigate whether the metal wall of reactor has an effect on reactions taking place during heating, the reaction products from heating at 150 °C for 1 h in a glass vial (b.1) was compared to that obtained by heating in direct contact with the stainless steel (b.4). Statistical significance of this difference can be claimed based on p-value which is less than 0.05, ensuring approximately 95 % confidence in the results (Table 3.5). Numerically there was a difference in the aromatic hydrogen content of reaction products (Table 3.4). The asphaltenes that were heated directly in contact with the stainless steel wall of the micro-batch reactors, gained slightly more aromaticity compared to those heated in glass vials.

As has been mentioned earlier, exposure time of reactors to heat was same for both cases despite of the somewhat longer heat-up time of glass vials to reach the set point. Therefore effect of the time might have played a role in the change of hydrogen content.

It appeared that the hydrogen distribution is somewhat dependent on the nature of reactor wall (glass or steel). This can be held as evidence that inner metal surface of the batch reactor might have a catalytic effect during the heating process, facilitating hydrogen disproportionation.

3.5 Conclusions

I. It was found that asphaltenes might exhibit some degree of heterogeneity in the reaction medium. Based on the ^{1}H NMR measurement, aromatic hydrogen content of product (17.98 %) extracted from bottom of reactor was higher than that of product (15.46 %) recovered from the top section. However, the confidence with which this statement can be made was eroded by the variability in analysis introduced the residual solvent in the reaction products.

II. It is preferable to recover the reacting product manually by scraping off the material from the reactor, rather than using a solvent for recovery. As can be seen from relatively higher value of aromatic hydrogen content of toluene extracted products, toluene evaporation was difficult, time consuming and did not lead to quantitative toluene removal. This might cause significant errors in product analyses.

III. Evidence was provided that the stainless steel wall might promote hydrogen disproportionation. However, confidence in this conclusion was eroded by the difference in the temperature versus time profile of reactions conducted in glass vials compared to that conducted in direct contact with the metal reactor.

References

1. Speight, J. G.; Long, R. B.; Trowbridge, T. D. Factors influencing the separation of asphaltenes from heavy petroleum feedstocks. *Fuel* **1984**, *63*, 616-620.

2. Speight, J. Petroleum Asphaltenes-Part 1: Asphaltenes, resins and the structure of petroleum. *Oil & gas science and technology* **2004**, *59*, 467-477.

3. Alboudwarej, H.; Beck, J.; Svrcek, W.; Yarranton, H.; Akbarzadeh, K. Sensitivity of asphaltene properties to separation techniques. *Energy Fuels* **2002**, *16*, 462-469.

4. Gray, M. R. *Upgrading oilsands bitumen and heavy oil;* University of Alberta: 2015; p 284.

5. Rahmani, S.; McCaffrey, W.; Gray, M. R. Kinetics of solvent interactions with asphaltenes during coke formation. *Energy Fuels* **2002***, 16*, 148-154.

6. Wiehe, I. A. *Process chemistry of petroleum macromolecules;* CRC press: 2008; p 27.

7. Larter, S. R.; Bennett, B.; Snowdon, L. R.; Jiang, C. D.; Adams, J. J.; Gates, I. D.; Noke, K. J. Method for measurement of crude oil and bitumen dead oil viscosity and density. U.S. Patent No. 8,336,370 , December 25, **2012**.

8. La Cava, A. I; Trimm, D. L.; Turner, C. E. Catalytic effects during the thermal cracking of hydrocarbons. *Revista portuguesa de quimica* **1977**, *19,* 345-349.

9. Styles, Y.; de Klerk, A. Sodium Conversion of Oilsands Bitumen-Derived Asphaltenes. *Energy Fuels* **2016***, 30 (7)*, 5214-5222.

10. Silverstein, R. M.; Webster, F. X.; Kiemle, D. J.; Bryce, D. L. *Spectrometric identification of organic compounds;* John Wiley & Sons: 2014.

4. LOW TEMPERATURE CONVERSION OF ASPHALTENES

Abstract

In this work, the conversion of industrial asphaltenes from Nexen's Long Lake upgrader without any catalyst was investigated over the temperature range of 100−150 °C under an inert atmosphere to limit the contribution of oxidation. With increasing fluidity of the asphaltenes with an increase in temperature, intramolecular hydrogen disproportionation and intermolecular hydrogen transfer reactions were favored. Eventually, these reactions could result in the formation of more condensed and potentially more aromatic products. Asphaltenes were found to be reactive for hydrogen disproportionation already at 150°C.

Keywords: Hydrogen, disproportionation, free radical, intermolecular, intramolecular

4.1 Introduction

Sodium conversion of asphaltenes was investigated in a recent study from our research group.[1] Reactions were performed at temperature ranges from 60 to 250 °C to limit thermal conversion of asphaltenes. However, control experiments revealed that industrially produced asphaltenes containing ~ 20 wt% maltenes presented significant changes in solubility and chemical composition when heated at low temperature. The maltenes fraction decreased with temperature increase and the maltenes obtained from thermal conversion at temperatures higher than 140 °C contained more aliphatic hydrogen. It was speculated that intermolecular hydrogen transfer is facilitated by increasing mobility of asphaltenes molecules, i.e. when asphaltenes were in a liquid state (~ 142 °C). Since hydrogen transfer of asphaltenes takes place at low temperatures, it intrigued us to investigate further what changes might occur at lower temperature.

The composition of gases evolved during pyrolysis of maltenes and asphaltenes fractions from the Cold Lake and Athabasca bitumen deposits was studied previously.[2] The rate of gas evolution was measured as 0.6×10^{-3} $\text{mol}\cdot\text{kg}^{-1}\cdot\text{h}^{-1}$ at 210 °C. It was also shown that the asphaltenes fraction of the bitumen is thermally less stable than the maltenes fraction based on the rate of thermolysis.

The reactivity of asphaltenes can be a very important concept in petroleum processes involving relatively mild heating, such as oil production by steam injection and refining. From the viewpoint of processing, any changes in the properties of oil, such as formation of insoluble material during preheating in refinery or storage, might induce fouling or it might cause flow assurance problems due to an increase in the viscosity.

The objective of this work was to investigate whether asphaltenes are affected by heating in the temperature range of 100 to 150 °C.

4.2 Experimental

4.2.1 Materials

A list of the chemicals used in this study is given in Table 4.1. The asphaltenes feed was obtained from the *n*-pentane based solvent deasphalting unit at the Long Lake Upgrader of Nexen Energy ULC. Detailed information for feed characterization was presented in Chapter 3.

Table 4.1. Materials employed in this study.

Compound	Formula	CASRN [a]	Mass fraction purity [b]	Supplier
Materials used for precipitation				
n-heptane	C_7H_{16}	142-82-5	0.99	Aldrich
Solvent for NMR				
chloroform-*d*	$CDCl_3$	865-49-6	0.99 [c]	Sigma-Aldrich
Cylinder gases				
nitrogen	N_2	7727-37-9	0.99[c]	Praxair
helium	H_2	7440-59-7	0.99[c]	Praxair

[a] CASRN = Chemical Abstracts Services Registry Number.

[b] This is the purity of the material guaranteed by the supplier; material was not further purified.

[c] Mole fraction purity.

4.2.2 Equipment and procedures

The experiments with industrial asphaltenes for this investigation were conducted in micro-batch reactors. The micro-batch reactors were constructed from Swagelok 316 stainless-steel 0.5 in. tubing (with 12.7 mm outside and 10.2 inside diameter), approximately 80 mm in length. These micro-batch reactors were not equipped with any form of agitation. The experimental setup was described in more detail in Chapter 3.

For each experiment, 5 ± 0.1 g of asphaltenes was loaded into reactors. Despite the observations in Chapter 3, it was decided not to make use of glass vial inserts. Since the product had to be recovered without the use of a solvent, the risk associated with the fragile glass vials was considered unacceptable. The possible contribution of the metal wall to promote reactions could therefore not be ruled out.

Before the reactions, reactors were leak-tested with nitrogen to confirm that no leaks developed during the experiments. The reactors were then pressurized with nitrogen to 4 MPa gauge. The micro-batch reactors were placed in a preheated fluidized sand bath heater, Omega fluidized bath FSB-3, to heat the reactors up to reaction temperature (Figure 3.1 in Chapter 3). The pressure inside was monitored with a pressure gauge installed on the reactors. The temperature inside the reactor was measured using a thermocouple. The heat-up time (7-8 min) was not taken into consideration for reaction time which was 1 h measured from the time that reactor internal temperature reached the set point. Asphaltenes were investigated over the temperature range 100-150 °C. The experiments and conditions are given in Table 4.2.

Table 4.2 Reaction conditions.

Reaction	Temperature [°C]	Time [h]	Pressure [MPa]	Atmosphere
Asphaltene heating	100-150	1	4	N_2
Asphaltene heating	150	5	4	N_2

At the end of the reaction period, reactors were removed from the sand bath and cooled down to room temperature. No significant pressure build-up was observed; overall pressure remained almost constant during the reactions. The reactors were connected to a sampling valve of a gas chromatograph right after the reaction in order to analyze the gases. Reactors and product were weighed at each step using a Mettler Toledo ML 3002 balance, which had a 3200 g capacity with 0.01 g readability. Products were recovered by scraping off the reactor tube without using any solvent. Since product was hardened after the reaction, more effort was required to take it off.

Above 97 % of material was recovered in all cases. Material balance closure was generally within 99 to 103 wt %. All experiments were performed in triplicate.

The *n*-heptane insoluble asphaltenes fraction was precipitated from the converted asphaltenes (reaction product) by using *n*-heptane as a solvent. A ratio of 40:1 of *n*-heptane to reaction product was mixed at ambient conditions, following the standard test method ASTM D 6560.[3] The final mixture was stirred around 2 h with a magnetic stirrer in a fume hood. The mixture was stored for 24 h to enable phase separation and was then filtered with a 0.22 μm Millipore Nitrocellulose membrane filter under vacuum while rinsing with *n*-heptane. Finally, unfiltered material (*n*-heptane insoluble asphaltenes) on the Millipore paper was transferred to aluminum cups and kept in the fume hood to dry. Subsequently, the solvent was evaporated from the soluble fraction (maltene) by rotary evaporation and the remainder of the products was left in a fume hood until constant mass was achieved. Products were classified into asphaltenes and maltenes for further analysis based on this separation.

Another set of experiments was designed to dynamically determine the nature of gaseous products formed at low temperature. The experimental setup is shown in the Figure 4.1.

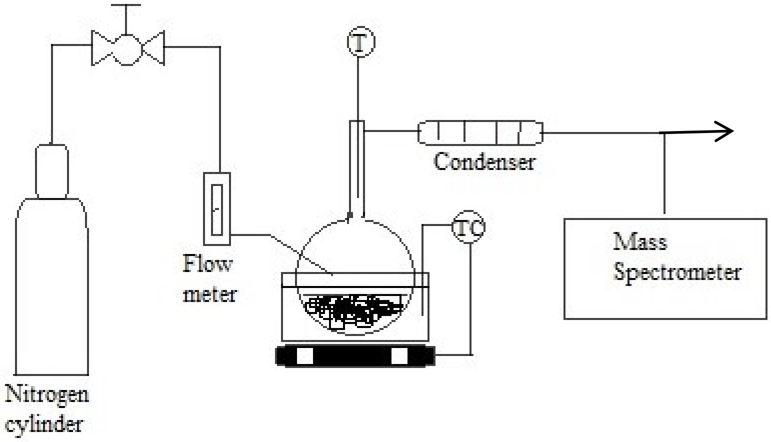

Figure 4.1 Experimental setup for gas measurements by mass spectrometer

In a typical experiment 30 g of the feed material (industrial asphaltenes) was placed in a 250 mL three-necked round bottom flask, which was connected to a reflux condenser. The reflux condenser was cooled with a chilled water supply that was maintained at 5 °C. Before the experiment the whole system was flushed with nitrogen. Nitrogen flow was controlled by a gas flow meter and maintained at a constant flow rate at the lower range of the flow meter (<20 mL min^{-1}).

The asphaltenes were heated and the temperature was maintained at 150 °C for different time periods up to 6 h. The temperature in the flask was controlled using a thermocouple in the oil bath connected to a Heidolph MR Hei-Standard heat-on-block. Gas production was continuously monitored by a mass spectrometer (ExtorrXT Series RGA, XT300 M, Extorr Inc., New Kensington, PA, USA).

4.2.3 Analyses

4.2.3.1 Proton magnetic nuclear resonance spectrometry (^{1}H NMR)

Proton magnetic nuclear resonance (^{1}H NMR) spectrometry was performed with Nanalysis 60 MHz spectrometer. Details of the equipment and analysis procedure can be found in Chapter 3.

4.2.3.2 Carbon-13 nuclear magnetic resonance spectrometry

Carbon-13 nuclear magnetic resonance (^{13}C NMR) spectrometry was performed by the Analytical Services of the Chemistry Department at University of Alberta using a 400 MHz Varian Unity Inova spectrometer.

For quantification of carbon, Chromium(III) acetylacetonate (MW 349) was employed as relaxation agent. 698 mg of Chromium(III) acetylacetonate in 10 ml of deuterated chloroform to make 0.2 M solution. Asphaltenes was dissolved in this solution to make about 0.7µL of sample height in NMR tube and then a NO NOE carbon experiment was set up where decoupling is on only during acquisition. Spectra were collected at 25.8 ºC and 100.577 MHz.

4.2.3.3 Gas chromatography

Still pressurized micro-batch reactors, after reaction and while being cooled down, were connected to a gas chromatograph (GC) to analyze the gas phase composition. Gases were slowly vented into the multi-port sampling valve of the GC by opening the valve on the reactor. The gas composition was analyzed using an Agilent 7890A gas chromatograph. The instrument is equipped with flame ionization and thermal conductivity detectors. Helium was used as carrier gas (25 mL/min) and a Hay Sep R column 2.44 × 0.003 m (8 ft × 1/8 in) was used for separation of compounds. The injector temperature was 200 °C and temperature program consisted of holding the column temperature at 70 °C for 7 minutes and increasing it to 250 °C at 10 °C/min. The temperature was kept at 250 °C for 2 minutes.

4.2.3.4 Infrared analysis

Infrared analyses were performed by using an ABB MB 3000 Fourier transform infrared (FTIR) spectrometer with Horizon MB FTIR software. Details of the equipment and analysis procedure can be found in Chapter 3.

4.2.3.5 Refractive Index

Refractive index of liquid samples was measured relative to air at 589 nm (sodium D-line). All analyses were performed at constant temperature of 20 °C using an Anton Paar Abbemat 200 refractometer. The direct refractive measurement of maltene was not possible because the maltenes were too dark. To overcome this problem the samples were dissolved in toluene to conduct measurement (100 mg sample/mL toluene).

4.2.3.6 Thermal gravimetric analysis

The mass loss and decomposition of the asphaltenes was studied by thermal gravimetric analysis (TGA) at 100-150 °C. The instrument used for the TGA investigations was a Mettler Toledo TGA with LF furnace, sample robot and, MX5 internal microbalance with a maximum weighing capacity of 5 g and a readability of 0.1 μg. All the measurements were performed under nitrogen by providing constant nitrogen flow at 100 $\mathrm{mL \cdot min^{-1}}$ to the reaction chamber. The sample mass was 9-11 mg. All experiments were performed in standard 70 μL alumina crucibles without lid and the crucibles were heated from 25 °C at 10 $°C \cdot min^{-1}$ to reach reaction temperature (100-150 °C) followed by an isothermal period of 2 h.

4.3 Results

4.3.1 Material balance

Material balance closure for the experiments performed in micro-batch reactors was calculated and it was found to be in the range of 99.5 to 103 wt% which can be considered acceptable. All the experiments were conducted in triplicate and results were reported as an average with one sample standard deviation, this is shown in Table B.4. Additionally, the mass of feed and the mass of the product that was recovered manually were reported in Table B.5.

Based on the material balance, the calculated gas yield lies between 0.004 and 0.008 g/g, which also includes nitrogen gas after initial purging. The mass due to N_2 gas was calculated by using the ideal gas law and the volume of the vapor space in the reactor left after loading of the asphaltenes feed (0.4-0.5 g). Calculated value for mass of N_2 is even higher than total mass of gases released after the heating reaction.

4.3.2 Yields of the asphaltenes at lower temperatures

Industrial asphaltenes obtained from *n*-pentane solvent deasphalting unit at the Long Lake Upgrader of Nexen Energy ULC was heated in the temperature range of 100 and 150 °C. Final products after heating reaction in batch reactors were classified after separation as maltene and asphaltenes as described in the section 4.2.2. Yields of the heptane insoluble and heptane soluble fractions of converted industrial asphaltenes are shown in Table 4.3.

Table 4.3 Product yields of the thermal conversion of the industrial asphaltenes at lower temperature for 1 h periods under N_2 air.

	Product yield (%)[a]			
Temperature	Asphaltenes		Maltenes	
	x	s	x	s
Feed[b]	66.9	1.7	32.5	1.5
100	66.5	2.1	33.2	0.3
110	64.3	1.3	35.1	0.9
120	67.1	0.8	32.6	0.5
130	67.5	1.4	31.9	0.4
140	71.1	1.2	28.9	1.7
150	74.8	3.1	25.3	1.0

[a] Average (x) and standard deviation (s) of triplicates are reported

[b] From Table 3.1 (Chapter 3) for ease of comparison

Asphaltene yield after thermal conversion at lower temperature indicated that temperature caused an increase in the amount of *n*-heptane precipitated materials. Relatively less amount of maltene was obtained from industrial asphaltenes after heating. Based on the visual inspection of the products, it can be stated that solid products became more hardened after each reaction with increasing temperature.

Asphaltene feed was also observed visually while heating in the glass beaker and it gradually turned to a viscous liquid form at around 150°C. This was consistent with the report of Styles, et al.[1] that reported a gradual change of phase between 124 and 142 °C using hot stage microscopy.

4.3.3 Composition of gases

Gases released from the reactors had a mild petroleum-like odor. Based on the material balance on the micro-reactors, very little gas was produced during heating of the asphaltenes feed. Some N_2 was also present in the released gases from the reactor due to initial purging. Since no information was found in the literature regarding the gaseous products from asphaltenes heated in the temperature range (100-150 °C), the components of gaseous and volatile materials were analyzed by using GC.

The composition of gases evolved from asphaltenes after heating in the micro-batch reactors is reported in Table 4.4.

Table 4.4. Compositions of gases evolved from the industrial asphaltenes at low temperatures ranging from 100 to 150 °C.

Compositions	Weight percentage (%)					
	100 °C	110°C	120°C	130°C	140°C	150°C
CO_2	-	-	-	-	-	-
C_1-C_4	-	-	-	-	-	-
C_5	0.15 ± 0.05	0.13 ± 0.03	0.24 ± 0.09	0.41 ± 0.07	0.71 ± 0.13	0.92 ± 0.04
C_6	-	-	-	-	-	-

The C_5 hydrocarbons were the only constituents in the gaseous product that were identified after the heating of asphaltenes for 1 h in the 100-150 °C temperature range (Table 4.4). The weight percentage of C_5 hydrocarbons increased with temperature and was yet very low (<1%) at 150 °C, indicating very small amount of gas evolved because of heating. Heating of the industrial asphaltenes did not yield C_1-C_4 hydrocarbons, H_2S and CO in the 100-150 °C temperature range.

Table 4.5. Compositions of gaseous volatiles from the industrial asphaltenes heated at 150 °C [a]

Compositions	Weight percentage (%)	10^{-4} [g] gas/[g] feed [b]
CO_2	0.26 ± 0.23	0.21
C_1-C_4 [c]	0.13 ± 0.14	-
C_5	2.13 ± 0.35	1.67
C_6	0.74 ± 1.17	0.58

[a] Experiments was run for 5 h only to see gases for analytic purposes.

[b] The gas product in terms of g gas/ g feed was calculated based on the total amount of gas released from reactor after heating.

[c] was not reproducible

The most abundant gase evolved from the asphaltenes feed after 5 h reaction time at 150°C was C_5 hydrocarbon content followed by C_6 hydrocarbons and CO_2. Overall only less than 3 % of gas compositions were evolved from asphaltenes and the rest was N_2 which was used as inert atmosphere for heating reactions. Large deviations were also very apparent in results especially in C_6 hydrocarbons.

No H_2S and CO were detected during the heating of asphaltenes at at 150 °C for 5 h. Despite of the presence of CH_4 in some experiments that were performed at 150°C for 5 h, it was not reproducible (Table 4.5).

This observation then led to a conclusion that decomposition of industrial asphaltenes (feed) to release gaseous products is very limited at 150°C. These C_5 hydrocarbon gases collected at 150 °C might be material that remained from the upgrading process (distillation units, *n*-pentane based solvent deasphalting unit).

It was not also possible to detect any reaction product (hydrocarbons) by using the experiment setup given in Figure 4.1.

Very small (<0.3 %) mass loss was recorded during the heating of industrial asphaltenes with TGA at 150°C for long period of time.

4.3.4 ^{1}H-NMR

^{1}H-NMR spectroscopic technique was used to estimate the ratio of aliphatic and aromatic hydrogen of maltene fraction of product from the residue. The whole spectrum was divided into aliphatic and aromatic regions based on the specific chemical shifts. Hydrogen type distribution of products was calculated by integrating corresponding peak intensities of aromatic range, H_{ar} (δ 6.0–9.0 ppm) and aliphatic range, H_{sat} (δ 0.5–4.5 ppm) as shown in Figure 4.2. It was found that aromatic hydrogen content of maltene fraction decreased upon increasing temperature from 100 to 150 °C (Table 4.6). Meanwhile, aromatic content of the asphaltenes fraction of the residue increased slightly over the same temperature range (Table 4.7).

Table 4.6. An estimation of the average amount of aromatic hydrogen of maltene fraction of residue from different temperatures.

	Ratio of aliphatic H to aromatic H				
Temperature	1	2	3	Average aromatic H (%)	St.Deviation
maltene[a]	10.11	10.05	9.98	9.05	0.05
100	10.38	10.59	10.38	8.73	0.09
110	10.77	11.02	10.85	8.42	0.09
120	11.04	11.22	11.23	8.22	0.07
130	11.51	11.2	11.25	8.12	0.11
140	10.98	11.61	11.54	8.08	0.23
150	11.54	12.14	12.66	7.63	0.33

[a] maltene fraction were separated from industrial asphaltenes without any heating.

Table 4.7. An estimation of the average amount of aromatic hydrogen of asphaltene fraction of residue from different temperatures.

Temperature (°C)	Ratio of aliphatic H to aromatic H			Average aromatic H (%)	St. Deviation
	1	2	3		
asphaltene[a]	11.05	10.98	11.21	8.28	0.08
100	10.84	10.56	10.58	8.58	0.11
110	10.45	10.26	10.78	8.70	0.20
120	9.61	9.56	9.9	9.35	0.16
130	9.78	9.57	9.78	9.34	0.11
140	9.37	9.33	9.6	9.58	0.13
150	8.78	8.75	8.9	10.19	0.08

[a] asphaltene fraction were separated from industrial asphaltenes without heating

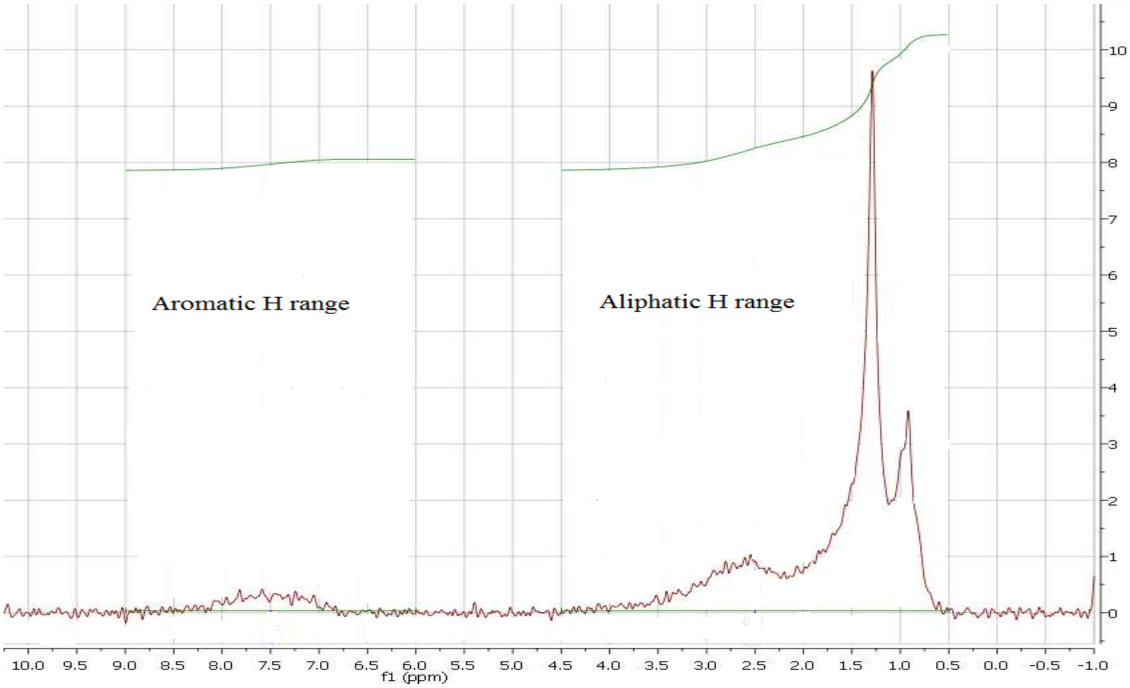

Figure 4.2 A typical ^{1}H NMR spectra of asphaltenes obtained from the asphaltenes feed without heating.

4.3.5 ^{13}C NMR

High resolution ^{13}C NMR was also employed to determine any change in aromaticity of fractions upon heating. Spectra of the asphaltenes which obtained without any heating of industrial asphaltenes feed and after heating of feed at 150 °C are presented in Figure 4.3 and Figure 4.4. The spectra of both fractions appear very similar, featuring a broad peak due to aromatics C and a broad hump due to napthenic C, and sharp peaks which appears for primary, secondary and tertiary carbons in straight chains. The region between 0 – 70 ppm and 110 – 160 ppm was ascribed to aliphatic and aromatic carbons respectively.[4] The approximate ratios of aromatic and aliphatic carbons were determined by integration of the corresponding peaks. There is approximately 2 % increase in aromatic carbon percentage after heating of the feed at 150 °C (Table 4.8). These results can be an indication of structural alteration due to mild heat treatment.

Table 4.8. An estimation of the average amount of aromatic carbon of asphaltene fraction of residue from different temperatures.

Temperature [°C]	Aromatic C/ Aliphatic C 1	Aromatic C/ Aliphatic C 2	Average Aromatic Carbon [%]	St. Deviation
Asphaltenes[a]	1.02	1.01	50.31	0.256685
150	1.10	1.07	52.01	0.578167

[a] asphaltene fraction were separated from industrial asphaltenes without heating

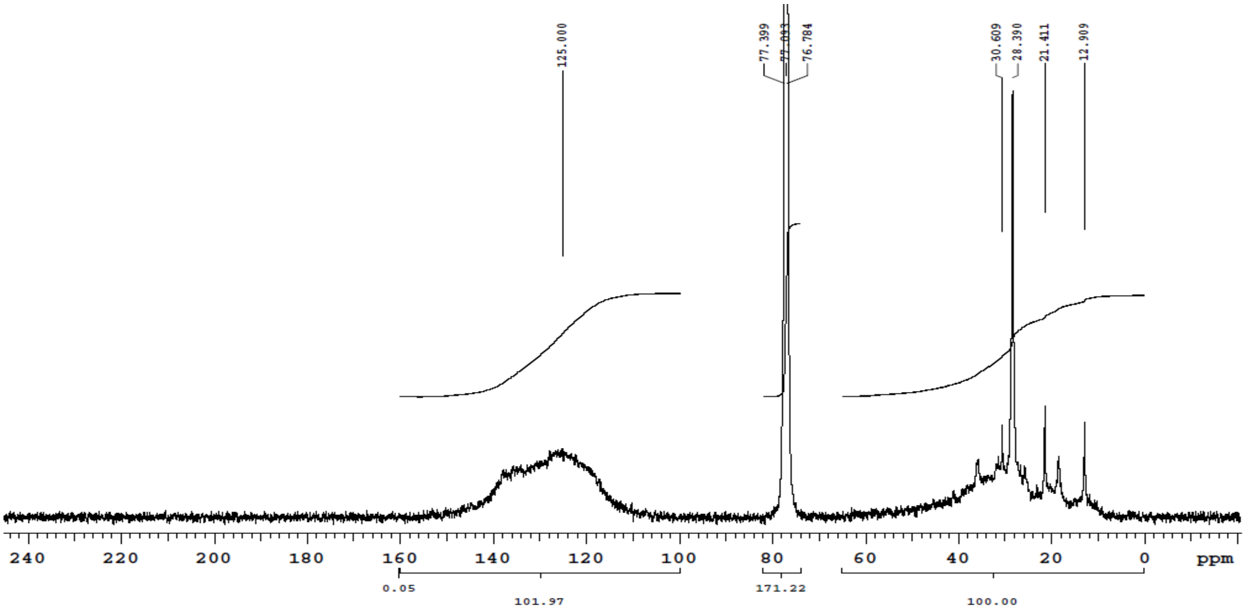

Figure 4.3. High resolution ^{13}C NMR spectrum of asphaltenes extracted from feed without any heating.

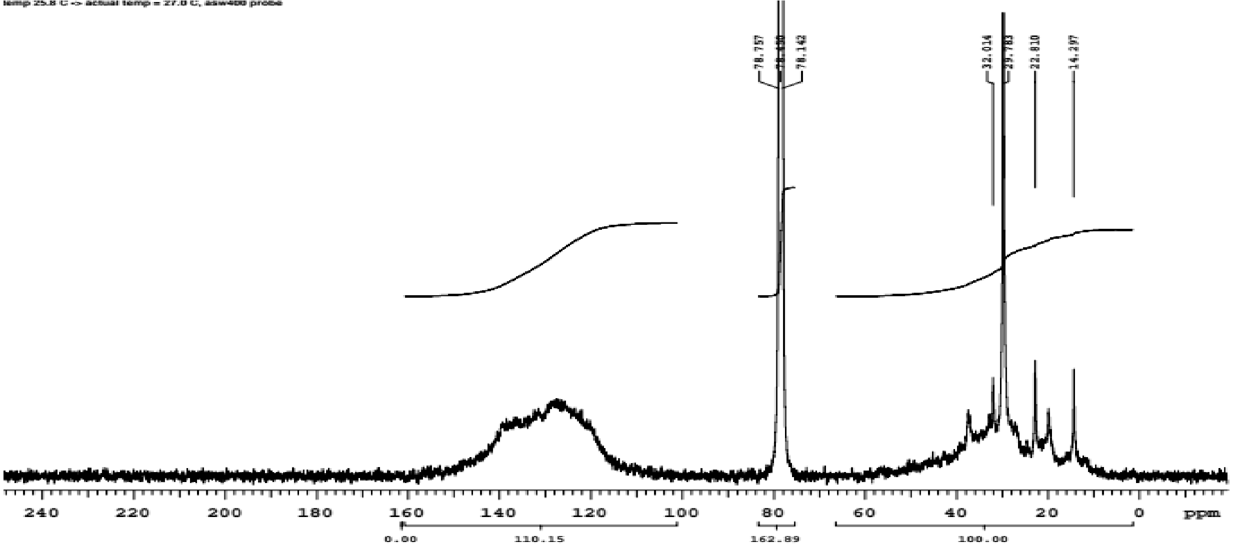

Figure 4.4. High resolution ^{13}C NMR spectrum of asphaltenes precipitated from feed after heating at 150 °C for 1 h.

4.3.6 Refractive index

The refractive index (RI) of maltenes cannot be measured directly, since they are very black and do not permit light transmission and clear refraction. But solution of it in toluene can still provide information about the possible chemical changes taking place during reaction. It is usually assumed that a complex mixture of a solvent and bitumen or its fractions (maltene, asphaltenes) behaves as an ideal binary mixture of the components.[5] It was found that the refractive index of the maltene fraction (*n*-heptane soluble) decreased with an increase in reaction temperature (Table 4.9).

Table 4.9. Refractive index of the mixture of toluene and maltene fraction produced at temperature range of 100-150 °C. The measurement temperature was set as 20 °C and the refractive index of 100 mg maltene dissolved in 1 mL toluene was recorded.

Temperature (°C)	Refractive Index 1	2	3	Average	Standard Deviation
100	1.5632	1.5629	1.5631	1.5631	0.00015
110	1.5631	1.5603	1.5643	1.5626	0.00205
120	1.5613	1.5604	1.5614	1.5610	0.00055
130	1.5622	1.5628	1.5614	1.5621	0.00070
140	1.5606	1.5595	1.5603	1.5601	0.00057
150	1.5579	1.5586	1.5588	1.5584	0.00047

The RI data for a mixture of maltenes, n_m , and toluene, can be used to estimate refractive index of maltene by following equation:

$$\frac{n^2-1}{n^2+1}=\left[\frac{n_m^2-1}{n_b^2+2}-\frac{n_s^2-1}{n_s^2+1}\right]f_m+\frac{n_s^2-1}{n_s^2+1}$$

where f_m is the volume fraction of bitumen, n_s is refractive index of solvent and n is refractive index of toluene and maltene mixtures. Density of maltenes needs to be measured for this calculation.

4.4 Discussion

There are several possible explanations can be made for the observed changes in asphaltenes after heating between 100 and 150 °C. Direct thermolytic cleavage of the C-C bond is not very likely in this temperature range because of high bond dissociation energy. But due to high free radical concentration of the asphaltenes and presence of different mineral constituents, one can expect some bimolecular reactions such as free radical addition reactions to occur at those temperatures. Electron spin resonance studies of the various asphaltenes have confirmed at least two different kinds of the free radicals are present in the petroleum asphaltenes: vanadyl porphyrin and carbon free radicals.[6,7] Considering the increasing mobility of asphaltenes medium with rising temperature, those so-called reactions might be favored.

It can also be speculated that physical change in the asphaltenes such as “melting” of the solid phase allows the trapped materials to be extracted easily. Since the asphaltene feed for this study was from *n*-pentane based solvent deasphalting unit, there is a chance of presence of pentane in the feed. Evolution of C_5 constituents was also detected with gas GC. But this alternative cannot be completely true since soluble fraction (maltene) of the industrial asphaltenes has been meaningfully reduced as result of heating (Figure 4.5). This small reduction in the extracted amount of the heptane soluble compounds may not be merely enough to ignore the effect of the physical phenomena happening in asphaltenes due to mild heating.

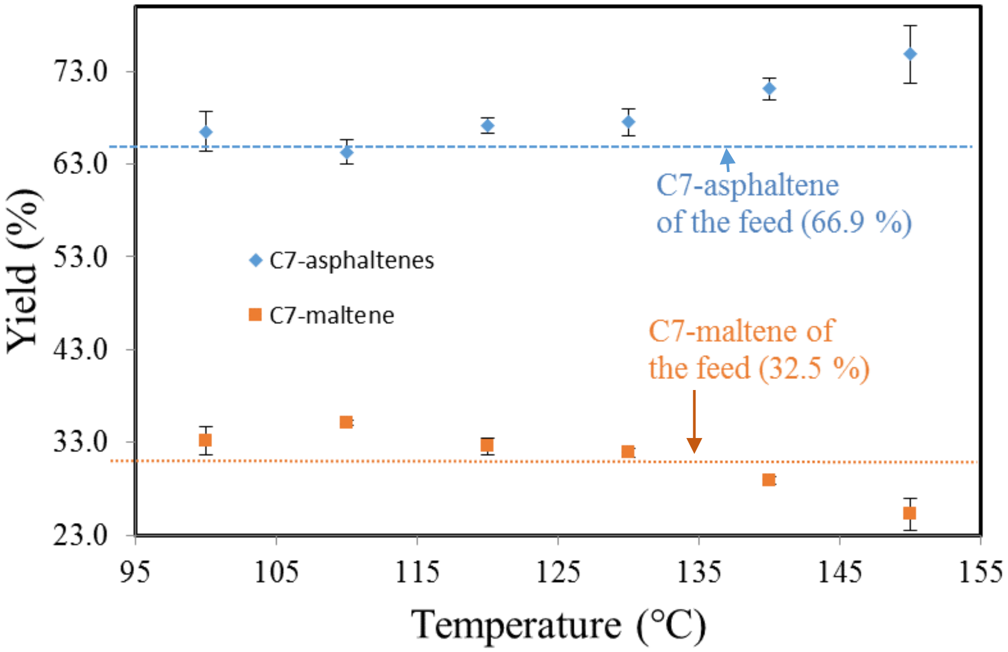

Figure 4.5. Solubility class distribution of products after conversion conducted with industrial asphaltenes feed at 100–150 °C for 1 h under 4 MPa N_2 pressure.

Based on the material balances, amount of the gases formed from each reaction is negligible, which means the overall H/C ratio has not changed significantly after the processing. TGA study of asphaltene did not exhibit any significant mass loss while heating at constant temperature of 150 °C for long period of time. No H_2S was detected by GC analysis, which indicates C-S bond is very unlikely to cleave at those temperatures. CO_2 was only observed when heating period was increased from 1 h to 5 h. One can suggest that CO_2 might have been identified because of the possible presence of air during measurements or oxidation reactions during heating. However, due to initial purging of the system with N_2, CO_2 is more likely to be released due to loss of carbonyl or carboxylic groups which are possibly present in asphaltenes.

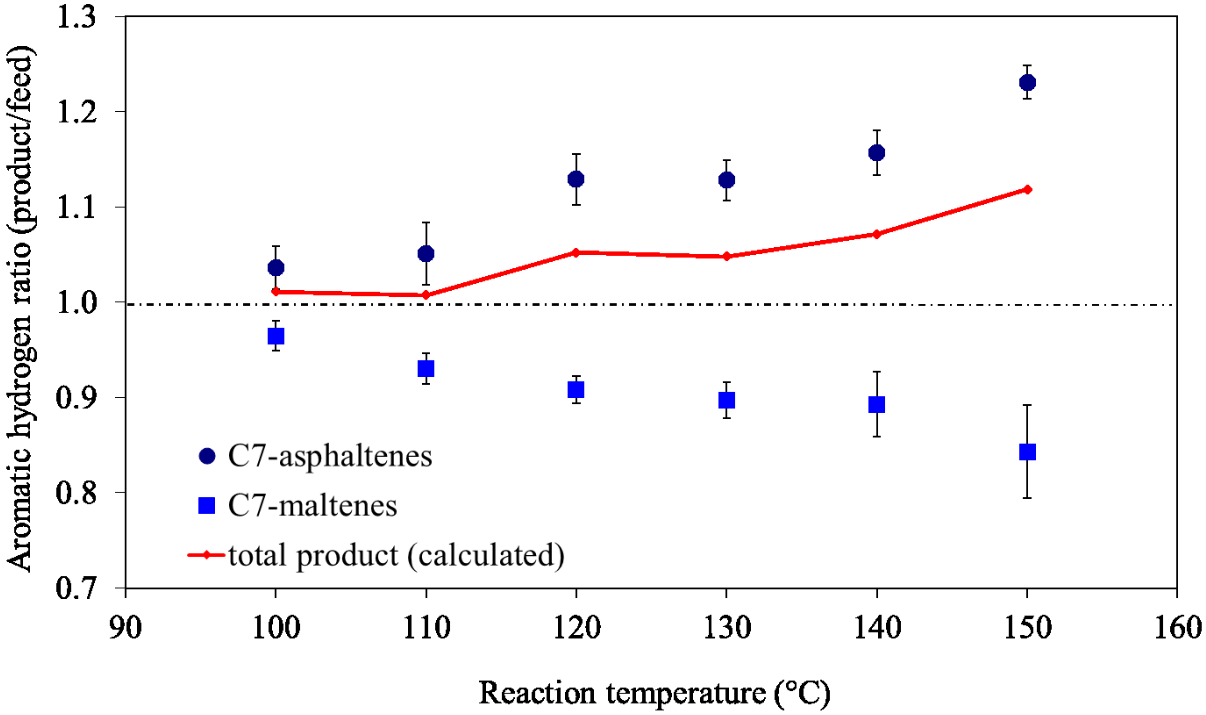

Figure 4.6. Aromatic hydrogen content relative to that of the feed of the *n*-heptane solubility class separated products after reaction at 100–150 °C for 1 h under 4 MPa N_2.

The ratio of aromatic hydrogen of the reaction products relative to that of the feed material was estimated based ^1H NMR results of the maltene fractions show that aromatic hydrogen content of each product has been reduced with increasing temperature (Figure 4.6). Meanwhile, increased aromatic hydrogen content of the asphaltenes fraction might indicate that asphaltenes has become more aromatic after heating the initial sample. These observations by the ^1H NMR can be attributed to the possible intermolecular or intramolecular hydrogen transfer which were likely to be restricted to take place at lower temperatures when the asphaltene was in solid state. To confirm and support this hydrogen transfer phenomena, one also should consider the decreased yield of the maltene fraction with increasing temperature (Figure 4.5). Based on the observations, some maltenes might have changed their solubility class after free radical type reactions which cause an increase in molecular weight. The solubility of the molecules can also be affected by the changes in the H/C ratio. This finding was also supported the solvent-resid phase diagram which provides insight on the transformation of one pseudo-component to another.[8] So *n*-heptane insoluble asphaltenes can be formed from maltenes by either molecular weight growth or by decreasing hydrogen content by aromatization of naphthenoaromatics or condensation reactions.

The aromatic hydrogen content of the total product was also calculated based on the material balance (Table 4.3) and ^{1}H NMR data (Table 4.6 and Table 4.7), and presented as a ratio of aromatic hydrogen content to that of feed (Figure 4.6). It appeared that there was an increase in the aromatic hydrogen content compared to that of the feed, reaching a ratio 1.12 at 150 °C. It implies that the hydrogen atoms are transferred to other aliphatic carbons, therefore there is a net increase in the aromatic hydrogen. If the hydrogen is transferred to other aromatic structures, there is no change in the aromatic to aliphatic ratios.

Average aromatic hydrogen content of asphaltene feed was also calculated based on analyzed values of its subfractions by performing a hydrogen material balance. Calculated value for average aromatic hydrogen (8.4 %) content was numerically different than that obtained from analysis (10.07 %) (Table 3.4 in Chapter 3). It can be speculated that possibly some residual *n*-heptane remained in the sub fractions of the feed after precipitation, which caused to a decrease in overall aromatic hydrogen percent.

Due to limited of ability of ^{1}H NMR to define the type of the carbon atom, ^{13}C NMR was also performed to determine any change in aromatic carbon of the fractions after mild heat treatment. Not necessarily all hydrogen disproportionation reaction converts aliphatic carbon to aromatic carbon. The following results can be inferred from the ^{13}C NMR spectrums of the fraction:

Carbon aromaticity of heptane insoluble asphaltene fraction has been increased at higher temperature which is in well agreement with the change in aromatic hydrogen content. A number of different mechanisms can also be suggested at this point such as dehydrogenation of the napthenic rings in aromatics, which are reportedly very good hydrogen donors and can easily undergo aromatization reaction.[9] Another alternative can be condensation of the aromatic rings by means of hydrogen loss, which does not affect aromatic carbon.[10]

The decrease in H/C ratio at the higher temperature range (> 400°C) reported in literature indicate an increase in aromaticity and provides good evidence for the cracking of alkyl chains which lowers aliphatic hydrogen content.[11] Changes in aromatic and aliphatic hydrogen content at lower temperatures cannot be interpreted in same way since decomposition has less or minimal effect based on the gas analysis. Our observations mainly support hydrogen loss mechanism from the napthenic ring, which fused into aromatics leading to an increase in aromatic compounds and to decrease in aliphatic hydrogen content. A variety of polycyclic aromatic hydrocarbons compounds which are more likely to present in asphaltenes are effective hydrogen transfer agents.[12] This proposed mechanism involves the transfer of weakly bound hydrogens atom which are readily available for the acceptor type compounds. Thermal hydrogen transfer reaction which is initiated by a bimolecular hydrogen atom transfer might give a rise to stable free radical concentration (see Chapter 5 for subsequent investigations to explore this). Considering naturally found hydrogen donor compounds of the asphaltenes, these free radicals can be self-stabilized by going under hydrogen disproportionation reactions. Some types of free radicals formed from naphteno-aromatics due to cleavage of C-H bond are unlikely to disproportionate, instead they will go under additional reactions to stabilize and subsequently form heavier compounds which might affect the solubility.

In addition to bimolecular hydrogen disproportionation reactions, ring closure via cyclodehydrogenation also may play a role in during this process. Formation of the phenanthrene from the 1,1–diphenylethane can be shown one of this example which gives a rise to aromatic carbon atom.[13] It can also be expected that high free radical concentrations in asphaltenes assist aromatization reaction (free-radical aromatic substitution reactions) which has been considered to take place in coal system at low temperature (Figure 4.7).[14] Overall, mechanisms of the hydrogen transfer are very ambiguous but all possible interactions has to be considered in order to understand the most likely reaction pathway.

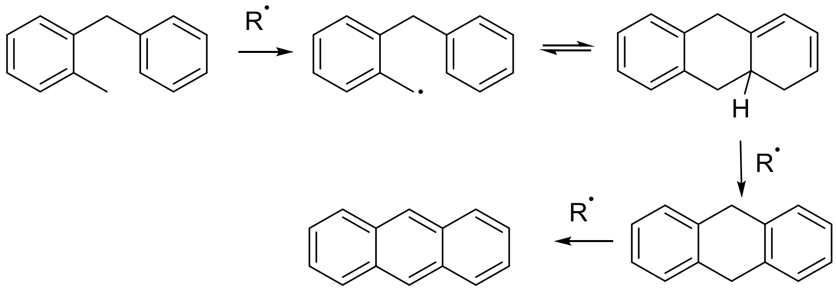

Figure 4.7. Free radical induced aromatization.

4.5 Conclusions

Based on the experimental results, following consideration can be made regarding the low temperature conversion of asphaltenes:

i. Yield of the industrial asphaltenes (*n*-heptane soluble and insoluble fractions) changed on heating to 100 to 150 °C for 1 h.

ii. After heating asphaltenes to 100 to 150 °C for 1 h, there were measurable changes in the nature of fractions, such as ratio of aliphatic and aromatic hydrogen and refractive index.

iii. The most important contribution of this work was to highlight the role of hydrogen disproportionation reactions between asphaltenes donor and acceptor molecules at 150 °C and even lower temperatures. This caused increased aromaticity and it is speculated that it also possibly cause a molecular weight growth due to free-radical additions.

References

1. Styles, Y.; de Klerk, A. Sodium Conversion of Oilsands Bitumen-Derived Asphaltenes. *Energy Fuels* **2016***, 30 (7)*, 5214-5222.

2. Jha, K.; Montgomery, D.; Strausz, O.; Strausz, O.; Lown, E. Chemical composition of gases in Alberta bitumens and in low-temperature thermolysis of oil sand asphaltenes and maltenes. In *Oil sand and oil shale chemistry*Verlag Chemie New York: 1978; pp 33-54.

3. Standard, A. D6560-12. *Test Method for Determination of Asphaltenes (Heptane Insolubles) in Crude Petroleum and Petroleum Products, ASTM International, West Conshohocken, PA* **2012**.

4. Strausz, O. P.; Lown, E. M. *The chemistry of Alberta oil sands, bitumens and heavy oils;* Alberta Energy Research Institute Calgary, Alberta, Canada: 2003.

5. Taylor, S. D.; Czarnecki, J.; Masliyah, J. Refractive index measurements of diluted bitumen solutions. *Fuel* **2001***, 80*, 2013-2018.

6. Morgenthaler, J.; Rüchardt, C. New hydrogen transfer catalysts. *European journal of organic chemistry* **1999***, 1999*, 2219-2230.

7. Saraceno, A.; Fanale, D.; Coggeshall, N. An electron paramagnetic resonance investigation of vanadium in petroleum oils. *Anal. Chem.* **1961***, 33*, 500-505.

8. Wiehe, I. A. A solvent-resid phase diagram for tracking resid conversion. *Ind Eng Chem Res* **1992***, 31*, 530-536.

9. Guo, A.; Zhang, X.; Zhang, H.; Wang, Z.; Wang, Z. Aromatization of naphthenic ring structures and relationships between feed composition and coke formation during heavy oil carbonization. *Energy Fuels* **2009***, 24*, 525-532.

10. Fetzer, J. The role of the Scholl condensation in the chemistry of catalytic hydrocrackers. *Polycyclic Aromatic Compounds* **1994***, 4*, 19-24.

11. Lababidi, H. M.; Sabti, H. M.; AlHumaidan, F. S. Changes in asphaltenes during thermal cracking of residual oils. *Fuel* **2014***, 117*, 59-67.

12. Yen, T. F.; Erdman, J. G.; Saraceno, A. Investigation of the Nature of Free Radicals in Petroleum Asphaltenes and Related Substances by Electron Spin Resonance. *Anal. Chem.* **1962***, 34*, 694-700.

13. Alshareef, A. H.; Scherer, A.; Tan, X.; Azyat, K.; Stryker, J. M.; Tykwinski, R. R.; Gray, M. R. Effect of chemical structure on the cracking and coking of archipelago model compounds representative of asphaltenes. *Energy Fuels* **2012***, 26*, 1828-1843.

14. S Stein, S. E. A fundamental chemical kinetics approach to coal conversion. In *New approaches in Coal Chemistry,* ACS Symposium Series, 169; Blaustein, B.D; Bockrath, B.C; Friedman, S., Eds.; American Chemical Society; Washington, DC, 1981; pp 97-129.

5. REACTIVITY OF ASPHALTENES AT LOWER TEMPERATURES

In this work, thermal reaction of industrial asphaltenes from the Long Lake Upgrading Unit of Nexen was investigated over the temperature range of 150-250 °C, which is representative conditions of *in situ* oil production. A more reactive hydrogen acceptor, α-methylstyrene, which has been used for mechanistic studies of bimolecular hydrogen transfer reactions, was successfully hydrogenated by asphaltenes at 180 °C, indicating that asphaltenes contain structurally reactive compounds that promote hydrogen transfer at low temperature. Hydrogen disproportionation reactions support the possibility of formation of intermediates that are prone to addition reactions. Addition reactions lead to the formation of higher molecular weight compounds at relatively low temperature, which can be detrimental in processes where similar conditions are applied. Electron spin resonance (ESR) studies of asphaltenes also supported the coupling of carbon-centered free radicals and hydrogen disproportionation reactions at 250 °C, which resulted in a decrease in the concentration of free radicals.

Key words: hydrogen transfer, dimerization, free radical

5.1 Introduction

This investigation is mainly concerned with thermal hydrogen transfer (uncatalyzed hydrogen transfer). Those reactions can be understood as bimolecular reactions involving free radical intermediates. Hydrogen (H•) transfer has been thoroughly investigated in coal chemistry, and different routes have been proposed.[1]

Simple hydrogen atom transfer from a donor molecule to an acceptor molecule proceeds by a two-step mechanism as a molecular disproportionation (reverse radical disproportionation), leading to the formations of two free radicals (Figure 5.1).[2] It was suggested that gas phase hydrogenation of ethylene with cyclopentene proceeded through a bimolecular radical mechanism at 400-500°C.[3] Molecular hydrogen disproportionation reactions between aromatic and hydroaromatic also have particular importance for coal liquefaction (and by extension heavy oil upgrading) in terms of free radical generation which facilitate cracking reactions.[2] A rate-determining molecular disproportionation was proposed for the reaction of 1,2-dihydronaphthalene to form tetralin and naphthalene at 300 °C that involves breaking the C-H bond on the 2-position to form 1-tetralyl radical and 1,4-dihydro-l-naphthyl radical, followed by disproportionation.[4] Kinetic studies of hydrogen migration between 9,l0-dihydroanthracene to 2-ethylanthracene (250-375 °C) showed that the reaction follows simple bimolecular hydrogen atom transfer as an initiation step, resulting in the formation of two stabilized free radicals.[5]

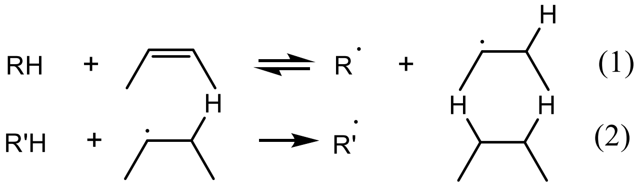

Figure 5.1 Molecular disproportionation mechanism for hydrogen atom transfer.[2]

Another competitive route of H atom transfer, which is often referred to in coal chemistry,[6] is radical induced hydrogen transfer. It is questionable whether H transfer is achieved in a single step similar to a simple hydrogen metathesis, which involves transition state (Figure 5.2) or in a multistep process.[7] This chemistry is explored in the chapter and therefore some additional background is given before presenting the experimental work that was performed.

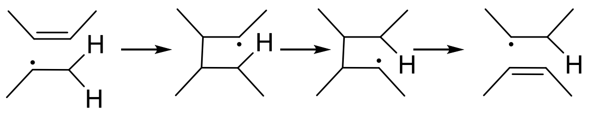

Figure 5.2. A simple hydrogen metathesis.

5.1.1 Structure reactivity of hydrogen donors

It has been postulated that H-donor compounds, which has more weakly bound H-atoms compared to typical C-H bonds, transfer hydrogen to an acceptor. The acceptor is a species that contains an unsaturated bond, such as C=C, C=O, C=N, N=O or N=N, or is a free radical. The uncatalyzed hydrogenation of α-methylstyrene with 9, 10-dihydroanthracene (9- or 10-position ΔH_{diss}(C-H) = 347.50 kJ/mol), which involves a molecular disproportionation followed by two radical reaction steps, were reported to produce cumene selectively, with a 98 % cumene yield at 280-320 °C (Figure 5.4).[8]

The reactivity of a series of H donor compounds with weaker C-H bond enthalpies was studied to determine if their structure influenced the disproportionation reactions with of α-methylstyrene.[9] The transfer of hydrogen from 9, 10-dihydroanthracene to α-methylstyrene occurred in the range of 220-260 °C instead of 280-320 °C after addition of compounds to the reaction medium that have C-H bonds with lower bond dissociation energy (ΔH_{diss}(C-H)) than typical C-H bonds. Examples of such compounds are: phenalene (ΔH_{diss}(C-H) = 295 kJ/mol), 6H-benzopyrene (ΔH_{diss}(C-H) = 323 kJ/mol), 7H-dibenzoanthracene (ΔH_{diss}(C-H) = 313 kJ/mol) or 4-methyl-7H-benzonapthacene (ΔH_{diss}(C-H) = 326 kJ/mol) (Figure 5.3).

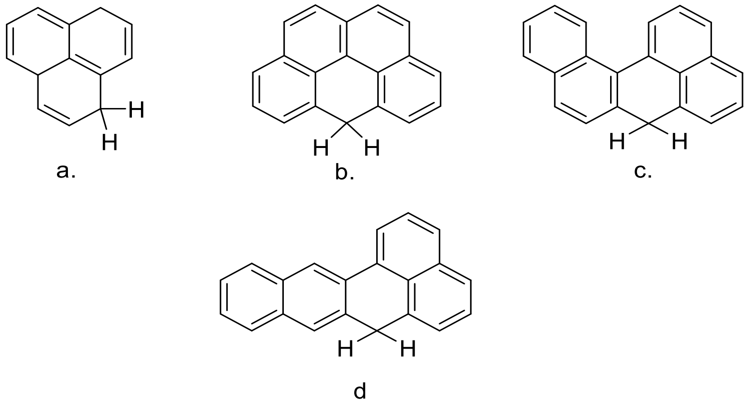

Figure 5.3. Polycyclic hydrocarbons with weaker C-H bonds: (a) phenalene; (b) 6H-benzopyrene ; (c) 7H-dibenzoanthracene; (d) 4-methyl-7H-benzonapthacene.

The key mechanism here is the molecular disproportionation step which involves initiation by the transfer of weakly bound H to the acceptor (Figure 5.4).[10] The kinetic and electron spin resonance spectroscopy studies strongly supported molecular disproportionation of two phenalene molecules, which formed phenalenyl and dihydrophenalenyl radicals which confirmed the radical mechanism during the hydrogen transfer reaction. The presence of a styrene-like double bond in those compounds enables them to function both as an H acceptor and H donor. Unlike phenalene, the other compounds listed above do not possess any styrene like double bond and that is why they remain constant during reaction due to their continuous regeneration.

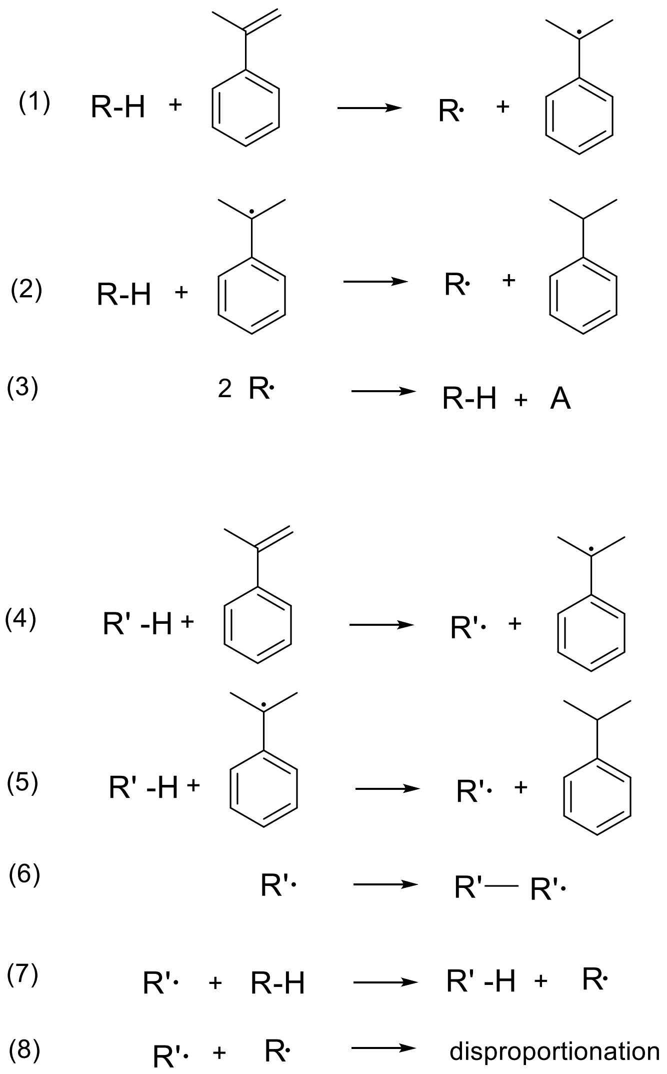

Figure 5.4 Hydrogen transfer from donor compounds (R-H: 9,10-dihydroanthracene, R'-H: hydroaromatics with weaker C-H bond enthalpy) to α-methylstyrene. Reactions given in lines 4-8 are additional steps are involved after addition of R'-H.

5.1.2 Hydrogen transfer from asphaltenes

The hydrogen donating ability and the hydrogen accepting ability of the different petroleum residues has long been recognized.[11] It has been reported that addition of good hydrogen donor compounds such as tetralin effectively suppresses coke, which was cut in half and also delayed the onset of coke formation, which is known as coke induction time.[12] More recently, it was reported that asphaltenes contains a high concentration of natural hydrogen donors.[13] This study also revealed that hydrogen donors of asphaltenes are significantly more reactive than saturates. Typically, naphthenic rings in aromatics (hydroaromatics) are known as the main hydrogen donor compounds, which undergo aromatization reactions rather than ring opening under cracking conditions.

Hydrogen transfer capabilities of petroleum residues have not been investigated extensively at low temperature. Moreover, there is only little information present in the literature regarding reactivity of the hydrogen donor compounds in asphaltenes. Most of the kinetic studies and hydrogen transfer reactions have been performed at higher temperatures at approximately 360-450 °C, which is under cracking conditions of the material.[14] The results obtained from Chapter 4 demonstrated some structural alteration at lower temperatures, which is far below the cracking temperature. It was proposed that yield changes in asphaltenes conversion at lower temperature (100-150 °C) is mainly caused by the hydrogen disproportionation and addition reactions.

Thermal instability of asphaltenes might have relevance to some existing processes. In situ oil production requires saturated steam temperatures ranging from 200 to 300 °C, which is not sufficiently high for appreciable amount of random thermal scission.[15] Therefore, the main focus of this study is to investigate asphaltenes at low temperature ranges to analyze hydrogen donor properties by using model compounds as hydrogen acceptors.

5.2 Experimental

5.2.1 Materials

A list of the chemicals used in this study is given in Table 5.11,9- dihydroanthracene and indene were used as hydrogen donor, α-methylstyrene and anthracene were used as hydrogen acceptor. Diphenyl ether was also used as a solvent for the reaction which facilitates hydrogen transfer.

Table 5.1 . List of the compounds used in this study.

Name	CAS[a]	Formula	Purity (%)[b]	Supplier
Chemicals				
Cumene	120-12-7	C_9H_{12}	98	Across Organics
α-Methylstyrene	98-83-9	C_9H_{10}	99	Sigma-Aldrich
Indene	95.13.6	C_9H_8	98	Sigma-Aldrich
Anthracene	120-12-7	$C_{14}H_{10}$	99	Across Organics
Biphenyl	92-52-4	$C_{12}H_{10}$	99.5	Sigma-Aldrich
9,10-dihydroanthracene	613-31-0	$C_{14}H_{12}$	97	Sigma-Aldrich
n-heptane	142-82-5	C_7H_{16}	99	Sigma-Aldrich
Diphenyl ether	101-84-8	$C_{12}H_{10}O$	99	Sigma-Aldrich
Methanol	67-56-1	CH_3OH	99.99	Sigma-Aldrich
Chloroform	67-66-3	$CHCl_3$	99	Sigma-Aldrich
d-chloroform	865-49-6	$CDCl_3$	0.9996 atom D	Sigma-Aldrich
Cylinder gases				
nitrogen	7727-37-9	N_2	0.99999[c]	Praxair
helium	7440-59-7	H_2	0.99999[c]	Praxair

[a] CASRN = Chemical Abstracts Services Registry Number.

[b] This is the purity of the material guaranteed by the supplier; material was not further purified.

[c] Mole fraction purity.

Industrially produced asphaltenes was used to investigate hydrogen transfer reactions at low temperatures without further solvent precipitation. The asphaltenes feed was obtained from the *n*-pentane based solvent deasphalting unit the Long Lake Upgrader of Nexen Energy ULC and detailed information for feed characterization is already presented in Chapter 3.

5.2.2 Procedure

The experiments with model compounds for this study were conducted in microbatch reactors. The microbatch reactors were constructed from Swagelok 316 stainless-steel 0.5 in. tubing. The inner and outer diameters of reactors were 2.7 and 3.3 cm respectively with a length equal at 8.7 cm. Reactors were heated inside silicon oil filled beakers on Fischer Scientific Isotemp hot plate. The beakers were wrapped with aluminum foil for thermal isolation. The temperature inside the heating medium and reactor was monitored using a thermocouple. To enable agitation inside the reactor, small magnetic stirrer was placed into the vial and the liquid was stirred at 250 rpm.

For each experiment, a mixture of asphaltenes and model compounds were loaded into glass vials and placed into microbatch reactor. Solid reactants were weighed by using the high precision Mettler Toledo XS 105, which had a 120 g max capacity and 0.1 mg readability. An Accumax micropipette (100-1000 μL) was used to transfer the liquid reactants (α-methylstyrene, indene, diphenyl ether) into reaction vials. The quantity of the liquid reagents was added volume-based to achieve the desired mass ratio of reagents and reagents with asphaltenes. Densities of the liquid reactants were confirmed and used to calculate required volume required for each reaction. Approximately equal weight ratio of diphenyl ether (1 mL) was added to improve mass transfer between reactants. The loaded reactors were purged and leak-tested with nitrogen at an absolute pressure of around 4 MPa. A schematic of the microbatch reactor is given in Figure 5.5. A temperature controller was installed in the system to control the oil temperature to keep the internal temperature of the reactor at set point.

Experiments were performed at various temperatures ranging from 150 to 250 °C for different period of time as presented in Table 5.2.

The run length of time was measured from the time when internal temperature of the reactor reached the set point. The heat-up time was measured as 15-16 minutes and excluded for the reaction time. After the reactions, reactors were cooled down by a continuous air flush over a period of 10 minutes. The temperature-time profiles for both heating and cooling period are presented in Figure C.3 and Figure C.4 can be found in Appendix C.1.

The same procedure was employed when only model compounds were loaded into the microbatch reactor. Products were washed off from the reactor with methanol thoroughly to recover and dissolved in known amount of solvent. The efficiency of recovery process was also tested (Appendix C.3). Mixture of products and asphaltenes were filtered and analyzed by GC MS.

For the set of experiments of indene which presented in Table 5.2 in row number 8, chloroform was used as solvent. Products was dissolved in chloroform and analyzed in GC MS.

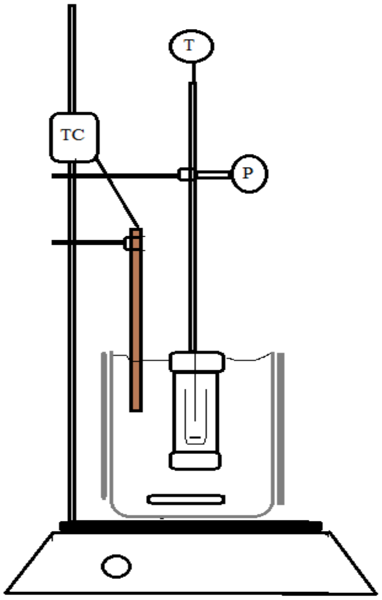

Figure 5.5. Schematic of the reaction system

Table 5.2. Process conditions for the reaction of asphaltene and model compounds.

Number	Reactants [a,b]	Weight Ratio of reactants	T (°C)	Time (min)
1[c]	Asphaltene : α-methylstyrene	1:1	150-250	60
2[c]	Asphaltene : cumene	1:1	250	60-120
3[c]	α-methylstyrene		250	120
4[c]	Asphaltene : α-methylstyrene	1:1	250	20-120
5[c]	Asphaltene : α-methylstyrene	1:1	250	240
	Asphaltene : 9, 10-dihydroanthracene : α-methylstyrene	0.5 : 0.5 : 1	250	60
	Asphaltene : α-methylstyrene	3:1	250	60
	1,9-dihdroanthracene : α-methylstyrene	1:1	250	60
6[d]	Asphaltene : α-methylstyrene	2:1 4:1 8:1	250	30-120
7	Asphaltene : anthracene	1:1	250	60
	Asphaltene : 9,10-dihydroanthracene	1:1	250	60
8	Indene : α-methylstyrene	1:1	250	60-120
	Indene : 9.10-dihydroanthracene : α-methylstyrene	0.5 : 0.5 : 1	250	60
	Indene		250	60

[a] Results from each set of reactions were presented in a separate results section.

[b] diphenylether was used as reaction solvent to facilitate hydrogen transfer.

[c] Initial mass of α-methylstyrene was 570 mg .

[d] Initial mass of α-methylstyrene was 150 mg.

5.2.3 Analyses

5.2.3.1 Gas chromatography

Gas chromatography coupled with mass spectrometry (GC-MS) was performed using an Agilent 7820 coupled with Agilent 5977E mass spectrometer. Separation was performed on an HP-5 column (30 m x 0.25 mm x 0.25 µm) using helium as a carrier gas at constant flow of 2 mL/min. The temperature program started at 90 °C and temperature was increased by 10 °C/min up to 320 °C.

GC-MS analysis was used to identify final products, which had been recovered by methanol extraction. Identification of individual products was accomplished by simultaneous evaluation of electron ionization mass spectra of products with the corresponding spectra from The National Institute of Standard and Technology (NIST). Despite of the presence of complex addition products in the chromatogram, all possible formulas were suggested to make a conclusion about the nature of reactions.

5.2.3.2 Quantification of cumene and α-methylstyrene

Quantification of the components was performed by using the biphenyl as internal standard throughout all analysis and the detailed procedure is presented in Appendix B. Biphenyl was selected based on following two criteria: Firstly, biphenyl is soluble in methanol which is used for selective recovery of cumene and α-methylstyrene. Secondly, its retention time does not interfere with cumene and α-methylstyrene. The calibration curves consist of three levels with concentrations up to 5 mg/mL for α-methylstyrene (0.5, 2 and 5mg/mL) and 0.2 mg/mL for a cumene (0.05, 0.1 and 0.2 mg/mL) with a constant concentration of biphenyl (0.1 mg/mL). All samples were injected in triplicate and each point on the curve corresponds to average value. Both calibration showed regression line coefficients R^2>0.96.

After each reaction products were washed off from the reactors and dissolved in known amount of methanol and stirred constantly for half an hour. Mixture was filtered and transferred into 10 ml volumetric beakers by using a syringe. 10 mg of biphenyl was added to each solution. Samples were analyzed by GC MS. Quantification was achieved by using the ratio of integrated peak area of each component to that of internal standard. The concentration of the cumene and α-methylstyrene were evaluated mathematically by using the linear equation, which indicates relation between the variable and peak area, given in the Figures B.3 and Figure B.4.

To ensure the complete extraction of products, control experiments were performed which involve known amount of concentration of cumene and α-methylstyrene. Experimentally determined concentration of cumene and α-methylstyrene were compared against initial values. Accuracy was also reported quantitatively by using percent error, indicating 3-5 % error over the concentration range 0.4 – 5.0 mg/mL, but higher error value was determined at lower concentration of cumene (Table C.8 and Table C.9).

The quantification of other compounds which employed in this study and the reaction products need be considered as semi-quantitative at best.

5.2.3.3 Thermal gravimetric analysis coupled with a Fourier-transform infra-red

Gaseous and volatile products of thermal decomposition were detected by ABB MB3000 FTIR spectrometer which equipped with thermal connector for gases released from the TGA and combined with Horizon MB^{TM} FTIR software. Details of the equipment and analysis procedure can be found in Chapter 3 and Chapter 4 for FTIR and TGA respectively.

The FTIR measurements were performed at a resolution of 8 cm^{-1} and an average of 20 scans over the spectral region of 4000-500 cm^{-1} to be able to record the spectra each two minutes.

In TGA, samples were heated from 25 °C at 10 °C·min^{-1} to reach reaction temperatures: 250 and 360 °C followed by an isothermal period of 2 h for each case.

5.2.3.4 Electron spin resonance

Electron spin resonance spectroscopy (ESR) analysis were performed using a Bruker Elexys E-500 spectrometer (Billerica, MA) with the following instrument parameters: frequency, 9.85 GHz; center field ranging from 3366.6 to 3666.31 G (336.66 to 366.63 mT); microwave power, 50 mW; modulation amplitude, 0.0001 T; modulation frequency, 100 kHz and receiver gain, 60 to observe any change in free radical concentration. 100 mg industrial asphaltenes in the glass vial (7mL) was placed into microbatch reactor and immersed into fluidized sand bath, Omega fluidized bath FSB-3, to heat at 250 °C for an hour period to prepare blank samples. Equal weight of 9, 10-dihydroanthracene (100 mg) was mixed with asphaltenes to run at same experimental conditions. After the reactions, asphaltenes samples (~100 mg) were dissolved and vortexed in toluene, transferred to NMR/EPR tube (4 mm OD, 3.2 mm ID) and measured. The ESR absorption lines were given in their corresponding first derivative form and line-width was corrected. The amount of free radicals of samples was compared by their derivative signal intensity, which is proportional to the concentration of free radicals (number of spins per gram of sample).[16]

5.2.4 Calculations

The conversion of α-methylstyrene calculated on a mass basis as shown in Equation 1.

$$conversion\ (\%) = \frac{m_i - m_f}{m_i}\ x\ 100 \quad (1)$$

where m_i is initial mass of of α-methylstyrene and m is final mass of of α-methylstyrene measured after the reaction.

Mass of byproducts were calculated semi-quantitatively relative to the mass of internal standard based on the GC MS integrated area (%) of products. Details were given in Appendix C.

Mass of unrecovered products was estimated based on total mass balance by not taking into account amount of hydrogen transferred from asphaltenes.

Selectivity was calculated by following equation (Equation 2):

$$Selectivity\ (\%) = \frac{m_i}{m_{\alpha-\text{methylstyrene consumed}}} \quad (2)$$

i – cumene, byproducts recovered, unrecovered products.

g-value for the ESR signal was calculated by the following equation (Equation 3):

$$g = \frac{71.4484 * v}{B} \qquad (3)$$

where v is microwave frequency (GHz) and B is the magnetic field (mT)

5.3 Results

5.3.1 α-Methylstyrene as hydrogen transfer probe

5.3.1.1 Identification of products from the reaction of α-methylstyrene with asphaltenes and α-methylstyrene with 1,9-dihydroantracene .

Hydrogen transfer from asphaltene to model compounds was investigated by using α-methylstyrene as hydrogen acceptor. α-Methylstyrene contains a C=C bond, which yield cumene after hydrogenation. It was preferred over the other common hydrogen acceptors as probe, such as anthracene and napthacene, because cumene formed during the reaction can be selectively removed from the asphaltenes medium for quantitative work. A series of experiments were conducted with different ratio of reactants at different conditions given in Table 5.2.

The overall chromatogram of the solvent extracted products after reaction at 250 °C is given in Figure 5.6. In addition to the hydrogenation product, a number of byproducts were determined in the reaction medium and were presented in Table 5.3. Electron impact mass spectrometry was used to determine the identities of by-products formed due to side reactions. Mass spectra of the individual compounds are given in the Appendix B. The quantity of by-products increased with reaction temperature, and also more addition products were formed when reactions were carried out for longer periods of time. The most abundant byproducts were the saturated dimer of α-methylstyrene which has a molecular formula $C_{18}H_{22}$ and unsaturated dimers of α-methylstyrene with a molecular formula $C_{18}H_{20}$.

The chromatogram of the products from the reaction of α-methylstyrene and 1,9-dihydroantracene at 250 °C is given in Figure C.7. A very small amount of the by-products of cumyl radicals was formed. However, there is also one major addition product that was identified and the corresponding mass spectrum was provided in Figure C.8. This product was suppressed very significantly after addition of asphaltenes to the reaction of α-methylstyrene and 1,9-dihydroantracene based on the relative area (Table C.16). Also, similar to the reaction of α-methylstyrene with asphaltenes, some dimerization products of cumyl radicals were identified (Table C.15).

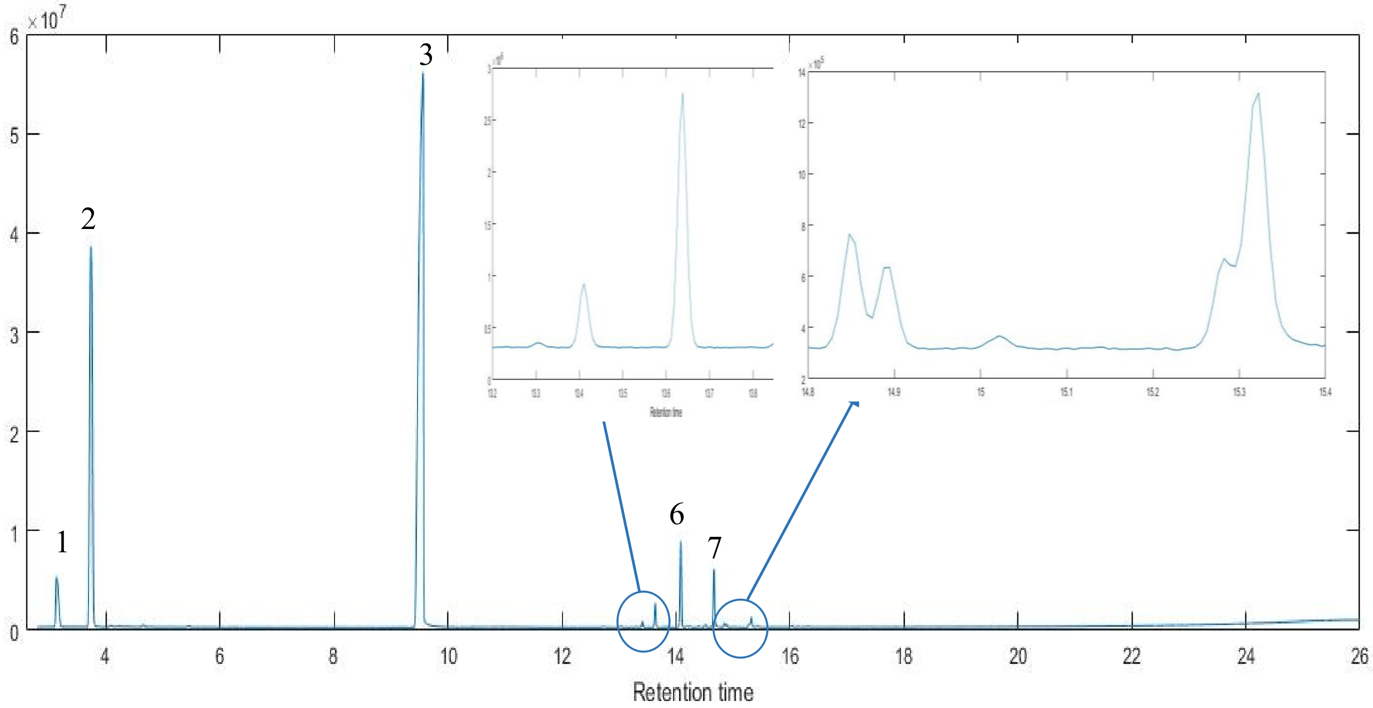

Figure 5.6. GC MS chromatogram of the reaction products of α-methylstyrene and asphaltene at 250 °C for 2 h period (details are given in Table 5.3).

Table 5.3. The list of the products was identified by GC-MS from the reaction of α-methylstyrene with asphaltene.

Number	Name	Retention time (min)	Formula	Structure
1[a]	Cumene	3.14	C_9H_{12}	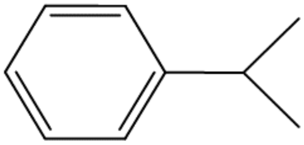
2[a]	α-methylstyrene	3.75	C_9H_{10}	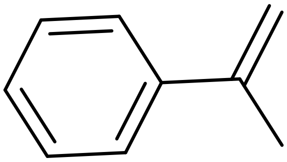
3[d]	Diphenylether	9.51	$C_{12}H_{10}O$	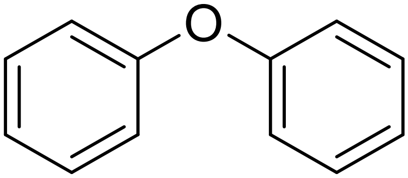
4	Not Identified	13.41		
5[b]	Benzene, 1,1'-(1,1,2,2-tetramethyl-1,2-ethanediyl)bis-	13.67	$C_{18}H_{22}$	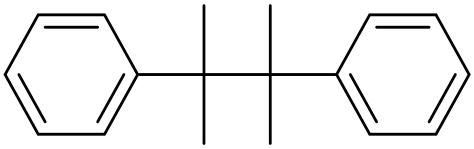
6[b]	2,4-Diphenyl-4-methyl-1-pentene	14.09	$C_{18}H_{20}$	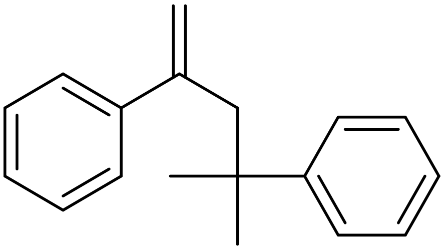

7[b]	Hex-1-ene,2,5-diphenyl-	14.67	$C_{18}H_{20}$	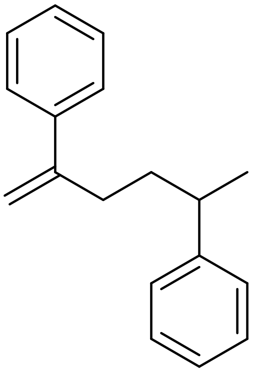
8[b,c]	1-phenyl-1,3,3-trimethylindane	14.85	$C_{18}H_{20}$	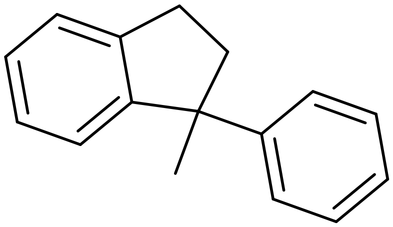
9[b,c]	2,4-Diphenyl-4-methyl-2(E)-pentene	14.89	$C_{18}H_{20}$	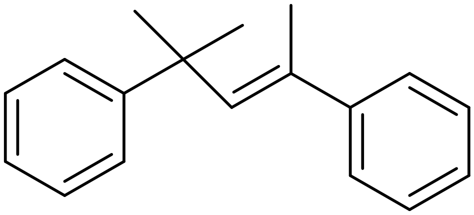
10[b,c]	2.5-Diphenyl-2,4-hexadiene	15.32	$C_{18}H_{18}$	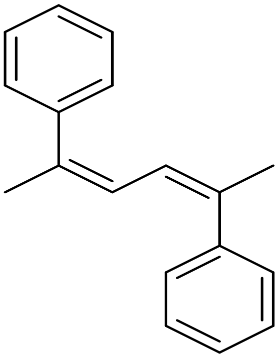

[a] Confirmed with standard compound.

[b] Confirmed based only on NIST library.

[c] Products were formed slightly when reaction was performed over 1 h.

[d] Reaction solvent.

5.3.1.2 The reaction of cumene and asphaltenes at 250°C

The irreversibility of the reaction was demonstrated by a control experiment which involved equal amount of cumene with asphaltenes to observe any α-methylstyrene. No α-methylstyrene was detected in the reaction products from the reaction of asphaltenes and cumene at 250 °C even after 2 h heating experiment. Another important finding from this reaction was the complete absence of any solvent extractable product which might have resulted from free radical reactions.

The absence of α-methylstyrene is not merely enough to exclude the likelihood of interaction of cumene with the asphaltenes. It can be speculated that cumene might formed α-methylstyrene as an intermediate product, which then reacted to asphaltenes to produce either cumene or some addition product with an asphaltene molecule that was too heavy to be extracted.

5.3.1.3 Heating of α-methylstyrene

No polymerization products were detected when α-methylstyrene was heated blank at 250 °C over 2 h period, making it a suitable probe for hydrogen transfer reactions in the temperature ranges of 150-250 °C. It has been reported that α -substituted styrenes are not polymerizable alone by means of heat.[17] In the presence of initiator, polymerization of α-methylstyrene does not occur above certain temperature known as the ceiling temperature (61 °C) where the rate of depolymerization exceeds that of propagation. [18]

5.3.1.4 The reaction of α-methylstyrene and asphaltenes between 150-250 °C.

The temperature range studied was from 150 to 250 °C, since it was speculated that hydrogen transfer might take place within this temperature range. Equal weight of asphaltene and α-methylstyrene was reacted in diphenyl ether with a residence time 1 h. The purpose of these experiments was to prove the possibility of hydrogen transfer from asphaltenes to an unsaturated system at lower temperature (<250 °C).

The conversion of α-methylstyrene and selectivity of cumene at each reaction temperature was shown in Table 5.4. The reaction did not yield any cumene as product at 150 °C and 1 h reaction time. However, the concentration of cumene increased with temperature from 180 °C, almost showed a monotonic increase. The conversion of α-methylstyrene increased with temperature, while the selectivity to cumene decreased substantially from the reaction temperature of 220 to 250 °C.

Table 5.4. Concentration of the cumene formed from the reaction α-methylstyrene with asphaltenes (1:1 wt/wt) as a function of temperature over 1 h period.

T [°C]	Cumene [mg/mL]	St.Dev.	Selectivity of Cumene [%]	α-methylstyrene [mg/mL]	St.Dev	Conversion of α-methylstyrene [%]
150[a]	0	0	0	5.69	0.01	x
180[a]	0.02	0.01	81.36	5.68	0.01	0.35
200[a]	0.08	0.01	86.29	5.62	0.	1.41
220	0.18	0.02	81.17	5.48	0.01	3.91
250	0.28	0.01	30.12	4.78	0.03	16.79

[a] Not any byproduct was identified in extracted products.
x – no product was identified.

The products were divided as following: cumene, recovered and unrecovered byproducts. Recovered product was calculated semi-quantitatively with respect to the internal standard. Then the mass of unrecovered product was only able to be determined indirectly by material balance closure. The selectivity of recovered and unrecovered products was calculated from material balance data for the experiments, and reported in Table C.11. No byproducts were identified in recovered products between 150 and 200 °C. But byproducts in methanol extract were found after reaction at 220 and 250 °C.

5.3.1.5 The reaction of α-methylstyrene and asphaltenes at 250 °C.

Time is another important factor to investigate especially in petroleum reactions. As it has been suggested that asphaltenes deplete their transferable hydrogen content very rapidly at higher temperatures and become hydrogen deficient and undergo coke formation. It is therefore increasingly important to take time into consideration while investigating hydrogen transfer reactions in asphaltenes.

Table 5.5. Concentration of the cumene formed from the reaction α-methylstyrene with asphaltenes (1:1 wt/wt) as a function of time.

Time [min]	Average Concentration [mg/mL]	St. Dev	Selectivity to cumene [%]
0	0	0	0
20	0.12	0.03	35.96
40	0.22	0.02	33.94
60[a]	0.28	0.01	30.12
80	0.37	0.02	37.45
100	0.40	0.01	39.16
120	0.46	0.02	44.25
240	0.65	0.04	34.59

[a] Repeated from Table 5.4

The reaction temperature that was chosen was 250 °C and the residence time was changed from 20 to 120 minutes to obtain an indication of reaction rate. The concentration of the hydrogenation product and α-methylstyrene are given in Table 5.5 and Table 5.7 respectively in different time ranges. As the concentration of α-methylstyrene decreases, the amount of the cumene increases with time over 2 h. The α-methylstyrene conversion is also reported in Table 5.7 which showed an increase with time.

Material balance was performed for the experiments to calculate mass of unrecovered products which presented in Table 5.6. Based on the data, selectivity into cumene, recovered products and unrecovered products were estimated. The selectivity of cumene was in the range 30- 45 %, and there was no relationship between selectivity to cumene and length of reaction period.

Table 5.6. Material balance for the experiments of the 1:1 asphaltenes to α-methylstyrene between 20 and 240 min at 250 °C.

	Mass [mg]				Selectivity [%]		
Time [min]	α-methylstyrene converted	Cumene	Recovered byproducts	Unrecovered byproducts	Cumene	Recovered byproducts	Unrecovered byroducts
20	31.99	11.51	17.21	3.27	35.96	53.80	10.22
40	64.74	21.98	35.65	7.11	33.94	55.07	10.99
60	93.05	28.02	57.37	7.65	30.12	61.66	8.22
80	94.28	35.30	49.23	9.74	37.45	52.22	10.33
100	100.97	39.54	51.24	10.19	39.16	50.75	10.09
120	103.71	45.89	43.90	13.91	44.25	42.33	13.42
240	188.61	65.24	99.41	23.96	34.59	52.71	12.70

[a] For measured concentration of cumene and methylstyrene, see Table 5.5 and Table 5.7.

Conversion of α-methylstyrene increased with reaction period (Table 5.7). No systematic relationship was observed between the cumene selectivity and α-methylstyrene conversion. Overall, the rate of conversion was high over the first one hour period, but then remained low within next one hour period.

Table 5.7 Concentration of the α-methylstyrene formed from the reaction α-methylstyrene with asphaltenes (1:1 wt/wt) as a function of time.

Time [min]	Average Concentration [mg/mL]	St. Dev	Conversion [%]
0	5.71		0
20	5.39	0.05	5.44
40	5.06	0.04	11.18
60[a]	4.78	0.03	16.15
80	4.77	0.03	16.36
100	4.70	0.03	17.54
120	4.67	0.04	18.02
240	4.28	0.05	33.15

[a] Repeated from Table 5.4.

5.3.1.6 Reactivity of asphaltenes and 9,10-dehydroanthracene.

Asphaltenes reactivity was also compared against 9,10-dehydroanthracene which is known as good hydrogen donor compound. To support the reactivity of asphaltenes compounds further, the reaction of α-methylstyrene and 9,10-dehydroanthracene was run in the presence of asphaltenes in the reaction medium.

Selectivity of cumyl dimers which are identified as by-products was also investigated which can be useful in the interpretation of hydrogen transfer capability of asphaltenes.

For the purpose of comparison, selectivity of the hydrogenated product and by-products are reported in Table 5.8. Interestingly, selectivity of cumyl dimers was decreased by 12 % when asphaltenes were reacted in excess amount. However, due to high amount of unrecovered mass this selectivity cannot be reliable for making this statement.

In terms of hydrogen transfer, asphaltene donated more hydrogen at 250 °C than 9,10-dehydroanthracene. The concentration of cumene formed increased even after 4 hours of reaction of α-methylstyrene and asphaltene. The amount of cumene increased significantly when α-methylstyrene was reacted with equal weight mixture of the asphaltenes and 9,10-dehydroanthracene.

Table 5.8. Selectivity of products from the reaction of α-methylstyrene with different H donors at 250°C: (1) α-methylstyrene + asphaltenes for 1 h (1:1); (2) α-methylstyrene + asphaltenes for 4 h (1:1); (3) α-methylstyrene+ asphaltene for 1 h (1:3); (4) α-methylstyrene + 9, 10-dihydroanthracene + asphaltenes for 1 h (2:1:1); (5) α-methylstyrene + 9, 10-dihydroanthracene for 1 h.

Reactants	T [°C]	Ratio	Time (min)	cumene [mg/ml]	Selectivity[a] [%]		
					Cumene	Recovered byproducts	Unrecovered Byproducts
α-methylstyrene + asphaltene [b]	250	1:1	60	0.28	30.12	61.66	8.22
α-methylstyrene + asphaltene [b]	250	1:1	240	0.65	34.59	52.71	12.70
α-methylstyrene + asphaltene	250	1:3	60	0.61	42.96	11.97	45.07
α-methylstyrene + asphaltene + 9,10-dihydroanthracene	250	2:1:1	60	0.84	83.03	15.84	1.13
α-methylstyrene + 9,10-dihydroanthracene	250	1:1	60	0.09	15.00	x	x

[a] Average of triplicate reactions, material balance is given in Table B.8.

[b] Repeated from Table B.7 for the purpose of comparison.

[x] due to dimerization product of 9,10-dehydroanthracene and α-methylstyrene, it was not possible to calculate selectivity.

Selectivity of cumene in the reaction of equal amounts of 9,10-dehydroanthracene and α-methylstyrene was only 15 %. However, this is primarily because of the identification of dimerization product of α-methylstyrene and 9,10-dehydroanthracene in methanol extract. Very small quantity of cumyl dimers can be observed in the reaction chromatogram given in Appendix C. After the addition of 9,10-dehydroanthracene to the reaction of asphaltenes and α-methylstyrene, formation of byproduct was also suppressed significantly, and selectivity of cumene and recovered by-products was 83.03 % and 15.84 % respectively.

Table 5.9. Concentration and conversion of α-methylstyrene from the reaction of α-methylstyrene with different H donors at 250°C: (1) α-methylstyrene + asphaltenes for 1 h (1:1); (2) α-methylstyrene + asphaltenes for 4 h (1:1); (3) α-methylstyrene+ asphaltene for 1 h (1:3); (4) α-methylstyrene + 9, 10-dihydroanthracene + asphaltenes for 1 h (2:1:1); (5) α-methylstyrene + 9, 10-dihydroanthracene for 1 h.

Reactants	T [°C]	Weight Ratio	Time [min]	α-Methylstyrene [mg/mL]	Conversion [%]
α-methylstyrene + asphaltene [a]	250	1:1	60	4.78	16.14
α-methylstyrene + asphaltene [a]	250	1:1	240	3.81	33.16
α-methylstyrene + asphaltene	250	1:3	60	4.28	29.71
α-methylstyrene + asphaltene + 9,10-dihydroanthracene	250	2:1:1	60	4.69	17.72
α-methylstyrene + 9,10-dihdroanthracene	250	1:1	60	5.1	10.53

[a] Repeated from Table 5.5 and Table 5.7 for the purpose of comparison.

There also appear to be a significant increase in the conversion of α-methylstyrene after addition of asphaltenes to the reaction of 9,10-dehydroanthracene and α-methylstyrene (Table 5.9).

5.3.1.7 The reaction of α-methylstyrene with excess amount of asphaltenes

In previous section while investigating selectivity of byproducts, it was observed that cumyl dimers formation is likely to be suppressed by increasing ratio of asphaltene to α-methylstyrene. Based on the material balance for the experiments with higher mass of asphaltenes, recovery efficiency decreased significantly.

That's why hydrogen transfer capability of asphaltenes was further investigated more elaborately with relatively lower mass of reagents. Based on the mass balance data shown in Table 5.11, recovery of products and dimers was sufficiently higher to make a conclusion regarding the selectivity of cumene and dimers. Selectivity of unrecovered products lies in the range of 0.5 and 5 % (Table 5.11).

Table 5.10 Concentration and selectivity of cumene, concentration and conversion of α-methylstyrene after the reaction of α-methylstyrene with different weight ratio of asphaltene.

Weight Ratio[a]	Time [min]	Cumene concentration[mg/mL]		Selectivity cumene [%]	α-Methylstyrene concentration [mg/mL]		Conversion [%]
		Average	St.Dev.		Average	St.Dev	
2:1	30	0.13	0.005	37.14	2.65	0.03	11.67
	60	0.27	0.002	52.05	2.48	0.02	17.29
	120	0.4	0.007	42.40	2.06	0.05	31.44
4:1	30	0.35	0.034	46.96	2.25	0.06	24.84
	60	0.65	0.032	61.90	1.95	0.01	35.00
	120	0.73	0.036	52.23	1.60	0.04	46.59
8:1	30	0.56	0.05	53.63	1.96	0.03	34.81
	60	0.84	0.091	66.30	1.73	0.04	42.23
	120	1.03	0.087	60.78	1.31	0.07	56.48

[a] Weight ratio of asphaltene to α-methylstyrene.

As seen from data in Table 5.10, concentration of cumene increased significantly with increasing ratio of asphaltene to α-methylstyrene. Overall, formation of cumyl dimers were appeared to significantly reduce with increasing ratio of asphaltene to α-methylstyrene.

Under each section of weight ratio, selectivity was reported at three different period of time. Not surprisingly, selectivity of cumene increased initially then reduced again when reactions were run over 2 h. The same relationship between the reaction time and selectivity was observed in each weight ratio.

In general, reactions of α-methylstyrene with excess amount of asphaltenes resulted in the significant amount of conversion of α-methylstyrene (Table 5.10). As the reaction time and weight of asphaltenes increases, there is a marked change in the conversion values of α-methylstyrene.

Table 5.11. Mass balance to estimate selectivity of recovered and unrecovered products.

	Mass [a,b] [mg]				Selectivity [a,b] [%]		
Ratio	methylstyrene converted [b]	Cumene recovered[c]	Recovered byproduct[d]	Unrecovered products[e]	Cumene	Recovered byproducts	Unrecovered products
2:1	17.50	6.50	10.50	0.50	37.14	60.00	2.86
	25.94	13.50	11.50	0.93	52.05	44.34	3.61
	47.17	20.00	25.50	1.66	42.40	54.07	3.53
4:1	37.27	17.50	19.00	0.76	46.96	50.99	2.05
	52.50	32.50	17.50	2.50	61.90	33.33	4.76
	69.88	36.50	32.50	0.88	52.23	46.51	1.26
8:1	52.21	28.00	22.50	1.71	53.63	43.10	3.27
	63.35	42.00	21.00	0.35	66.30	33.15	0.55
	84.72	51.50	30.50	2.72	60.78	36.00	3.22

[a] Average of two run.

[b] Sample calculation was given in Appendix B.

5.3.2 Indene as a Hydrogen Donor

To explain the formation of higher molecular weight products during the hydrogen disproportionation reactions, indene was used as a hydrogen donor due to its weak benzylic C-H bond and addition prone C=C bond.

The reaction of indene with α-methylstyrene also yielded cumene at 250 °C for 1 h (Figure C.19, Appendix C). Major components identified after the reaction were considered as recombination products of formed radicals due to disproportionation reactions.

Based on the integrated peak areas in GC MS (Table 5.12), conversion of methylstyrene and indene calculated which were equal to 35.22 and 79.82 % respectively. Main underlying assumption was that the detector responds identically to all compounds.

After addition of 9, 10-dehydroanthracene, not qualitative difference was observed in terms of products formation for reactions with and without 9,10-dehydroanthracene. The presence of 9,10-dehydroanthracene greatly reduced conversion of indene by around 30 % by suppressing formation of addition products.

Table 5.12. Integrated peak areas of the reaction products of α-methylstyrene and indene.

Compounds	Area
cumene	2.51E8
α-methylstyrene	1.85E9
indane	2.07E7
indene	7.29E8
cumyl dimers[a]	7.53E8
indene dimers[a]	1.37E9
Addition products[a]	1.49E9

[a] Lumped area of corresponding peaks

GC MS results showed that there were very diverse ranges of products formed in this reaction, especially at the higher mass range than dimer of cumyl radicals (Figure C.19).

To interpret the results more clearly, indene was heated at 250 °C to investigate whether additional reactions occur at this temperature due to indene on its own. As presented in the chromatogram in Figure C.22, which can be found in Appendix C, there are many products formed during indene conversion including indane. The mass spectra of the addition products which were considered to form due to dimerization of indenyl radicals are given in Appendix C (Figure C.23-Figure C.28). Indene conversion was estimated as 86.39 % based on the data shown in Table 5.13. For this calculation, it was assumed that the response of the detector is the same for each compound.

Table 5.13. Integrated peak areas of the reactions products of indene conversion.

Compounds	Area
indane	7.66E8
indene	4.89E9
indene dimers[a]	1.50E10
Addition products[a]	1.53E10

[a] Lumped areas of corresponding peaks

Table 5.14 shows the product list identified by GC MS from indene conversion at 250 °C. Electron ionization mass spectra were used to identify compounds, which were grouped together as isomers without identifying each isomer. Mass spectra of the individual compounds are given in the Appendix B.

Table 5.14. The product list identified by GC MS from indene conversion at 250 °C.

Name	Symbol	Molecular weight	General Formula	Structure
1[a]	Indane	118	C_9H_{10}	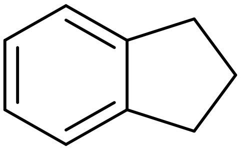
2[a]	Indene	116	C_9H_8	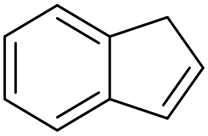
3	Not identified			
4	2-indanone	132	C_9H_8O	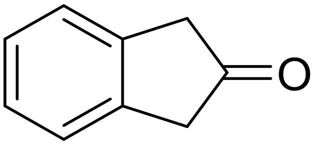
6	1,2-indane dimer	234	$C_{18}H_{18}$	
7[b]	2,2'-Bi-1H-indene	230	$C_{18}H_{14}$	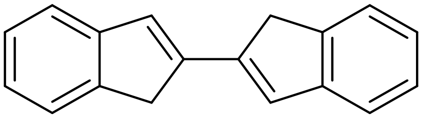
8[b]	D11-H-Benzofluorene	216	$C_{17}H_{12}$	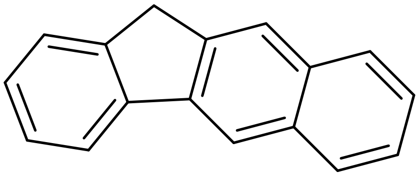

[a] Confirmed with commercial products.

[b] Given as an example (isomer)of certain type of compound.

The dimers which have molecular weight 232 and 230 g/mol are the main products and were identified after indene conversion. Most of the spectra exhibited a base peak of m/z 116 and major fragment of m/z = 232 (> 20%) which were considered as possible isomers of $C_{18}H_{16}$. There are also several spectra have the same base peak and with a major fragment m/z = 230, indicating the presence of different isomers of $C_{18}H_{14}$. Another possible dimer forms could be indane dimers based on the mass spectra which showed a molecular fragment m/z = 234 with a base peak m/z 117.

In addition to dimers, some higher molecular weight compound class also was observed. This series of compounds can be related to polymers which formed due to free radical addition reactions. This can be suggested based on the mass spectra of so called higher molecular weight compounds which featuring mainly some dominating base peaks at m/z 117, m/z 116 and major fragments m/z 346, m/z 348, m/z 350. They can be understood as isomeric forms of certain type of compounds.

5.3.3 Reaction of 9,10-dihydroanthracene and anthracene with asphaltenes

Hydrogen donor and acceptor capability of asphaltene was also investigated with the anthracene and 9, 10-dihydroanthracene at 250 °C. GC data for the extraction product after reaction for both the reaction of anthracene and 9, 10-dihydroanthracene was presented in Figure C.30 and Figure C.31 and can be found in Appendix C. As a qualitative work, GC MS chromatograms provided enough evidence regarding the occurrence of the hydrogen transfer reaction between the asphaltenes and model compounds. Asphaltenes donated and accepted hydrogen at 250 °C, which again confirms the presence of both donor and acceptor type of molecules in the feed.

Table 5.15. Integrated peak areas of 9, 10-dihydroanthracene and anthracene from the reaction with asphaltenes at 250 °C (1 h).

Reactions	Peak Area	
	Anthracene	9,10-dihydroanthracene
Asphaltene : Anthracene	4.84E8	1.36E7
Asphaltene : 9,10-dihydroanthracene	1.07E8	1.39E9

Due to partial solubility of 9,10-dihydroanthracene and anthracene in methanol, full recovery of products was not possible. That is why quantification of products was unlikely to be done after the reaction. Since the partition coefficients do not change, relative ratio of concentration of compounds can still be useful as an indirect measure of hydrogen transfer capability of asphaltenes.

Areas of each corresponding peak was integrated and reported in Table 5.15. Relative concentration of anthracene and 9,10-dihydroanthracene was calculated approximately as 97 and 3 % respectively for the reaction of anthracene and asphaltenes based on peak area. On the other hand, relative concentration of anthracene and 9,10-dihydroanthracene corresponded to 7 and 93 % respectively for the reaction of 9,10-dihydroanthracene and asphaltenes. Thus it can be suggested that transfer rate of hydrogen from asphaltenes to anthracene was slower than that from 9,10-dihydroanthracene to asphaltenes based on relative concentration of products in each reaction.

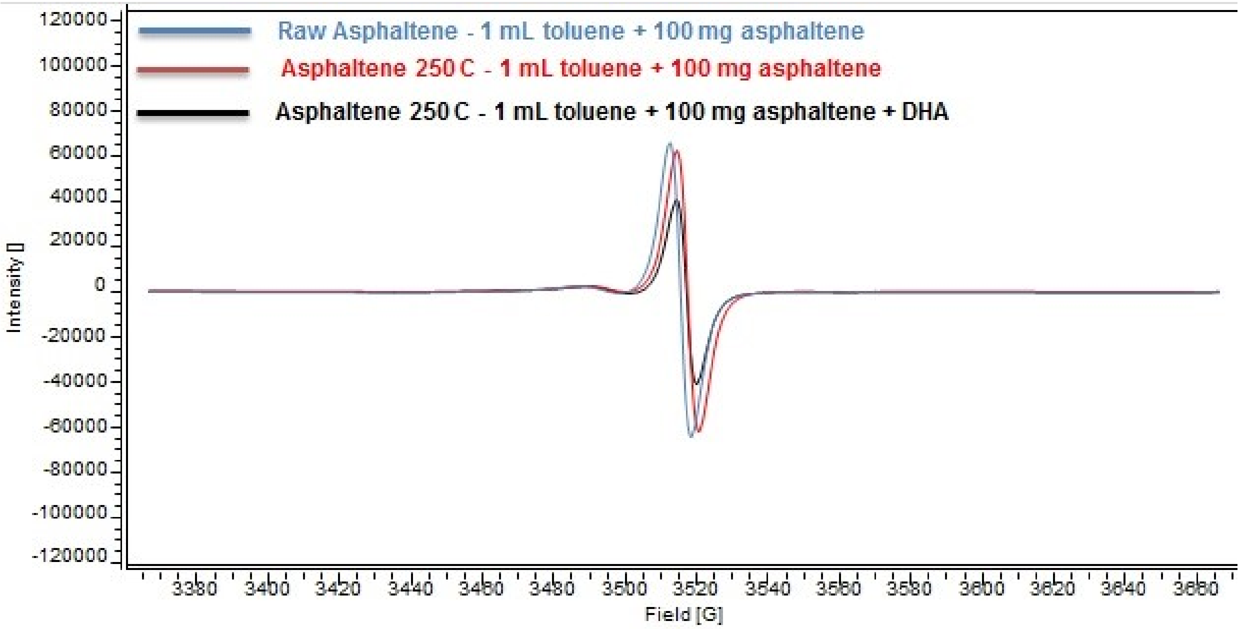

Figure 5.7. ESR spectra of blank aspaltenes (blue), converted asphaltenes at 250 C (red) and asphaltene converted in the presence of DHA (black)

To better understand the role of free radicals in asphaltenes at 250 °C, asphaltenes were studied by ESR (Figure 5.7). The amount of free radicals of asphaltenes was compared by their derivative signal intensity, which is proportional to the concentration of free radicals in the sample.

Clearly, there is a slight change in the detected free radical concentration of asphaltenes after heating. In the presence of 9,10-dihydroanthracene, the concentration of the stable radicals shows a different behavior in comparison to that in the absence of 9,10-dihydroanthracene, free radical concentration dropped based on the ESR spectra. Estimated g-values was reported in Table 5.16. Not significant shift was observed in g-values.

Table 5.16. Calculated g-values for the samples.

Samples	T [°C]	Frequency of microwave [GHz]	Magnetic field [G]	g-value
Asphaltenes	0	9.855778	3516.45	2.00253
Asphaltenes	250	9.861576	3516.45	2.00371
Asphaltenes + DHA	250	9.859388	3516.45	2.00326

5.3.4 Pyrolysis of asphaltenes feed

The pyrolysis behavior of asphaltenes at two temperatures: 250°C and 360°C was investigated by using a thermogravimetric analyzer coupled with Fourier transform infrared spectrometer (TG-FTIR). The results indicate that the release of volatiles takes place mainly above 300°C. Absorption bands appear in the region of 2830- 2900 cm^{-1} which is shown in circle (A) are arising in general from the C-H stretching of aliphatic hydrocarbons (Figure 5.8). Description of each peaks are given in Table 5.17. Intensity of those peaks increased as the time proceeds, indicating that cracking intensified with time. No aromatic C-H stretching bands were observed in the figure, which generally appears as a weaker broad band in the region 3000 – 3100 cm^{-1}.

The characteristic bands at the range of 2280 and 2400 cm^{-1} (B) can be ascribed to the C=O stretching which absorbs at a wavenumber of 2349 cm^{-1} with the overtones of the band, indicating the formation of CO_2. CO_2 might be mainly released due to cracking of carbonyl or carboxylic groups possibly present in asphaltenes, since the experiments were conducted under inert air. CO_2 was observed at both temperature level and decreased progressively upon increased time. Some H_2O also detected which can be observed as absorption peaks at 3500- 4000 cm^{-1}.

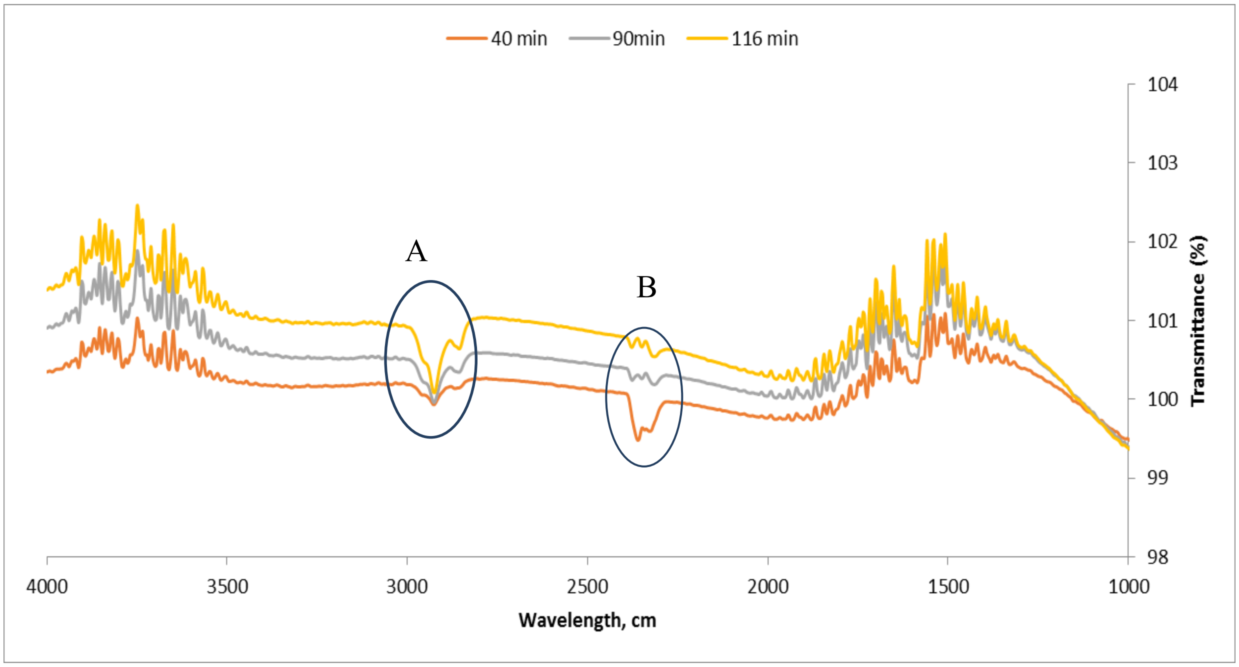

Figure 5.8. FTIR spectrum of the volatiles from asphaltene at 360°C. The recorded spectra is shown for different time intervals.

Those peaks, which appeared in the region of 2830- 2900 cm^{-1}, were not detected at 250 °C might to be due to absence of any significant dissociation. However, there are a few small molecular gaseous products released, such as CO_2 and H_2O.

Table 5.17. FT-IR wavenumbers of gases evolved from asphaltenes at 360 °C.

Wave number [cm^{-1}]	Functional groups	Description[a]
2831-2885	C-H	Assymetrical streching of methylene groups (CH_2) at 2853 cm^{-1}
2908-2943	C-H	Symmetrical streching of methylene groups (CH_2) at 2853 cm^{-1}
2950-2977	C-H	C-H streching of methyl groups (CH_3)
2280-2400	C=O	CO_2 absorbs at a wavenumber of 2349 cm^{-1} and overtones of the band.

[a] Characteristic band frequencies and their relationship with functional groups (Silverstein et al., 1981).[19]

TGA analysis confirmed the mass loss is approximately 0.2-0.4 % at 250 °C over a two hours of period of isothermal heating. In average, 16.5 % mass loss was recorded over same period of heating of asphaltenes at 360 °C.

5.4 Discussion

5.4.1 Structure reactivity of asphaltenes

Structural reactivity of the hydrogen donors appears to be very important concept for the asphaltenes. The conversion of α-methylstyrene with asphaltenes at 180 °C can be attributed to weak C-H bonds (compared to typical C-H bonds), which are contained in the asphaltenes. This shows that thermal reactivity of asphaltenes molecules is very high even at lower temperatures. There was clear evidence for the hydrogen transfer when asphaltenes heated (Figure 5.9).

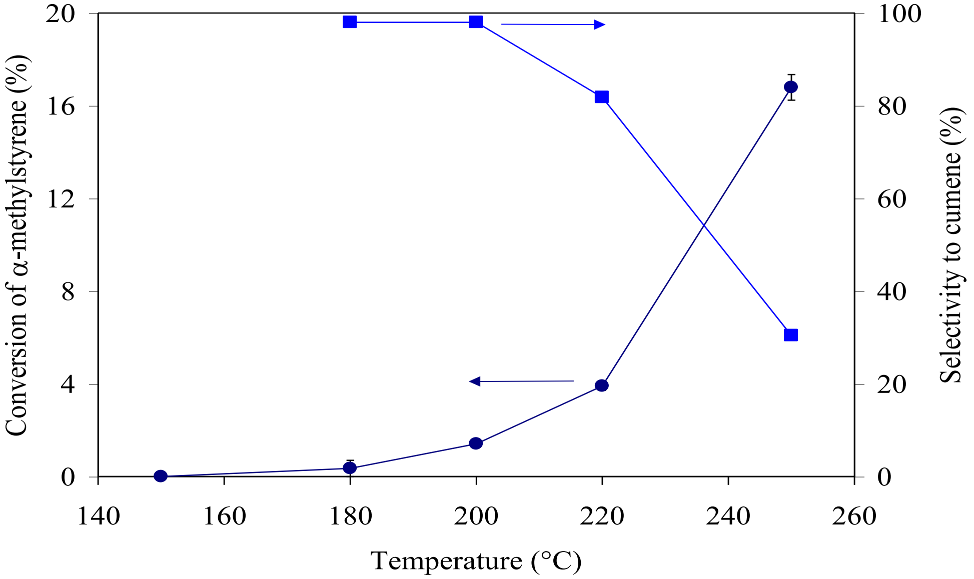

Figure 5.9. Conversion of α-methylstyrene (●) and selectivity to cumene (■) during the reaction of a 1:1 mixture of α-methylstyrene and asphaltenes for 1 h under 4 MPa N_2.

Despite of the very complex structure of the asphaltenes, it is well known that asphaltenes are more likely to contain naphthenic rings fused into polycyclic aromatic hydrocarbons. Interestingly the presence of the polyaromatic hydrocarbons during the reaction of α-methylstyrene and 9, 10-dihydroanthracene promotes hydrogenation reactions at considerably lower temperatures due to having C-H bonds with lower bond dissociation energy.[20] Similarly, the addition of asphaltenes to the reaction of α-methylstyrene and 9, 10-dihydroanthracene caused significantly higher amount of hydrogenated product (Table 5.8). These phenomena might explain possibility of hydrogen transfer from asphaltenes at lower temperature.

The "catalytic" effect of the asphaltenes on overall reaction is ease of formation of radicals through molecular disproportionation due to having lower C-H bond dissociation energy of polycyclic compounds. Of course, H transfer pathways that are induced by free radicals are also a feasible reaction pathway that might occur and will be discussed later.

The by-product which formed in the reaction of α-methylstyrene and 9, 10-dihydroanthracene was speculated to be product of an ene-reaction which is known as addition of a compound with a double bond (enophile) to an olefin possessing an allylic hydrogen (ene).[21] The molecular ion, M^+ at m/z = 298, and a base peak of m/z 179 can be interpreted as dimer of m/z = 119 (M^+-1 of α-methylstyrene) and m/z 179 (M^+-1 of 9,10-dihydroanthracene), indicating formation of an ene product by combination of 9, 10-dihydroanthracene and α-methylstyrene (Figure C.8). Under the applied condition (250 °C) it might not undergo homolytic decomposition. However, at relatively higher temperature this reaction may likely to occur to form cumyl and a well stabilized 9-hydroanthryl radical. That's why no addition products might have been identified from the reaction of α-methylstyrene and 9, 10-dihydroanthracene at 280 – 320 °C which automatically disfavored this type of hydrogen pathway over molecular disproportionation.[22]

In contradiction to this finding, it has also been suggested that molecular disproportionation was favored over the ene-reaction enthalpically, since the enthalpy of activation ($\Delta H°$) of the transfer hydrogenation of 9, 10-dihydroanthracene and α-methylstyrene was experimentally determined to be 133 kJ·mol^{-1} (31.8 kcal·mol^{-1}), which is approximately 63 kJ·mol^{-1} (15 kcal·mol^{-1}) lower than of a pericyclic process.[22] The reaction mechanisms are given in Figure 5.10. It has been also assumed that for termination reactions of radicals produced during molecular disproportionation proceed through without requiring any enthalpy of activation.

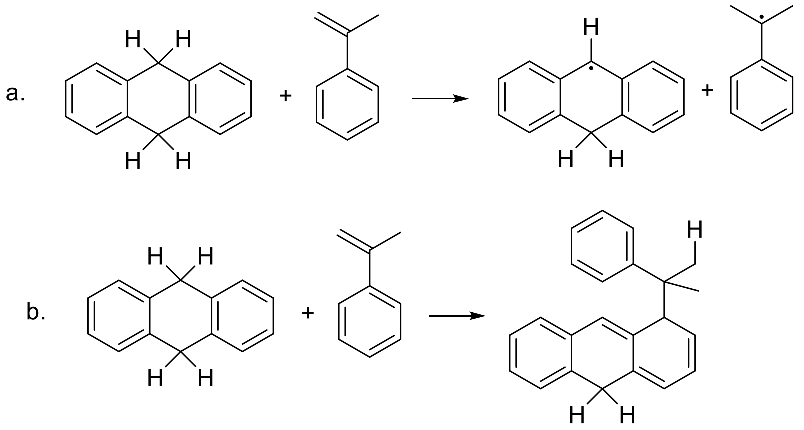

Figure 5.10. Mechanism of molecular disproportionation (a) and ene reaction between 9, 10-dihydroanthracene and α-methylstyrene.

The presence of asphaltenes in the reaction of α-methylstyrene and 9, 10-dihydroanthracene at 250 °C significantly suppressed this by-product, which formed only slightly (Table C.15). Similarly, no ene-product has been derived from the reaction of α-methylstyrene and 9, 10-dihydroanthracene in the presence of polycyclic donor hydrocarbons at temperatures in the range 200 – 260°C.[20] It can be speculated that the donor-to-acceptor weight ratio can be another reason favored the formation of this type of product over cumene statistically or thermochemically in the reaction of α-methylstyrene and 9, 10-dihydroanthracene at 250 °C which was 1:1 in this reaction compared to previous works (10:1).[8] Relative bond stregth of C-H being broken and C-C being formed can also favor the formation of this product. It can also be proposed that it is easier for 9-hydroanthryl radical to form C-C bond by addition to an unsaturated bond rather than loss of a hydrogen atom.

This finding tells more about hydrogen transfer ability of asphaltene which has been considered to take place at higher temperatures. It has been shown that hydrogen donor ability of residue starts to decrease after an initial rise at early stage of heating when anthracene was used as hydrogen acceptor.[11] The severe decomposition of asphaltene structures occurs at elevated temperatures above 350 °C. When asphaltene molecules thermally rupture they give a rise to the formation of a higher concentration of free radicals. More hydrogen is required to terminate those free radicals to prevent recombination and addition reactions of polyaromatics. Fast depletion of the donor hydrogen in asphaltene molecules might have reversed the hydrogen transfer from model compounds back to asphaltenes. Therefore, it has been concluded that asphaltenes typically accepts more hydrogen than the amount they donate at the conditions where severe cracking occurs.[11] Heating of asphaltenes feed under N_2 atmosphere at 360 °C for 2 h gave an average weight loss of 16.5 %. Through carefully analyzing the FT IR spectra, it can be concluded that the evolved products mainly consist of saturated and unsaturated hydrocarbons, CO_2 and likely some water (Figure 5.8). The release of CO_2 might be attributed to the cracking carbonyl and carboxyl groups.

In case of α-methylstyrene as a hydrogen probe the reverse reaction is very unlikely to occur as it was discussed for a reaction of asphaltenes with cumene 250°C. This could be one reason no decrease was observed in formation of cumene over time.

It has been shown that asphaltenes dissociated slightly at 250°C.[23] Some gases (CO_2, CH_4, C_2H_6) are evolved due to decomposition of carboxylic functional groups and thermally unstable alkyl moieties on the asphaltene molecules.[24]

To further demonstrate cracking propensity of asphaltenes feed which used in this study at 250 °C, mass loss was recorded trough TGA analysis, indicating approximately 0.2-0.4 % at 250°C over two hours period of isothermal heating. Based on the mass loss it could be suggested that thermal cracking reactions take place at 250 °C is not severe enough to make a substantial contribution to free radical concentration.

This might explain why the time corresponding to hydrogen donation ability of asphaltenes is longer at low temperatures. Thus asphaltenes can probably donate more hydrogen to an unsaturated system for longer period of time at low temperatures where hydrogen disproportionation is favored over cracking reactions. This might suggest that asphaltenes can possibly be benefit more in terms of hydrogen transfer at low temperatures without cracking the material appreciably and forming a coke.

Lacking the side alkyl groups may be even more favorable for the hydrogen disproportionation reactions due to absence of steric hindrance. But the investigation of reaction of donor molecules (substituted 9, 10-dihydroanthracene derivatives) with α-methylstyrene showed that steric effects has little or no observable effect on the molecular disproportionation step.[25] Steric effects can still be an issue between asphaltenes molecules.

5.4.2 Interpretation of cumyl dimers

Electron ionization mass spectrum was used as a tool to deduce and confirm the structure of dimers formed in the reaction of asphaltene and α-methylstyrene. The mass spectra of cumene and α-methylstyrene are shown in Appendix B (Figure C.10 and Figure C.11), which were assisted the interpretation of the additional products. Two main addition products: Benzene, 1,1'-(1,1,2,2-tetramethyl-1,2-ethanediyl)bis and 2,4-diphenyl-4-methyl-1-pentene are of particular interest for the overall reaction mechanism, due to their high selectivity compared to other by products. These two products were detected respectively in the spectrum of compounds which appeared at 13.672 (5) and 14.086 min (6) (Table 5.3). Both spectra are dominated mainly by a peak at m/z 119 and m/z 91 which represents a cumyl radical and a benzyl ion (through multiple fragmentation pathways) (Figure 5.10). They can be distinguished from one another by the presence of following peaks at m/z = 238, m/z = 236, which are the highest dominant molecular ions. The molecular ion, M^+ at m/z = 238, can be explained as dimer of m/z = 119. It can be thought a molecular ion (M^+ - 1) of the highest dominant fragment of cumene (M^+ at m/z = 120) which is produced due to loss of a hydrogen radical. In similar fashion, M^+ = 236 can be represented as dimerization of m/z = 117 (M^+-1 of α-methylstyrene) and m/z = 119. Those fragments proved that all dimerization products are formed by C-C linkage. In a similar way, identification of the rest of the dimers was corroborated by using mass spectra of cumene and α-methylstyrene along with the electron ionization mass spectra of corresponding compound. Mass spectra of the dimers are given in Figure C.12- Figure C.18. Upon examination of matched mass spectra in NIST Mass spectral library, identity of compound was confirmed. Those higher-molecular-weight compounds were formed due to addition reactions and their structure would provide an indication about the reaction mechanism of hydrogen transfer. The reaction mechanisms for the formation of dimers are given in Figure 5.15.

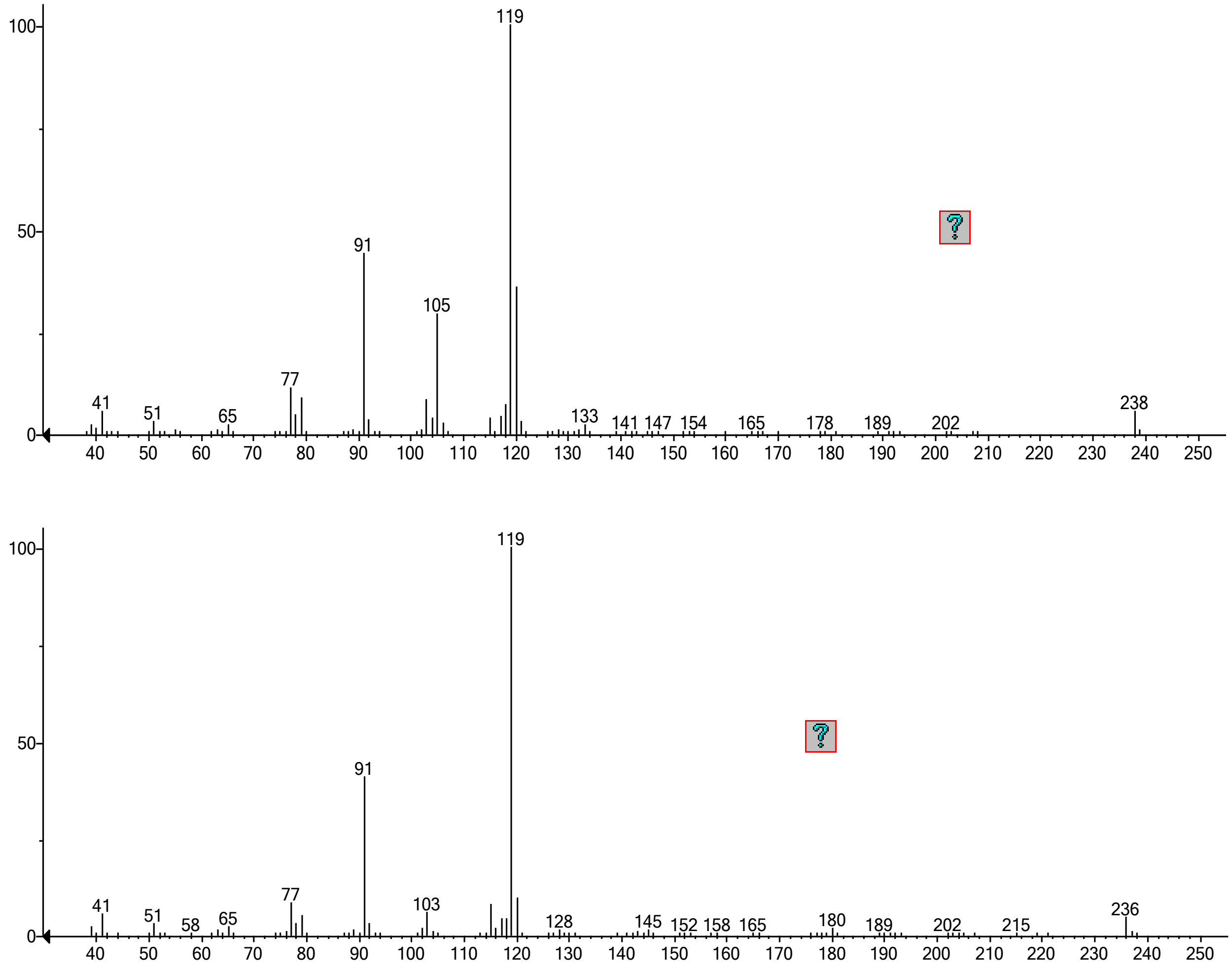

Figure 5.11. Electron impact mass spectrums of two main dimers: a) Benzene, 1,1'-(1,1,2,2-tetramethyl-1,2-ethanediyl)bis (top) b) 2,4-Diphenyl-4-methyl-1-pentene (bottom)

5.4.3 Hydrogen transfer via molecular disproportionation.

Benzene, 1,1'-(1,1,2,2-tetramethyl-1,2-ethanediyl)bis which is the most dominant byproduct may propose that considerable amount of cumyl radicals have been formed during the reactions which later participate dimerization and disproportionation reactions to terminate. Cumyl radicals are more likely to generate in the molecular disproportionation which is primarily known as the initiating step of the hydrogen transfer reaction. Thermal initiation of styrene polymerization at relatively higher temperature was explained by a transfer of weakly bound hydrogen atom to a styrene monomer which has an unsaturated C=C bond.[26] This finding again accentuates that hydrogen transfer proceeds through a molecular disproportionation, leading to formations of radicals, which has been differentiated from the hydride ion transfer mechanism proposed for dehydrogenation of hydrocarbons with quinones.[27,28] The molecular disproportionation as the initial step of two-step transfer hydrogenation of ethene with cyclopentene has also been proposed before at elevated temperatures in gas phase.[29] The formation of two alkyl radicals has been reported in free radical chain reaction between alkane and alkene (ane reaction).[30]

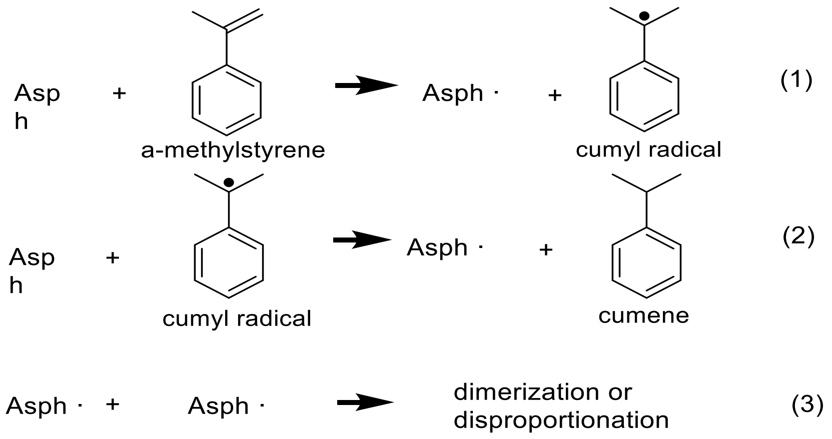

Figure 5.12. Reaction mechanisms for the hydrogenation of α-methylstyrene with asphaltenes: Asph (Asphaltene), Asph · (Asphaltene Radical)

This phenomenon might have an important implication in regard to low temperature hydrogen transfer in asphaltenes which might be taken as advantages during thermal processing. The initiation step to produce radicals in cracking reactions occurs as a homolytic bond cleavage, which later propagates through β-scission and hydrogen abstraction of free radicals.[31] Cracking of side alkyl chains of feed used in this study in initial thermal upgrading might have leaded to formation of olefin products. These olefin products might function as a hydrogen acceptor for the donor type of molecules or participate in additional reactions, ultimately leading to the formation of higher molecular weight compounds at lower temperature. The simplified mechanism was suggested for the molecular disproportionation reaction between hydrogen donors of asphaltenes and α-methylstyrene which can be understood as representative for unsaturated compounds in the feed (Figure 5.12).

5.4.4 Dimerization and disproportionation of cumyl radicals

A further point of discussion can be made here is that selectivity of the dimerization and disproportionation reactions. Relatively high concentration of addition products can be attributed to exceptionally fast initiation step, which increases the free radical concentration, which in turn increases the possibility of recombination reactions. However, it is hard to draw a conclusion here whether disproportionation favored over dimerization reactions. One can suggest here that there is an intense competition for H atoms between free radicals from asphaltenes, hydrogen acceptors in asphaltene molecules, and cumyl radicals. When there is not sufficient available hydrogen for stabilization of cumyl radicals, it might favor the dimerization reactions.

The selectivity to cumene increased from 30 % up to 83 % after addition of 9,10-dihydroanthracene to the reaction of α-methylstyrene and asphaltenes (Table 5.8). It suggests that addition of 9, 10-dihydroanthracene greatly reduced the formation of cumyl dimers by stabilizing cumyl radicals which formed due to fast molecular disproportionation of α-methylstyrene and asphaltenes molecules. For this conclusion, the mass of unrecovered products also needs to be considered which is very low (1.13 %) especially if some by-products were discounted during extraction. It is also worthwhile here to show the almost absence of cumyl dimers in the reaction of 9, 10-dihydroanthracene and α-methylstyrene (Figure C.9). Availability of transferrable hydrogen appeared to be important factor to control dimer formation.

Table 5.18. Conversion and selectivity in control experiments involving 9,10-dihydroanthracene at 250 °C for 1 h under 4 MPa N_2.

Reaction mixture	Conversion of α-methylstyrene (%)	Selectivity to cumene (%)	Relative concentration (%)	
			anthracene	9,10-dihydroanthracene
asphaltenes : α-methylstyrene : 9,10-dihydroanthracene	18	83	56	44
α-methylstyrene : 9,10-dihydroanthracene	11	15	10	90

With regard to olefin addition to asphaltenes, there is no enough evidence. Based on the mass of unrecovered products, it can be concluded indirectly that addition of α-methylstyrene to asphaltenes is not very significant if it takes place (Table 5.11). However as presented in Table 5.18, a low cumene selectivity and high combination and addition product selectivity was obtained in the reaction with only α-methylstyrene and 9,10-dihydroanthracene. This can be interpreted as an effect of steric constraint of the hydrogen donors. In the case of α-methylstyrene and 9,10-dihydroanthracene, after molecular disproportionation, two sterically unconstrained radicals are in closer proximity, which increased likelihood of radical recombination. Radical recombination might be limited in the case of asphaltenes due to possible steric constraints.

A further proof can be shown here is conversion of α-methylstyrene with different mass ratio of asphaltenes to α-methylstyrene, which increased with increase in the asphaltenes content in the reaction medium (Figure 5.13).

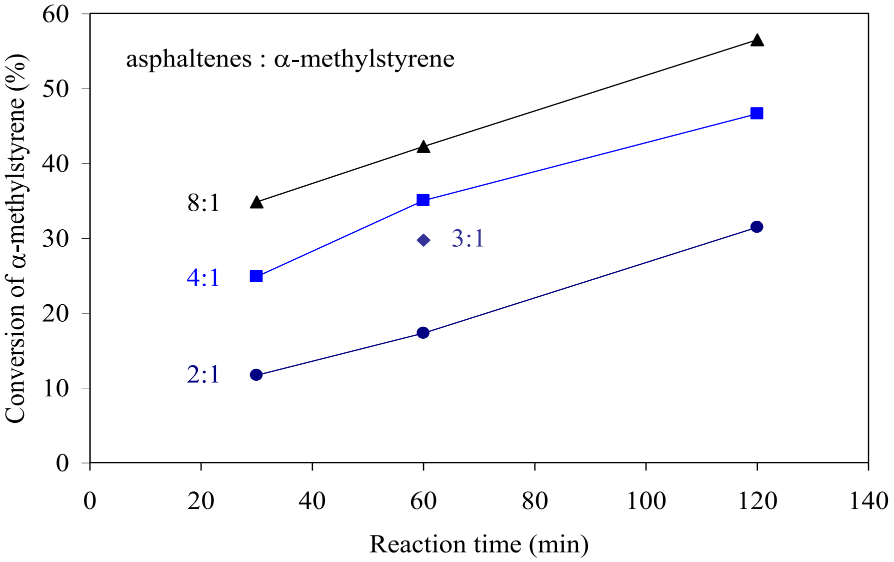

Figure 5.13. Conversion of α-methylstyrene in the reaction of asphaltenes and α-methylstyrene at 250 °C under 4 MPa N_2.

The average selectivity to each group of products was estimated based on Table 5.10 and Table 5.11 ,and presented in Figure 5.14. Some general observations can be made based on the trends. The selectivity to cumene appeared to increase slightly with an increase in the asphaltenes mass fraction, whereas there was a decrease in the selectivity of recovered byproducts with an increase in the asphaltenes content. The unrecovered byproduct selectivity was less than 15 % and decreased as asphaltenes content increased. The formation of cumene might have been favored due to the presence of more available hydrogen by asphaltenes in reaction environment, which also resulted in suppression of dimer formation.

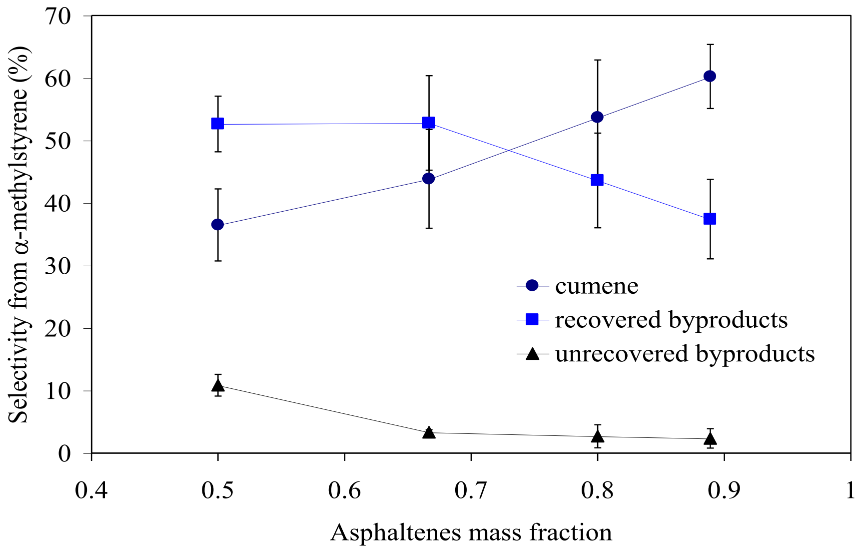

Figure 5.14. Average product selectivity after reaction of 1:1 to 8:1 asphaltenes to α-methylstyrene ratio at 250 °C under 4 MPa N_2.

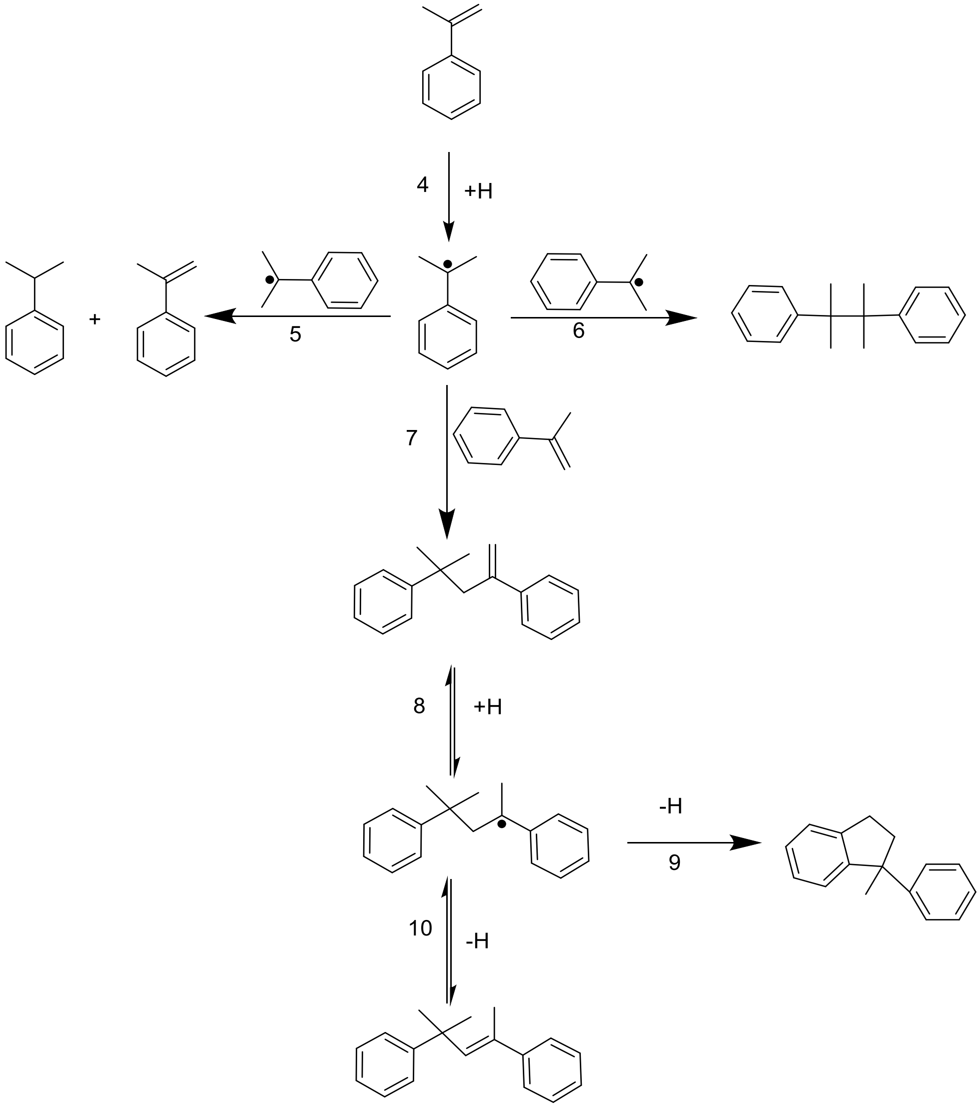

Figure 5.15. Reaction pathway for dimerization and disproportionation of cumyl radicals into more stable forms.

As seen in Figure 5.15 the formation of cumene can also take place during the disproportionation of cumyl radicals which accompany dimerization reactions. Because of the steric effects and and possession of β-Hydrogen, disproportionation reaction between cumyl radicals is also likely to occur however it was concluded which one is more favored. Abnormally low values of $k_{disproportionation}/k_{combination}$ have been reported indicating combinations of cumyl radicals are stabilized predominantly by recombination.[32]

Based on the observation mentioned above, it can also be concluded dimerization of cumyl radicals is more favorable rather than disproportionation. This can be claimed according to the estimated selectivity of dimers when reaction was run for longer period of time. Thus it can be hypothesized the main route for hydrogen atom transfer is from donor molecules contained in asphaltenes to the double bond in α-methylstyrene. Also because when asphaltenes was reacted in excess amount, selectivity to cumene increased significantly. Reaction step 6 Figure 5.15) becomes more favorable over reaction step 2 (Figure 5.10), due to production of more cumyl radicals which cannot abstract hydrogen atom.

5.4.5 Evaluation of hydrogen transfer

The emphasis is also on measurement of the amount of transferrable hydrogen which is very important parameter for heavier feedstock. This could be identifiable due to irreversibility of hydrogen transfer from cumene unlike the aromatic hydrogen acceptors such as anthracene. However, as mentioned earlier that possibility of the formation of some addition products of cumene with asphaltene molecules cannot be eliminated altogether. One can suggest that it is very unlikely for C-H in cumene to break at 250 °C, since bond dissociation energy for weakest C-H, which is tertiary C-H in alkyl group, is around 353 ± 6 kJ/mol.[33] This value is significantly higher than bond dissociation energy of C-H at the 9- or 10-positions of 9, 10-dihydroanthracene which has also been reported in the same study of McMillen and Golden as 315 ± 6 kJ/mol. The bond strength of C-H in 9, 10-dihydroanthracene reported by McMillen and Golden is approximately 32 kJ smaller than the recommendations of Gerst and Rüchardt.[22]

Even tough hydrogen transfer from cumene cannot be ruled out completely, the control experiment provided no evidence if cumene participated in reactions. The reverse of the hydrogen transfer: from cumene to asphaltenes was not found at 250 °C (Figure 5.16). Thus it can be deduced that asphaltenes free radicals are incapable of forming bond with hydrogen which stronger than weakest C-H in cumene (353 ± 6 kJ/mol).

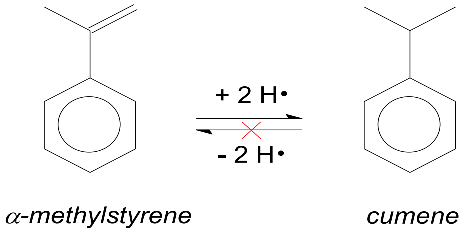

Figure 5.16. Hydrogen transfer between α-methylstyrene and cumene.

The amount of hydrogen that could be transferred from asphaltenes to α-methylstyrene was estimated based on the combined conversion and selectivity data. It is found that of the order of 1.8 mg H/g asphaltenes is transferred within 1 h at 250 °C and as much as 3.8 mg H/g asphaltenes in 4 h at 250 °C (Figure 5.17).

This calculation is based on the stoichiometry of the products formed by the conversion of α-methylstyrene. To produce cumene from α-methylstyrene, 2 mol H/mol α-methylstyrene must be transferred. To produce the other products, which were addition products, one C–C bond and one C–H is formed for each α-methylstyrene molecule that reacted and only 1 mol H/mol α-methylstyrene must be transferred to satisfy the reaction stoichiometry.

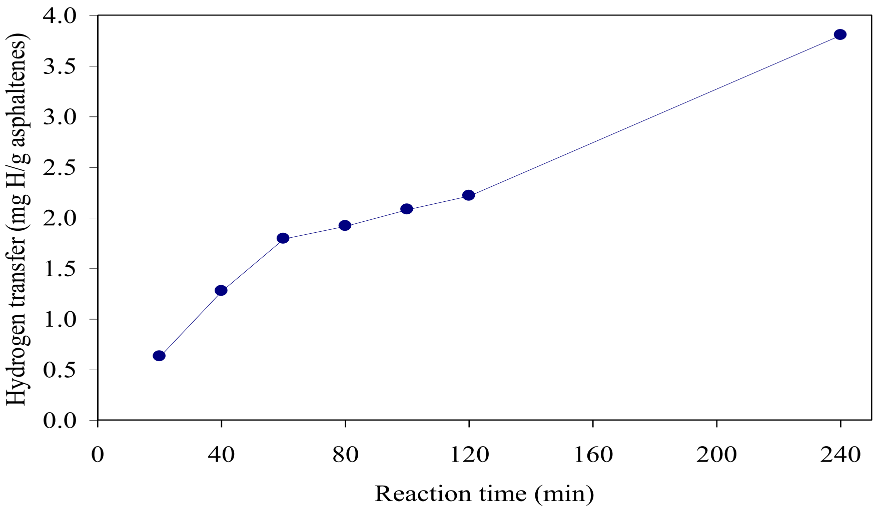

Figure 5.17. Amount of hydrogen transferred from asphaltenes to α-methylstyrene during reaction at 250 °C under 4 MPa N_2 pressure.

Main underlying assumption here was that hydrogen disproportionation reactions of cumyl radicals were not taken into consideration as mentioned previously hydrogen transfer from asphaltene was dominant way of hydrogenation of α-methylstyrene. Before making this conclusion, also it needs to be verified that cumene has been recovered efficiently. This was only checked for 1:1 weight ratio of reactants. This strategy can give an idea about transferrable hydrogen content of asphaltenes. Reactivity of the polyaromatic hydrocarbons in asphaltene can also be rationalized on the basis of the hydrogen amount transferred.

5.4.6 Formation of free radicals during molecular disproportionation

Some radicals formed from the cleavage of C-H bonds in molecular disproportionation step are not able to take place in disproportionation reactions. Loss of one H from this radical creates a resonance stabilized radical. Instead of disproportionation, radical-radical combinations occurs leading to aromatic growth. Importance of resonance stabilized radicals has been investigated and some mechanisms have been proposed for cyclopentadienyl and indenyl radicals from indene pyrolysis.[34]

The reaction of the indene with α-methylstyrene yielded variety of compounds due to recombinations of free radicals formed in the molecular disproportionation. Based on the electron ionization mass spectrum, it can be suggested that dimer radicals have mainly formed through C-C linkage. As an evidence, presence of m/z = 232 in the fragmentation of products can be represented here which can be considered as a dimer of m/z = 116. A scheme of the proposed reaction pathway is given Figure 5.18. It can be concluded that indene showed similar chemical reactivity to the asphaltenes based on the cumyl dimers, which did not form in the reaction of 9, 10-dihydroanthracene and α-methylstyrene in the absence of asphaltenes.

To assign every peak to a dimer, mass fragmentation spectra were taken into account (Appendix B). Knowing the structure of certain compounds would allow us to propose a reaction pathway for the overall reaction. The presence of indenyl groups in the isomers of can be confirmed with the loss of 116 atomic mass units, which form another fragment ion of 116 m/z, which appeared as base peak. By analogy the same can be applied to the isomers of $C_{18}H_{14}$ in which indene units are connected via single C-C bond. The identification of addition products clearly indicated that indene has undergone a dimerization reaction at 250 °C. All these observations indicate that the additional products are consequence of free radicals formed in initiation step which is unlikely to undergo disproportionation reactions. Due to the insensitivity of mass spectrometry for distinguishing isomers, no attempt was made to determine via which carbon atoms indene dimers are linked through and the position of the double bonds. The presence of the single bond carbon linkage does not violate both proposed model structures of asphaltenes: archipelago and island models.[35] Recently, AFM (Atomic force microcopy) and STM (Scanning tunneling microscopy) investigations of the asphaltenes revealed the presence of single covalent bond in minor quantities between polycyclic aromatic cores.[36]

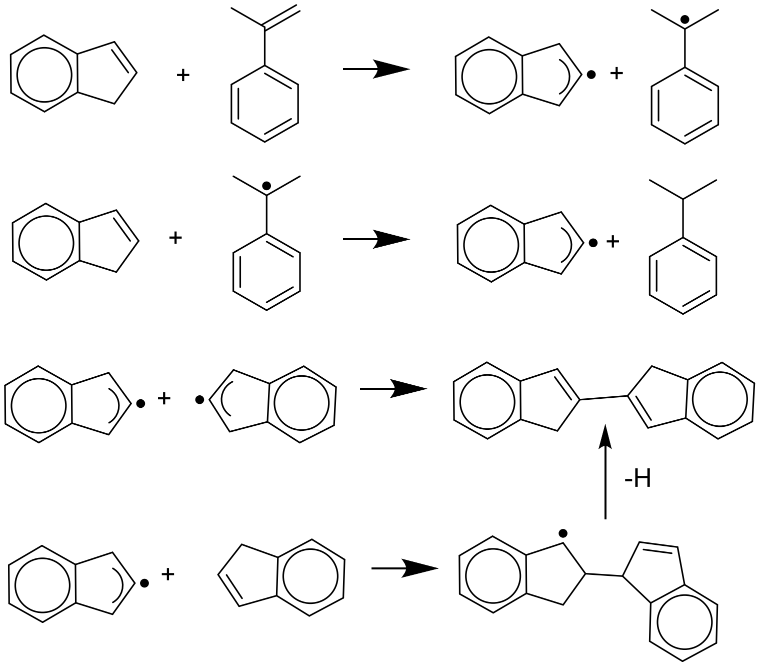

Figure 5.18. Proposed mechanism for hydrogen transfer from indene to α-methylstyrene at 250 °C

Unlike 9,10-dihydroanthracene, this phenomenon can be also observed in phenalene, which leads to the formation of complex dimers after a molecular disproportionation step. The complex products of the dimerization have not been observed when α-methylstyrene was reacted with phenalene by addition of an excess amount of 9, 10-dihydroanthracene as a radical scavenger.[37] Electron resonance spectroscopy studies have given more evidence about formation of free radicals such as the formation of 6-H-benzopyrenyl (5.14b) and 7-H-dibenzoanthracenyl (5.14c) radicals from their corresponding hydroaromatic derivatives.[20] All attempts to synthesize the following radicals (Figure 5.19 d) and (Figure 5.19 f) have been failed because those diradicals are very unstable and will polymerize immediately.[38] Dehydrogenation of (Figure 5.19 g) with palladium-charcoal yielded a non-volatile polymer and a high molecular condensation product which again indicated their intermediate diradicals cannot exist.[39] It has been suggested hydrocarbons with condensed hexagonal rings but without Kekule structure (aromatic sextet structure) are not aromatic but radicals with high reactivity. Asphaltenes might contain some of this type of molecules, which promote hydrogen transfer reaction at low temperature and also very vulnerable to free radical addition type reactions.

Reaction of indene with α-methylstyrene showed that not all hydrogen donor compounds undergo aromatization reactions while donating hydrogens, but instead only dimerize. Even addition of 9, 10-dihydroanthracene did not suppress formation of recombination products completely (Table C.17). This might give an alternative explanation for the possibility of formation higher molecular weight components at lower temperature. Also dimerization of α-methylstyrene in the presence of asphaltenes can provide indirect evidence for the recombination reactions taking place in asphaltenes.

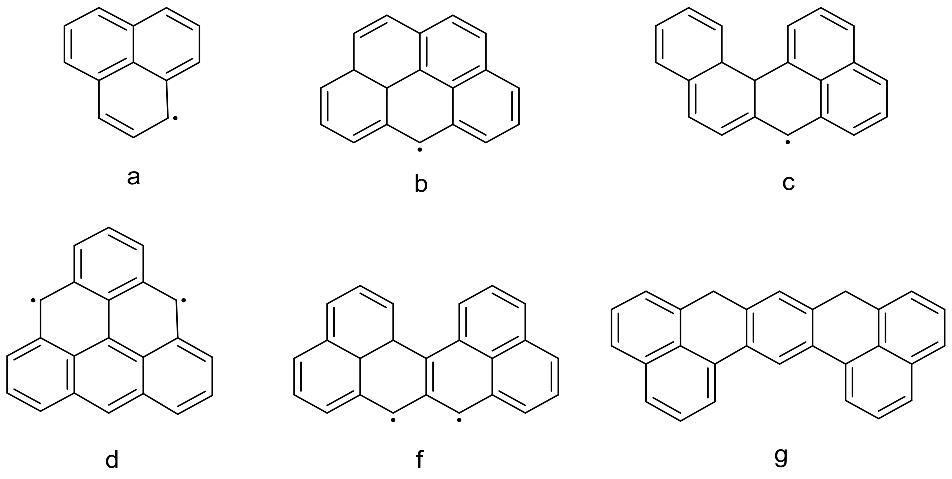

Figure 5.19. Structures of diradicals and hydrocarbons found in literature.

5.4.7 Significance of free radicals in hydrogen transfer reactions

An alternative possibility which might explain occurrence of hydrogen transfer reactions at relatively low temperature is the possession of considerable amount of natural free radicals in the asphaltenes, as shown in Figure 5.7 and reported in literature.[40] Organic free radicals can play an important role in the chemical properties of the asphaltenes at low temperature. Due to presence of considerable amount of free radical species, there is no need for a free radical initiation step.

The radical hydrogen transfer reaction is thought to be important in coal liquefaction. In this reaction, radical donates a hydrogen atom to an acceptor molecule rather than abstracting hydrogen from donor molecules (ArH• + `Ar→ Ar + `ArH•; Ar ≡ aromatic). The driving force for free radical hydrogen transfer is related to the relative stability of free radicals. Due to the difficulty to obtain thermochemical data, such as activation barrier of free radical hydrogen transfer pathway due to this transition state, there is no rigorous proof for this mechanism.[41] However, it cannot be ruled out.

For the radical hydrogen transfer reaction to be important in hydrogenation of α-methylstyrene, its activation barrier or bond dissociation energy has to be sufficiently low to compete with molecular disproportionation pathway. Bond dissociation energy for aromatic compounds increases, because their radicals derive more resonance energy from delocalization. As a radical having particular importance for the reaction of α-methylstyrene and 9,l0-dihydroanthracene, 9-hydroanthryl radical stability can be considered. The stability of the 9-hydroanthryl radical formed by abstraction of an H-atom from 9, l0-dihydroanthracene corresponds to a C-H bond strength of 180 kJ/mol which was estimated by Billmers and Stein.[5] It was concluded bond strength of C-H in the radical is too high to involve a free hydrogen atom transfer at 350 °C. On the other hand, this pathway for bimolecular H-transfer from a cyclohexadienyl radical intermediate to a closed-shell π-system has been considered as a main contributor to condensed phase pyrolysis of polycyclic aromatic hydrocarbons.[41]

The inhibiting effect of asphaltenes has been investigated during styrene polymerization. It has been proposed that the polymerization inhibition is caused mainly by active participation of free radicals in the reaction.[42] It could be also explained by the hydrogen disproportionation reactions which might terminate the styrene radicals via a hydrogen abstraction. As an indirect evidence, mixture of asphaltenes and α-methylstyrene gained plasticity at room temperature which was not observed with other organic solvents such as toluene. This might be attributed to presence of high concentration of free radicals in asphaltenes that turned the product into a viscous plastic material. Polymerization of α-methylstyrene with asphaltenes was not observed at higher temperature which was above the known ceiling temperature of α-methylstyrene.

Understanding of hydrogen disproportionation and addition reactions is very important from the viewpoint of free radical reactions. Ex situ ESR studies of industrial asphaltenes showed that significant amount of stable free radicals present in the mixture (Figure 5.7). After heating of asphaltenes at 250 °C there was a slight decrease in the free radical concentration. Since it was already confirmed that no significant pyrolysis occurred at this temperature, free radicals generated due to cleavage of covalent bonds are not significant contributors to the overall free radical content. But free radical formation cannot be excluded during hydrogen disproportionation reactions, which were mentioned earlier. It has been suggested hydrogen transfer during hydrogen disproportionation does not produce free radicals.[43] Thus reduction of the free radical concentration might be attributed to the coupling reaction between free radical fragments and hydrogen disproportionation reactions. It shows some free radicals that were originally present in the asphaltenes do not couple with each other, probably due to steric hindrance, but are exposed sufficiently to be stabilized by 9,10-dihydroanthracene. Some stable free radicals still continued to persist, which might be confined in the rigid structure and therefore cannot acquire hydrogen from 9,10-dihydroanthracene.

Transfer of hydrogen from 9,10-dihydroanthracene suggests that hydrogen transfer leads to the formation of the C-H bonds with radical species which become stronger than the weakest C-H of 9,10-dihydroanthracene (315 ± 6 kJ/mol). Thus, radical H atom transfer reaction become favorable due to the differences between the bond strength of C-H being formed and C-H which is being broken. More hydrogen was transferred from 9,10-dihydroanthracene to asphaltenes, than that was transferred from asphaltenes to anthracenes (Table 5.19). It can be deduced that asphaltenes contains more accessible free radicals, which are capable of forming bonds with hydrogen with bond strength higher than 315 kJ/mol, compared to its transferrable hydrogen with bond strength less than 315 kJ/mol. It is also worth mentioning that none of the free radicals are capable of forming bond with hydrogen stronger than 353 kJ/mol.

Table 5.19. Relative product selectivity from conversion of anthracene and 9,10-dihydroanthracene with asphaltenes at 250 °C for 1 h under 4 MPa N_2.[a]

Reaction mixture	Relative concentration (%)	
	anthracene	9,10-dihydroanthracene
asphaltenes : anthracene	97	3
asphaltenes : 9,10-dihydroanthracene	7	93

[a] Calculated based on the Table 5.15.

The formation of heavier products by coupling reactions of free radicals that generated through hydrogen disproportionation as shown in case of indene conversion, and also aromatization through molecular disproportionation can be speculated based on ESR data, which showed a decrease in free radical concentration after heat treatment. The ESR data is consistent with either explanation. Due to lack of knowledge about nature of transferrable hydrogen atom in asphaltenes, it cannot be said whether aromatization or dimerization are predominant. Hydrogen donor molecules in asphaltenes are not necessarily hydro-aromatics like tetralin or 9, 10-dihydroanthracene. They can possibly be classified according to the number of transferrable hydrogen atom per molecule. The heavier products which formed at lower temperature were interpreted as *n*-heptane insoluble in our previous study, revealed itself as a change in asphaltenes yield. However, they do not necessarily need to be asphaltenes, toluene soluble or toluene insoluble (coke). It has been shown that higher molecular weight g.p.c (gel permeation chromatography) fraction of asphaltenes has more pronounced polymer-forming propensity and form an insoluble material (CH_2Cl_2 -insoluble) at lower pyrolysis temperature (<300°C).[44] This formed polymer does not appear to be related to the coke produced over 500 °C. Heating of the whole asphaltene did not produce polymer and relatively depolymerization was observed. This effect was explained by the presence of some type of asphaltenes species that might act as chain terminator or stabilizer, preventing the recombination of free radicals.

Although hydrogen disproportionation or hydrogen transfer reactions have not been mentioned specifically, it is necessary to note the importance of these reactions. Overall results from ESR are in well agreement with our speculations about formation of additional products at lower temperature range, which indicated a minor decrease in free radical content. It has been shown that structural properties of asphaltenes such as average aromaticity may vary upon production with an experimental study of the chemical composition of asphaltene samples, collected at three different stages of the production process: well extraction, storage and refining.[45]

5.4.8 Implications for the industry

The phase separation model for coke formation depicts that converted asphaltenes undergoes liquid-liquid phase separation and forms a phase which is lean in abstractable hydrogen.[46] This model was partly contradicted later when asphaltenes was revealed to contain only slightly less concentration of donor hydrogen than its full residue.[13]

Maintaining of solubility of converted asphaltenes is a challenge to improve the extent of thermal conversion without forming a coke. One of the more practical ways is stripping out of the distillable liquid product, which is usually a non-solvent for asphaltenes, during visbreaking where asphaltenes limits compatibility of liquids.[13]

This work revealed that asphaltenes possibly donate hydrogen at mild temperatures (<250°C) where not appreciable amount of cracking occurs. The reactivity of hydrogen donors in asphaltenes can be advantage at mild heating processes where coke formation and phase separation can be limited.

Since asphaltene cores cannot be converted into light products during the thermal conversion, it is desirable to benefit from its transferable hydrogen content as much as possible. It was also suggested that hydrogen disproportionation reactions will possibly cause growth in aromatic cores at lower temperatures. Co-processing of asphaltene with an olefin rich or aromatic oil while controlling thermal cracking reactions might cause an increase in hydrogen content of the liquid yield due to possible hydrogenation reactions.

5.5 Conclusion

It was postulated that hydrogen disproportionation and free radical addition reactions are likely to take place between asphaltene molecules at 250 °C and lower temperatures. The following observation and conclusions can be made based on this work:

i. Asphaltenes hydrogenated α-methylstyrene to cumene at temperature as low as 180 °C. Reaction did not take place at 150 °C within 1 h reaction time, but this does not exclude the possibility of hydrogen disproportionation reactions between asphaltenes species at 150 °C.

ii. Asphaltenes molecules are structurally reactive due to their large polycyclic aromatic core, which was confirmed with reaction of α-methylstyrene. Considering significant free radical concentration of asphaltenes free radical induced hydrogen transfer, which involves a bimolecular hydrogen atom transfer from a radical to an unsaturated bond, could be considered as well. Based on study of hydrogen transfer, insufficient information was presented to identify the main hydrogen transfer pathway with certainty. In this work, it was concluded only that hydrogen transferred from asphaltenes to an unsaturated bond at lower temperatures than cracking temperatures, regardless of the pathway.

iii. Some radicals formed from hydrogen donors after cleavage of C-H bond cannot disproportionate to form a stabilized product on its own, but will dimerize instead (as shown by the reaction of indene and α-methylstyrene). Even addition of a good hydrogen donor cannot suppress the formation of addition products, probably due to fast dimerization step compared to the disproportionation. Asphaltenes might include this type of compounds that can form high molecular weight compounds at low temperatures.

iv. It was proposed that the dominant pathway for addition reactions is the dimerization of free radicals which are formed in the initiation step or free radicals the persisted and were generated in previous processes. Free-radical addition proceeds through the formation of C−C bonds which was explained by indene conversion.

v. ESR results also confirmed that coupling of free radicals and hydrogen disproportionation occurs at lower temperature than cracking temperature, leading to a decrease in overall free radical concentration. Some free radical fragments are sterically hindered with respect to each other, which were stabilized by addition a hydrogen donor. The asphaltene feed used in this work has a significant amount of free radicals, some of which might have been generated in atmospheric and vacuum distillation units due to cracking reactions, but could not form addition products due to steric constrains.

References

1. Franz, J.; Camaioni, D.; Alnajjar, M.; Autrey, T.; Linehan, J. Fundamental hydrogen transfer studies in coal liquefaction: Understanding the answers and questions. *Prepr. Pap.Am. Chem.* Soc., *Div. Fuel Chem.* **1995**, *40*, 203−*207.*

2. S Stein, S.E. A fundamental chemical kinetics approach to coal conversion. In *New Approaches in Coal Chemistry*, ACS Symposium Series, 169; Blaustein, B.D; Bockrath, B.C; Friedman, S., Eds.; Americal Chemical Society; Washington, DC, 1981; pp 97-129.

3. Benson, S. W. On the reaction between ethylene and cyclopentene, a radical mechanism. *Int J Chem Kinet* **1980***, 12*, 755-760.

4. Poutsma, M. L. Free-radical thermolysis and hydrogenolysis of model hydrocarbons relevant to processing of coal. *Energy Fuels* **1990***, 4*, 113-131.

5. Billmers, R.; Griffith, L.; Stein, S. Hydrogen transfer between anthracene structures. *J. Phys. Chem.* **1986***, 90*, 517-523.

6. McMillen, D. F.; Malhotra, R.; Nigenda, S. E. The case for induced bond scission during coal pyrolysis. *Fuel* **1989***, 68*, 380-386.

7. Stein, S. E. Thermal reactions and properties of polycyclic aromatic hydrocarbons. *Acc. Chem. Res.* **1991***, 24*, 350-356.

8. Rüchardt, C.; Gerst, M.; Nölke, M. The Uncatalyzed Transfer Hydrogenation of α-Methylstyrene by Dihydroanthracene or Xanthene—a Radical Reaction. *Angewandte Chemie International Edition in English* **1992***, 31*, 1523-1525.

9. Gerst, M.; Rüchardt, C. Bimolekulare Radikalbildung durch H-Transfer, 2. H-Transferreaktionen mit Phenalen. *Chem. Ber.* **1993***, 126*, 1039-1045.

10. Morgenthaler, J.; Rüchardt, C. Bimolecular Formation of Radicals by Hydrogen Transfer, 11. Transfer Hydrogenation of Conjugated Cyclic Dienes and Trienes. *Liebigs Annalen* **1996**, 1529-1532.

11. Guo, A.; Wang, Z.; Zhang, H.; Zhang, X.; Wang, Z. Hydrogen transfer and coking propensity of petroleum residues under thermal processing. *Energy Fuels* **2010***, 24*, 3093-3100.

12. Sanford, E. C.; Xu, C. M. Relationship between solids formation, residuum conversion, liquid yields and losses during athabasca bitumen processing in the presence of a variety of chemicals. *The Canadian Journal of Chemical Engineering* **1996***, 74*, 347-352.

13. Gould, K. A.; Wiehe, I. A. Natural hydrogen donors in petroleum resids. *Energy Fuels* **2007***, 21*, 1199-1204.

14. Wang, Z.; Ji, S.; Liu, H.; Chen, K.; Guo, A. Hydrogen Transfer of Petroleum Residue Subfractions During Thermal Processing under Hydrogen. *Energy Technology* **2015***, 3*, 259-264.

15. Harding, T. G.; Zanon, S.; Imran, M.; Kerr, R. K. In *In In-Situ Reflux: An Improved In-Situ Recovery Method for Oil Sands;* SPE Canada Heavy Oil Technical Conference; Society of Petroleum Engineers: 2016; .

16. Yen, T. F.; Erdman, J. G.; Saraceno, A. Investigation of the Nature of Free Radicals in Petroleum Asphaltenes and Related Substances by Electron Spin Resonance. *Anal. Chem.* **1962***, 34*, 694-700.

17. Palmer, R. C. Developments in terpene chemicals. *Industrial & Engineering Chemistry* **1942***, 34*, 1028-1034.

18. McCormick, H. Ceiling temperature of α-methylstyrene. *Journal of Polymer Science* **1957***, 25*, 488-490.

19. Silverstein, R. M.; Bassler, G. C.; Morrill, T. C. *Spectroscopic identification of organic compounds*. Wiley, New York **1981**, 95-105.

20. Morgenthaler, J.; Rüchardt, C. New Hydrogen Transfer Catalysts. *European Journal of Organic Chemistry* **1999**, 2219-2230.

21. Hoffmann, H. The ene reaction. *Angewandte Chemie International Edition in English* **1969***, 8*, 556-577.

22. Rüchardt, C.; Gerst, M.; Ebenhoch, J. Uncatalyzed Transfer Hydrogenation and Transfer Hydrogenolysis: Two Novel Types of Hydrogen Transfer Reactions. *Angewandte Chemie International Edition in English* **1997***, 36*, 1406-1430.

23. Zou, R.; Liu, L. Role of Asphaltenes in Petroleum Cracking and Refining. *Developments in Petroleum Science* **1994***, 40*, 339-363.

24. Strausz, O.; Jha, K. N.; Montgomery, D. S. Chemical composition of gases in Athabasca bitumen and in low-temperature thermolysis of oil sand, asphaltene and maltene. *Fuel* **1977***, 56*, 114-120.

25. Rüchardt, C.; Gerst, M.; Ebenhoch, J. Uncatalyzed Transfer Hydrogenation and Transfer Hydrogenolysis: Two Novel Types of Hydrogen-Transfer Reactions. *Angewandte Chemie International Edition in English* **1997***, 36*, 1406-1430.

26. Campbell, J.; Teymour, F.; Morbidelli, M. High temperature free radical polymerization. 1. Investigation of continuous styrene polymerization. *Macromolecules* **2003***, 36*, 5491-5501.

27. Braude, E.; Jackman, L.; Linstead, R. Hydrogen transfer. Part II. The dehydrogenation of 1: 4-dihydronaphthalene by quinones. Kinetics and mechanism. *Journal of the Chemical Society (Resumed)* **1954**, 3548-3563.

28. Braude, E.; Jackman, L.; Linstead, R. Hydrogen transfer. Part III. The dehydrogenation of hydroaromatic hydrocarbons by quinones. Quantitative comparison of donors. *Journal of the Chemical Society (Resumed)* **1954**, 3564-3568.

29. Benson, S. W. On the reaction between ethylene and cyclopentene, a radical mechanism. *Int J Chem Kinet* **1980***, 12*, 755-760.

30. Metzger, J. O. Bildung von Alkylradikalen durch thermische bimolekulare Reaktion von Alkanen und Alkenen. *Angewandte Chemie International Edition in English* **1983***, 22*, 1256-1267.

31. Kossiakoff, A.; Rice, F. O. Thermal Decomposition of Hydrocarbons, Resonance Stabilization and Isomerization of Free Radicals1. *J. Am. Chem. Soc.* **1943***, 65*, 590-595.

32. Neuman Jr, R. C.; Alhadeff, E. S. Coupling and disproportionation reactions of cumyl radical--cyclohexyl radical pairs from. alpha.-cumylazocyclohexane. *J. Org. Chem.* **1970***, 35*, 3401-3405.

33. McMillen, D. F.; Golden, D. M. Hydrocarbon bond dissociation energies. *Annu. Rev. Phys. Chem.* **1982***, 33*, 493-532.

34. Lu, M.; Mulholland, J. A. Aromatic hydrocarbon growth from indene. *Chemosphere* **2001***, 42*, 625-633.

35. Mullins, O. C.; Sabbah, H.; Eyssautier, J.; Pomerantz, A. E.; Barré, L.; Andrews, A. B.; Ruiz-Morales, Y.; Mostowfi, F.; McFarlane, R.; Goual, L. Advances in asphaltene science and the Yen–Mullins model. *Energy Fuels* **2012***, 26*, 3986-4003.

36. Schuler, B.; Meyer, G.; Pena, D.; Mullins, O. C.; Gross, L. Unraveling the molecular structures of asphaltenes by atomic force microscopy. *J. Am. Chem. Soc.* **2015***, 137*, 9870-9876.

37. Roth, W. R.; Unger, C.; Wasser, T. Resonanzenergie von Diradikalen—1, 8-Naphthoquinodimethan. *Liebigs Annalen* **1996***, 1996*, 2155-2169.

38. Clar, E.; Kemp, W.; Stewart, D. G. The significance of Kekulé structures for the stability of aromatic systems. *Tetrahedron* **1958***, 3*, 325-333.

39. Clar, E.; Macpherson, I. A. The significance of Kekulé structures for the stability of aromatic systems—II. *Tetrahedron* **1962**, *18*, 1411-1416.

40. Niizuma, S.; Steele, C. T.; Gunning, H. E.; Strausz, O. P. Electron spin resonance study of free radicals in Athabasca asphaltene. *Fuel* **1977**, *56*, 249-256.

41. McMillen, D. F.; Malhotra, R.; Chang, S.; Ogier, W. C.; Nigenda, S. E.; Fleming, R. H. Mechanisms of hydrogen transfer and bond scission of strongly bonded coal structures in donor-solvent systems. *Fuel* **1987**, *66*, 1611-1620.

42. Bukowski, A.; Milczarska, T. Asphalts as inhibitors of radical polymerization. *J Appl Polym Sci* **1983**, *28*, 1001-1009.

43. Zachariah, A.; de Klerk, A. Thermal Conversion Regimes for Oilsands Bitumen. *Energy Fuels* **2016**, *30*, 239-248.

44. Ignasiak, T. M.; Kotlyar, L.; Samman, N.; Montgomery, D. S.; Strausz, O. P. Preparative gel permeation chromatography of Athabasca asphaltene and the relative polymer-forming propensity of the fractions. *Fuel* **1983**, *62*, 363-369.

45. Daaou, M.; Larbi, A.; Martínez-Haya, B.; Rogalski, M. A Comparative study of the chemical structure of asphaltenes from Algerian petroleum collected at different stages of extraction and processing. *Journal of Petroleum Science and Engineering* **2016**, *138*, 50-56.

46. Wiehe, I. A. A phase-separation kinetic model for coke formation. *Ind Eng Chem Res* **1993**, *32*, 2447-2454.

6. CONCLUSIONS

6.1 Introduction

It was postulated that asphaltenes are possibly participating in free radical reactions at temperatures below typical thermal cracking processes. The purpose of this study was to investigate the changes in asphaltenes macroscopic properties, as well as chemical changes and reactions in the temperature range 100–250 °C.

6.2 Major conclusions

i. It was found that asphaltenes undergoes some changes in the temperature range 100–250 °C. One observable change was in the ratio of aromatic and aliphatic hydrogen, as determined by ^{1}H NMR. The most intriguing change was the increase in aromatic hydrogen content of the product relative to that of the feed. There was also an increase in aromatic carbon content by a factor 1.12 relative to the feed after the heating asphaltenes to 150 °C for 1 hour. These changes were accompanied by an increase in the *n*-heptane insoluble content of the product.

ii. Almost no lighted decomposition products were found during heating to 250 °C for 1 hour, with exception of some trapped C_5 constituents. It indicated that cracking was a minor contributor to the reactions in the temperature range studied.

iii. The presence of free radical species in the feed and product was confirmed. The ESR analyses indicated that there was a minor decrease in free radical concentration of product after heating relative to the feed.

iv. Taken collectively (points i to iii), the results suggested that the most important free radical type reactions were hydrogen transfer reactions. Hydrogen transfer reactions could explain the increase of aromatic hydrogen content, as well as free radical addition-combination reactions, which led to an increase in the yield of *n*-heptane insoluble fraction of product due to formation of higher molecular weight addition products.

v. Hydrogen transfer reactions were further investigated by reactions involving mixtures of asphaltenes and model compounds. The extent of hydrogen transfer from asphaltenes was estimated to be around 1.8 mg H/g asphaltenes in 1 h at 250 °C, based on the conversion of α-methylstyrene to cumene.

vi. Cumene did not transfer hydrogen to the asphaltenes, indicating that the free radicals in the asphaltenes are incapable of forming bonds with hydrogen that are stronger than the weakest C–H bond (353 ± 6 kJ/mol) in cumene.

vii. A study of conversion of anthracene and 9,10-dihydroanthracene with asphaltenes at 250 °C suggested that asphaltenes have both acceptor and donor type of compounds. Hydrogen was transferred from asphaltenes to anthracene to produce 9,10-dihydroanthracene, indicating asphaltenes have transferable hydrogen with a bond strength of less than 315 kJ/mol, which is the homolytic bond dissociation energy of the C–H at the 9- and 10-positions of 9,10-dihydroanthracene. On the other hand, twice more hydrogen transferred from 9,10-dihydroanthracene to asphaltenes. Thus, it was deduced that there are also free radicals in asphaltenes capable of forming bonds with hydrogen that were stronger than 315 kJ/mol.

viii. Indirect evidence of the involvement of asphaltenes in the formation of combination or addition products was provided. Cumyl dimers, the products of free radical combination or addition reactions of α-methylstyrene, were identified in the reaction product after reaction of α-methylstyrene in the presence of asphaltenes. No cumyl dimers were found when α-methylstyrene was heated on its own. Thus, the formation of cumyl dimers was induced by the asphaltenes.

ix. Both the temperature and the availability of hydrogen affected the selectivity of hydrogen transfer as opposed to combination or addition reactions.

6.3 Suggested future work

i. The free radical reactions might also be affected by possible involvement of foreign substances, such as mineral constituents that are present in the asphaltenes. This was observed in a related study (not this work) involving transfer reactions in asphaltenes in the presence of metal halides. There are consequently other potential pathways that may lead to analogous observations and these should be explored.

ii. Some important information can be brought to light by studying asphaltenes obtained at various stages of production, or obtained from different sources with different porcessing history. As mentioned, in this work only industrially *n*-pentane extracted asphaltenes from one specific process have been employed. Asphaltenes from different sources do not necessarily have identical compositional properties or reactivity.

6.4 Presentation & Publication

Naghizada, N. ; Prado, G. H. C. and De Klerk, A. Reactivity of Asphaltenes at Low Temperature. In: at the 66th Canadian Chemical Engineering Conference, 2016, Quebec city, Canada.

Naghizada, N. ; Prado, G. H. C. ; De Klerk, A. "Uncatalyzed hydrogen transfer during 100–250 °C conversion of asphaltenes", The manuscript was submitted for publication to *Energy & Fuels*.

BIBLIOGRAPHY

Acevedo, S.; Escobar, G.; Ranaudo, M. A.; Pinate, J.; Amorín, A.; Díaz, M.; Silva, P. Observations about the structure and dispersion of petroleum asphaltenes aggregates obtained from dialysis fractionation and characterization. *Energy Fuels* **1997***, 11*, 774-778.

Acevedo, S.; Escobar, G.; Ranaudo, M. A.; Rizzo, A. Molecular weight properties of asphaltenes calculated from GPC data for octylated asphaltenes. *Fuel* **1998***, 77*, 853-858.

Akbarzadeh, K.; Hammami, A.; Kharrat, A.; Zhang, D.; Allenson, S.; Creek, J.; Kabir, S.; Jamaluddin, A.; Marshall, A. G.; Rodgers, R. P. Asphaltenes—problematic but rich in potential. *Oilfield Review* **2007***, 19*, 22-43.

Alboudwarej, H.; Beck, J.; Svrcek, W.; Yarranton, H.; Akbarzadeh, K. Sensitivity of asphaltene properties to separation techniques. *Energy Fuels* **2002***, 16*, 462-469.

Alemán-Vázquez, L. O.; Torres-Mancera, P.; Ancheyta, J.; Ramírez-Salgado, J. Use of Hydrogen Donors for Partial Upgrading of Heavy Petroleum. *Energy Fuels* **2016***, 30*, 9050-9060.

Alshareef, A. H.; Scherer, A.; Tan, X.; Azyat, K.; Stryker, J. M.; Tykwinski, R. R.; Gray, M. R. Effect of chemical structure on the cracking and coking of archipelago model compounds representative of asphaltenes. *Energy Fuels* **2012***, 26*, 1828-1843.

Baltus, R. E.; Andersen, J. L. Comparison of gpc elution characteristics and diffusion coefficients of asphaltenes. *Fuel* **1984***, 63*, 530-535.

Bansal, V.; Kumar, R.; Krishna, G.; Patel, M.; Sarpal, A.; Basu, B. Transferable hydrogen by 1H nuclear magnetic resonance spectroscopy–Vital structural aspects of petroleum heavier ends (370–660° C) feed stocks. *Fuel* **2014***, 118*, 148-155.

Benson, S. W. On the reaction between ethylene and cyclopentene, a radical mechanism. *Int J Chem Kinet* **1980***, 12*, 755-760.

Billmers, R.; Brown, R.; Stein, S. Hydrogen transfer from 9, 10-dihydrophenanthrene to anthracene. *Int J Chem Kinet* **1989***, 21*, 375-386.

Billmers, R.; Griffith, L.; Stein, S. Hydrogen transfer between anthracene structures. *J. Phys. Chem.* **1986***, 90*, 517-523.

Braude, E.; Jackman, L.; Linstead, R. Hydrogen transfer. Part II. The dehydrogenation of 1: 4-dihydronaphthalene by quinones. Kinetics and mechanism. *Journal of the Chemical Society (Resumed)* **1954**, 3548-3563.

Braude, E.; Jackman, L.; Linstead, R. Hydrogen transfer. Part III. The dehydrogenation of hydroaromatic hydrocarbons by quinones. Quantitative comparison of donors. *Journal of the Chemical Society (Resumed)* **1954**, 3564-3568.

Bukowski, A.; Milczarska, T. Asphalts as inhibitors of radical polymerization. *J Appl Polym Sci* **1983***, 28*, 1001-1009.

Campbell, J.; Teymour, F.; Morbidelli, M. High temperature free radical polymerization. 1. Investigation of continuous styrene polymerization. *Macromolecules* **2003***, 36*, 5491-5501.

Clar, E.; Kemp, W.; Stewart, D. G. The significance of Kekulé structures for the stability of aromatic systems. *Tetrahedron* **1958***, 3*, 325-333.

Clar, E.; Macpherson, I. A. The significance of Kekulé structures for the stability of aromatic systems—II. *Tetrahedron* **1962***, 18*, 1411-1416.

Cyr, N.; McIntyre, D.; Toth, G.; Strausz, O. Hydrocarbon structural group analysis of Athabasca asphaltene and its gpc fractions by 13C nmr. *Fuel* **1987***, 66*, 1709-1714.

Cyr, N.; Selucky, M. L. Nuclear magnetic resonance studies of asphaltenes and coals. A new approach to obtaining asphaltene structural parameters with dipolar dephasing. *Liquid fuels technology* **1985***, 3*, 377-396.

da Costa, L. M.; Stoyanov, S. R.; Gusarov, S.; Tan, X.; Gray, M. R.; Stryker, J. M.; Tykwinski, R.; de M. Carneiro, J Walkimar; Seidl, P. R.; Kovalenko, A. Density functional theory investigation of the contributions of π- π stacking and hydrogen-bonding interactions to the aggregation of model asphaltene compounds. *Energy Fuels* **2012***, 26*, 2727-2735.

Daaou, M.; Larbi, A.; Martínez-Haya, B.; Rogalski, M. A Comparative study of the chemical structure of asphaltenes from Algerian petroleum collected at different stages of extraction and processing. *Journal of Petroleum Science and Engineering* **2016***, 138*, 50-56.

Del Bianco, A.; Zaninelli, M.; Girardi, E. Determination of transferable hydrogen in coal liquefaction solvents by spectroscopic methods. *Fuel* **1986***, 65*, 1062-1066.

Dutta Majumdar, R.; Gerken, M.; Hazendonk, P. Solid-State 1H and 13C Nuclear Magnetic Resonance Spectroscopy of Athabasca Oil Sands Asphaltenes: Evidence for Interlocking π-Stacked Nanoaggregates with Intercalated Alkyl Side Chains. *Energy Fuels* **2015***, 29*, 2790-2800.

Espinat, D.; Fenistein, D.; Barre, L.; Frot, D.; Briolant, Y. Effects of temperature and pressure on asphaltenes agglomeration in toluene. A light, X-ray, and neutron scattering investigation. *Energy Fuels* **2004***, 18*, 1243-1249.

Fetzer, J. The role of the Scholl condensation in the chemistry of catalytic hydrocrackers. *Polycyclic Aromatic Compounds* **1994***, 4*, 19-24.

Franz, J.; Camaioni, D.; Alnajjar, M.; Autrey, T.; Linehan, J. *Fundamental hydrogen transfer studies in coal liquefaction: Understanding the answers and questions* **1995**.

Gerst, M.; Rüchardt, C. Bimolekulare Radikalbildung durch H-Transfer, 2. H-Transferreaktionen mit Phenalen. *Chem. Ber.* **1993***, 126*, 1039-1045.

Gould, K. A.; Wiehe, I. A. Natural hydrogen donors in petroleum resids. *Energy Fuels* **2007***, 21*, 1199-1204.

Gray, M. R. *Upgrading oilsands bitumen and heavy oil;* University of Alberta: 2015; p 284.

Gray, M. R.; Le, T.; McCaffrey, W. C.; Berruti, F.; Soundararajan, S.; Chan, E.; Huq, I.; Thorne, C. Coupling of mass transfer and reaction in coking of thin films of an Athabasca vacuum residue. *Ind Eng Chem Res* **2001***, 40*, 3317-3324.

Gray, M. R.; Tykwinski, R. R.; Stryker, J. M.; Tan, X. Supramolecular assembly model for aggregation of petroleum asphaltenes. *Energy Fuels* **2011***, 25*, 3125-3134.

Groenzin, H.; Mullins, O. C. Asphaltene molecular size and structure. *The Journal of Physical Chemistry A* **1999***, 103*, 11237-11245.

Guillén, M. D.; Díaz, C.; Blanco, C. G. Characterization of coal tar pitches with different softening points by 1H NMR: role of the different kinds of protons in the thermal process. *Fuel Process Technol* **1998***, 58*, 1-15.

Guo, A.; Wang, Z.; Zhang, H.; Zhang, X.; Wang, Z. Hydrogen transfer and coking propensity of petroleum residues under thermal processing. *Energy Fuels* **2010***, 24*, 3093-3100.

Guo, A.; Zhang, X.; Zhang, H.; Wang, Z.; Wang, Z. Aromatization of naphthenic ring structures and relationships between feed composition and coke formation during heavy oil carbonization. *Energy Fuels* **2009***, 24*, 525-532.

Harding, T. G.; Zanon, S.; Imran, M.; Kerr, R. K. In *In In-Situ Reflux: An Improved In-Situ Recovery Method for Oil Sands;* SPE Canada Heavy Oil Technical Conference; Society of Petroleum Engineers: 2016; .

Hoffmann, H. The ene reaction. *Angewandte Chemie International Edition in English* **1969***, 8*, 556-577.

Hortal, A. R.; Martínez-Haya, B.; Lobato, M. D.; Pedrosa, J. M.; Lago, S. On the determination of molecular weight distributions of asphaltenes and their aggregates in laser desorption ionization experiments. *Journal of mass spectrometry* **2006***, 41*, 960-968.

Hurtado, P.; Hortal, A. R.; Martínez-Haya, B. Matrix-assisted laser desorption/ionization detection of carbonaceous compounds in ionic liquid matrices. *Rapid Communications in Mass Spectrometry* **2007***, 21*, 3161-3164.

Ignasiak, T. M.; Kotlyar, L.; Samman, N.; Montgomery, D. S.; Strausz, O. P. Preparative gel permeation chromatography of Athabasca asphaltene and the relative polymer-forming propensity of the fractions. *Fuel* **1983***, 62*, 363-369.

Ignasiak, T.; Kemp-Jones, A.; Strausz, O. The molecular structure of Athabasca asphaltene. Cleavage of the carbon-sulfur bonds by radical ion electron transfer reactions. *J. Org. Chem.* **1977***, 42*, 312-320.

Jha, K.; Montgomery, D.; Strausz, O.; Strausz, O.; Lown, E. Chemical composition of gases in Alberta bitumens and in low-temperature thermolysis of oil sand asphaltenes and maltenes. In *Oil sand and oil shale chemistry*; Strausz, O. P., Lown, E. M., Eds.; Verlag Chemie: New York, 1978; pp 33-54.

Karimi, A.; Qian, K.; Olmstead, W. N.; Freund, H.; Yung, C.; Gray, M. R. Quantitative evidence for bridged structures in asphaltenes by thin film pyrolysis. *Energy Fuels* **2011***, 25*, 3581-3589.

Kossiakoff, A.; Rice, F. O. Thermal Decomposition of Hydrocarbons, Resonance Stabilization and Isomerization of Free Radicals1. *J. Am. Chem. Soc.* **1943***, 65*, 590-595.

La Cava, A. I; Trimm, D. L.; Turner, C. E. Catalytic effects during the thermal cracking of hydrocarbons. *Revista portuguesa de quimica* **1977**, *19,* 345-349.

Lababidi, H. M.; Sabti, H. M.; AlHumaidan, F. S. Changes in asphaltenes during thermal cracking of residual oils. *Fuel* **2014***, 117*, 59-67.

Larter, S. R.; Bennett, B.; Snowdon, L. R.; Jiang, C. D.; Adams, J. J.; Gates, I. D.; Noke, K. J. Method for measurement of crude oil and bitumen dead oil viscosity and density. U.S. Patent No. 8,336,370 , December 25, **2012**.

Le Page, J.; Chatila, S. G.; Davidson, M. *Resid and heavy oil processing;* Editions Technip: Paris, 1992.

Lian, H.; Lin, J.; Yen, T. F. Peptization studies of asphaltene and solubility parameter spectra. *Fuel* **1994***, 73*, 423-428.

Liao, Z.; Zhao, J.; Creux, P.; Yang, C. Discussion on the structural features of asphaltene molecules. *Energy Fuels* **2009***, 23*, 6272-6274.

Lu, M.; Mulholland, J. A. Aromatic hydrocarbon growth from indene. *Chemosphere* **2001***, 42*, 625-633.

Malhotra, V. M.; Buckmaster, H. A. 34 GHz epr study of vanadyl complexes in various asphaltenes: Statistical correlative model of the coordinating ligands. *Fuel* **1985***, 64*, 335-341.

Manka, M.; Brown, R.; Stein, S. Rate constants for hydrogen abstraction by resonance stabilized radicals in high temperature liquids. *Int J Chem Kinet* **1987***, 19*, 943-957.

Mannistu, K.; Yarranton, H.; Masliyah, J. Solubility modeling of asphaltenes in organic solvents. *Energy Fuels* **1997***, 11*, 615-622.

Martínez Haya, B.; Hortal, A. R.; Hurtado, P.; Lobato, M. D.; Pedrosa, J. M. Laser desorption/ionization determination of molecular weight distributions of polyaromatic carbonaceous compounds and their aggregates. *Journal of mass spectrometry* **2007***, 42*, 701-713.

McCormick, H. Ceiling temperature of α-methylstyrene. *Journal of Polymer Science* **1957***, 25*, 488-490.

McMillen, D. F.; Golden, D. M. Hydrocarbon bond dissociation energies. *Annu. Rev. Phys. Chem.* **1982***, 33*, 493-532.

McMillen, D. F.; Malhotra, R.; Chang, S.; Ogier, W. C.; Nigenda, S. E.; Fleming, R. H. Mechanisms of hydrogen transfer and bond scission of strongly bonded coal structures in donor-solvent systems. *Fuel* **1987***, 66*, 1611-1620.

McMillen, D. F.; Malhotra, R.; Nigenda, S. E. The case for induced bond scission during coal pyrolysis. *Fuel* **1989***, 68*, 380-386.

Metzger, J. O. Bildung von Alkylradikalen durch thermische bimolekulare Reaktion von Alkanen und Alkenen. *Angewandte Chemie International Edition in English* **1983***, 22*, 1256-1267.

Morgenthaler, J.; Rüchardt, C. Bimolecular Formation of Radicals by Hydrogen Transfer, 11. Transfer Hydrogenation of Conjugated Cyclic Dienes and Trienes. *Liebigs Annalen* **1996**, 1529-1532.

Morgenthaler, J.; Rüchardt, C. New hydrogen transfer catalysts. *European journal of organic chemistry* **1999***, 1999*, 2219-2230.

Moschopedis, S. E.; Parkash, S.; Speight, J. G. Thermal decomposition of asphaltenes. *Fuel* **1978***, 57*, 431-434.

Mujica, V.; Nieto, P.; Puerta, L.; Acevedo, S. Caging of molecules by asphaltenes. A model for free radical preservation in crude oils. *Energy Fuels* **2000***, 14*, 632-639.

Mullins, O. C. Review of the molecular structure and aggregation of asphaltenes and petroleomics. *Spe Journal* **2008***, 13*, 48-57.

Mullins, O. C. The asphaltenes. *Annual Review of Analytical Chemistry* **2011***, 4*, 393-418.

Mullins, O. C.; Sabbah, H.; Eyssautier, J.; Pomerantz, A. E.; Barré, L.; Andrews, A. B.; Ruiz-Morales, Y.; Mostowfi, F.; McFarlane, R.; Goual, L. Advances in asphaltene science and the Yen–Mullins model. *Energy Fuels* **2012***, 26*, 3986-4003.

Neuman Jr, R. C.; Alhadeff, E. S. Coupling and disproportionation reactions of cumyl radical--cyclohexyl radical pairs from. alpha.-cumylazocyclohexane. *J. Org. Chem.* **1970***, 35*, 3401-3405.

Niizuma, S.; Steele, C. T.; Gunning, H. E.; Strausz, O. P. Electron spin resonance study of free radicals in Athabasca asphaltene. *Fuel* **1977***, 56*, 249-256.

Palmer, R. C. Developments in terpene chemicals. *Industrial & Engineering Chemistry* **1942***, 34*, 1028-1034.

Parsons, A. F. *An introduction to free radical chemistry;* Wiley-Blackwell: 2000.

Ping'an, P.; Angelina, M. I.; Alan, H.; and Otto, P. S. Molecular Structure of Athabasca Asphaltene: Sulfide, Ether, and Ester Linkages. **1997***, 11 (6)*, 1171–1187.

Poutsma, M. L. Free-radical thermolysis and hydrogenolysis of model hydrocarbons relevant to processing of coal. *Energy Fuels* **1990***, 4*, 113-131.

Rahmani, S.; McCaffrey, W.; Gray, M. R. Kinetics of solvent interactions with asphaltenes during coke formation. *Energy Fuels* **2002***, 16*, 148-154.

Rodgers, R. P.; Marshall, A. G. Petroleomics: Advanced characterization of petroleum-derived materials by Fourier transform ion cyclotron resonance mass spectrometry (FT-ICR MS). In *Asphaltenes, Heavy Oils, and Petroleomics*Springer; Mullings, O. C., Sheu, E.Y., Hammami, A., Marshall, A.G., Eds.; Springer: New York, 2007; pp 63-93.

Roth, W. R.; Unger, C.; Wasser, T. Resonanzenergie von Diradikalen—1, 8-Naphthoquinodimethan. *Liebigs Annalen* **1996***, 1996*, 2155-2169.

Rüchardt, C.; Gerst, M.; Ebenhoch, J. Uncatalyzed Transfer Hydrogenation and Transfer Hydrogenolysis: Two Novel Types of Hydrogen-Transfer Reactions. *Angewandte Chemie International Edition in English* **1997***, 36*, 1406-1430.

Rüchardt, C.; Gerst, M.; Nölke, M. The Uncatalyzed Transfer Hydrogenation of α-Methylstyrene by Dihydroanthracene or Xanthene—a Radical Reaction. *Angewandte Chemie International Edition in English* **1992***, 31*, 1523-1525.

Rüchardt, C.; Gerst, M.; Nölke, M. The Uncatalyzed Transfer Hydrogenation of α-Methylstyrene by Dihydroanthracene or Xanthene—a Radical Reaction. *Angewandte Chemie International Edition in English* **1992***, 31*, 1523-1525.

S Stein, S.E. A fundamental chemical kinetics approach to coal conversion. In *New Approaches in Coal Chemistry*, ACS Symposium Series, 169; Blaustein, B.D; Bockrath, B.C; Friedman, S., Eds.; Americal Chemical Society; Washington, DC, 1981; pp 97-129.

Sanford, E. C.; Xu, C. M. Relationship between solids formation, residuum conversion, liquid yields and losses during athabasca bitumen processing in the presence of a variety of chemicals. *The Canadian Journal of Chemical Engineering* **1996***, 74*, 347-352.

Saraceno, A.; Fanale, D.; Coggeshall, N. An electron paramagnetic resonance investigation of vanadium in petroleum oils. *Anal. Chem.* **1961***, 33*, 500-505.

Schuler, B.; Meyer, G.; Pena, D.; Mullins, O. C.; Gross, L. Unraveling the molecular structures of asphaltenes by atomic force microscopy. *J. Am. Chem. Soc.* **2015***, 137*, 9870-9876.

Schultz, K. F.; Selucky, M. L. Esr measurements on asphaltene and resin fractions from various separation methods. *Fuel* **1981***, 60*, 951-956.

Silverstein, R. M.; Bassler, G. C.; Morrill, T. C. Spectroscopic identification of organic compounds. *Wiley, New York* **1981**, 95-105.

Silverstein, R. M.; Webster, F. X.; Kiemle, D. J.; Bryce, D. L. *Spectrometric identification of organic compounds;* John Wiley & Sons: 2014.

Speight, J. G.; Long, R. B.; Trowbridge, T. D. Factors influencing the separation of asphaltenes from heavy petroleum feedstocks. *Fuel* **1984***, 63*, 616-620.

Speight, J. Petroleum Asphaltenes-Part 1: Asphaltenes, resins and the structure of petroleum. *Oil & gas science and technology* **2004***, 59*, 467-477.

Speight, J.; Wernick, D.; Gould, K.; Overfield, R.; Rao, B. Molecular weight and association of asphaltenes: a critical review. *Revue de l'Institut français du pétrole* **1985***, 40*, 51-61.

Standard, A. D6560-12. *Test Method for Determination of Asphaltenes (Heptane Insolubles) in Crude Petroleum and Petroleum Products, ASTM International, West Conshohocken, PA* **2012**.

Stein, S. E. Thermal reactions and properties of polycyclic aromatic hydrocarbons. *Acc. Chem. Res.* **1991***, 24*, 350-356.

Strausz, O. P.; Lown, E. M. *The chemistry of Alberta oil sands, bitumens and heavy oils;* Alberta Energy Research Institute Calgary, Alberta, Canada: 2003.

Strausz, O. P.; Mojelsky, T. W.; Faraji, F.; Lown, E. M.; Peng, P. Additional structural details on Athabasca asphaltene and their ramifications. *Energy Fuels* **1999***, 13*, 207-227.

Strausz, O. P.; Mojelsky, T. W.; Lown, E. M. The molecular structure of asphaltene: an unfolding story. *Fuel* **1992***, 71*, 1355-1363.

Strausz, O.; Jha, K. N.; Montgomery, D. S. Chemical composition of gases in Athabasca bitumen and in low-temperature thermolysis of oil sand, asphaltene and maltene. *Fuel* **1977***, 56*, 114-120.

Strausz, O.; Lown, E. *The Chemistry of Alberta Oil Sands, Bitumens and Heavy Oils.* Alberta Energy Research Institute (AERI): Calgary, Alberta, 2003.

Styles, Y.; de Klerk, A. Sodium Conversion of Oilsands Bitumen-Derived Asphaltenes. *Energy Fuels* **2016***, 30 (7)*, 5214-5222.

Tan, X.; Fenniri, H.; Gray, M. R. Water enhances the aggregation of model asphaltenes in solution via hydrogen bonding. *Energy Fuels* **2009***, 23*, 3687-3693.

Taylor, S. D.; Czarnecki, J.; Masliyah, J. Refractive index measurements of diluted bitumen solutions. *Fuel* **2001***, 80*, 2013-2018.

Thawer, R.; Nicoll, D. C.; Dick, G. Asphaltene deposition in production facilities. *Spe production engineering* **1990***, 5*, 475-480.

Wang, Z.; Ji, S.; Liu, H.; Chen, K.; Guo, A. Hydrogen Transfer of Petroleum Residue Subfractions During Thermal Processing under Hydrogen. *Energy Technology* **2015***, 3*, 259-264.

Wiehe, I. A. A phase-separation kinetic model for coke formation. *Industrial and Engineering Chemistry Research;(United States)* **1993***, 32*.

Wiehe, I. A. A phase-separation kinetic model for coke formation. *Ind Eng Chem Res* **1993***, 32*, 2447-2454.

Wiehe, I. A. *Process chemistry of petroleum macromolecules.* CRC press: Boca Raton, FL, 2008.

Wiehe, I. A. *Process chemistry of petroleum macromolecules;* CRC press: 2008; p 27.

Yen, T. F.; Erdman, J. G.; Saraceno, A. Investigation of the Nature of Free Radicals in Petroleum Asphaltenes and Related Substances by Electron Spin Resonance. *Anal. Chem.* **1962***, 34*, 694-700.

Yen, T. F.; Erdman, J. G.; Saraceno, A. Investigation of the Nature of Free Radicals in Petroleum Asphaltenes and Related Substances by Electron Spin Resonance. *Anal. Chem.* **1962***, 34*, 694-700.

Zachariah, A.; de Klerk, A. Thermal Conversion Regimes for Oilsands Bitumen. *Energy Fuels* **2016***, 30*, 239-248.

Zou, R.; Liu, L. Role of Asphaltenes in Petroleum Cracking and Refining. *Developments in Petroleum Science* **1994***, 40*, 339-363.

Appendix A Support information for the chapter 3

Appendix A.1 Schematic of the reactor

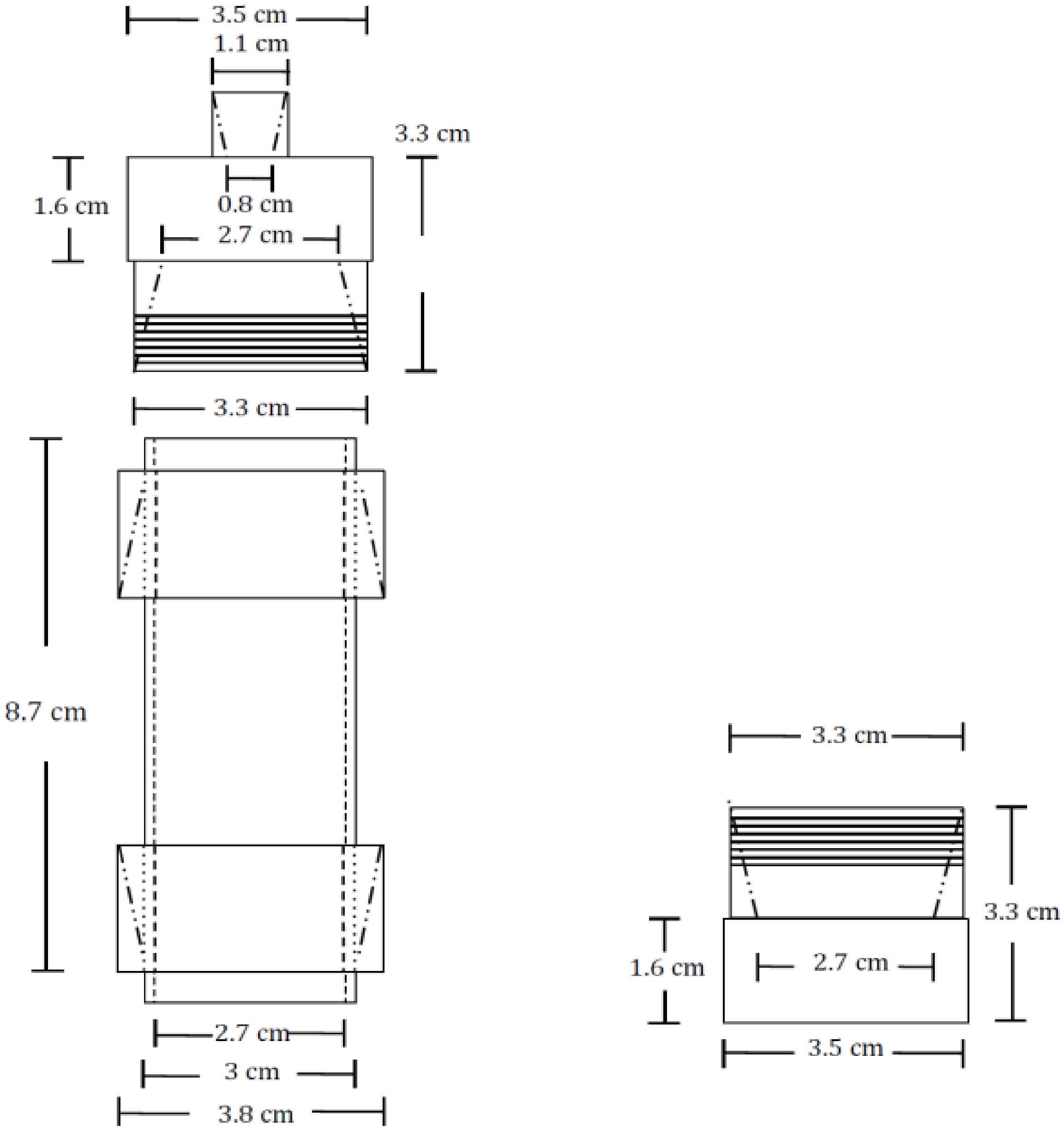

Figure A.1. A schematic of the batch reactor

Appendix A.2 ^{1}H NMR spectra of asphaltenes

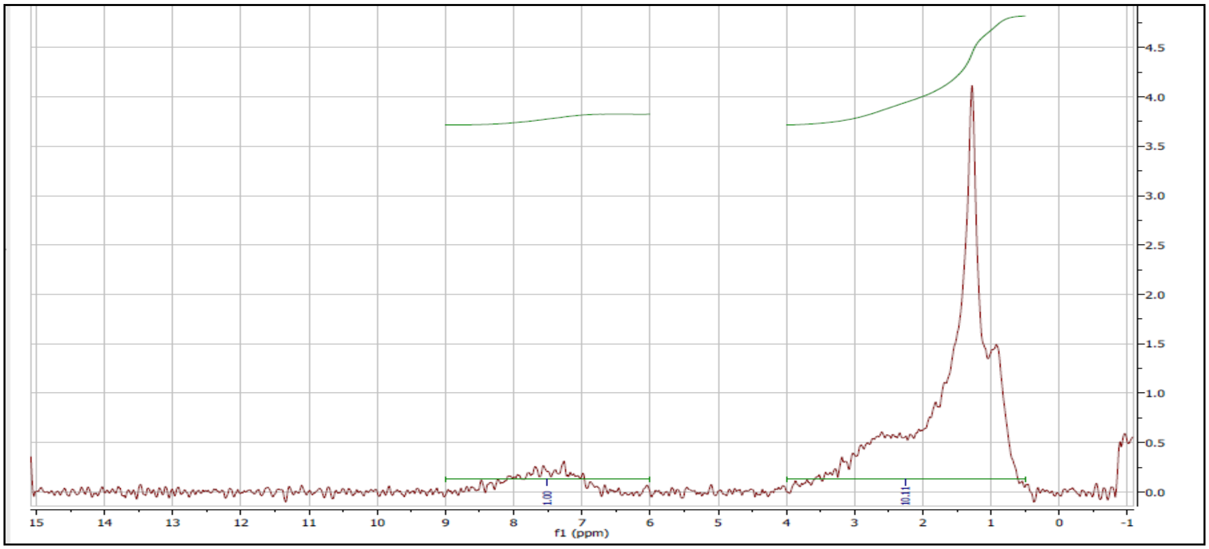

Figure A.2. ^{1}H NMR spectra of asphaltenes

Appendix A.3 Material Balance

All the experiments were conducted in triplicate and results were reported as an average with one sample standard deviation, this is shown in Table A.1. .

Table A.1. Mass balance (wt %) for thermal conversion reactions at 150 °C and initial pressure of 4 MPa.

	Material balance [wt %]	
Samples	x	s
(b.1)	99.2	1.2
(b.2) and (b.3) [b]	101.8	0.89
(b.4)	98.6	0.66

[a] Average (x) and sample standard deviation (s) of three experiments are reported
[b] (b.2) and (b.3) are from same vial.

Amount of feed and amount of toluene used for the recovery of the following samples: (b.2) and (b.3) has been reported in Table A.2. The data in Table A.3 include mass of asphaltenes feed for the preparation of samples: (b.1) and (b.4) that were recovered manually from the vial and micro-batch reactor respectively.

Table A.2 Mass of feed loaded into vials, mass of product recovered and amount of toluene used for procedure

	(b.2)		(b.3)	
Mass loaded into vial [g]	Product recovered manually [g]	Toluene amount to dissolve [g]	Product recovered with solvent [g]	Toluene amount used for recovery [g]
4.03	1.13	77	2.9	200
4.13	1.36	100	2.77	215
4.1	1.23	92	2.87	210

In each case, (b.2) and (b.3) has same concentration.

Table A.3. Mass loaded into reactor and mass of product recovered.

Samples	Mass loaded [g]		Mass recovered [g]	
	x	s	x	s
(b.1)	4.11	0.02	4.05	0.06
(b.4)	4.15	0.04	4.02	0.04

Appendix B Support information for the chapter 3

Appendix B.1 Material Balance

All the experiments were conducted in triplicate and results were reported as an average with one sample standard deviation, this is shown in Table B.4. Additionally, the mass of feed and the mass of the product that was recovered manually were reported in Table B.5.

Table B.4. Mass balance (wt %) for thermal conversion reactions at 100-150 °C and initial pressure of 4 MPa for different reaction times.

Reaction temperature [a] [°C]	Material balance [wt %]	
	x	s
100	101.8	0.73
110	102.8	0.51
120	99.5	0.34
130	101.2	1.1
140	100.8	0.35
150	101.1	0.48

[a] Average (x) and sample standard deviation (s) of three experiments are reported.

Table B.5 Mass of feed loaded, mass of product recovered manually and mass of gas released from the reactor

Temperature [a] [°C]	Mass loaded [g]		Mass unloaded [g]		Gas [g]	
	x	s	x	s	x	s
100	5.05	0.01	4.92	0.08	0.03	0.01
110	5.01	0.00	4.90	0.03	0.02	0.02
120	5.03	0.02	4.88	0.07	0.03	0.02
130	5.05	0.02	4.90	0.02	0.04	0.01
140	5.06	0.01	4.91	0.04	0.04	0.00
150	5.09	0.02	4.94	0.01	0.04	0.01

[a] Average (x) and sample standard deviation (s) of three experiments are reported

Appendix C Support information for the CHAPTER 5

Appendix C.1 Temperature time profile for batch reactors.

The temperature-time profiles for both heating and cooling period were recorded and presented in Figure C.3 and Figure C.4.

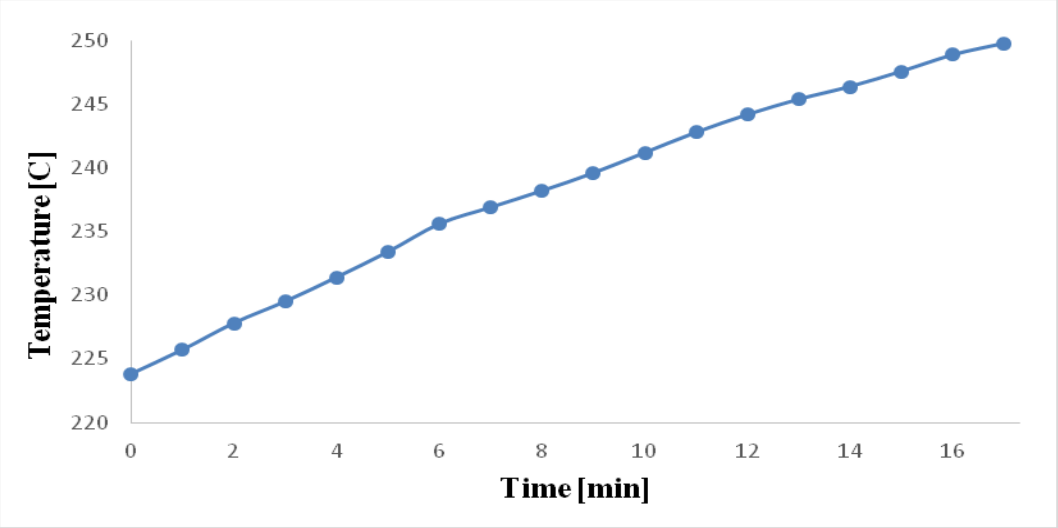

Figure C.3 Temperature time profile for batch reactors.

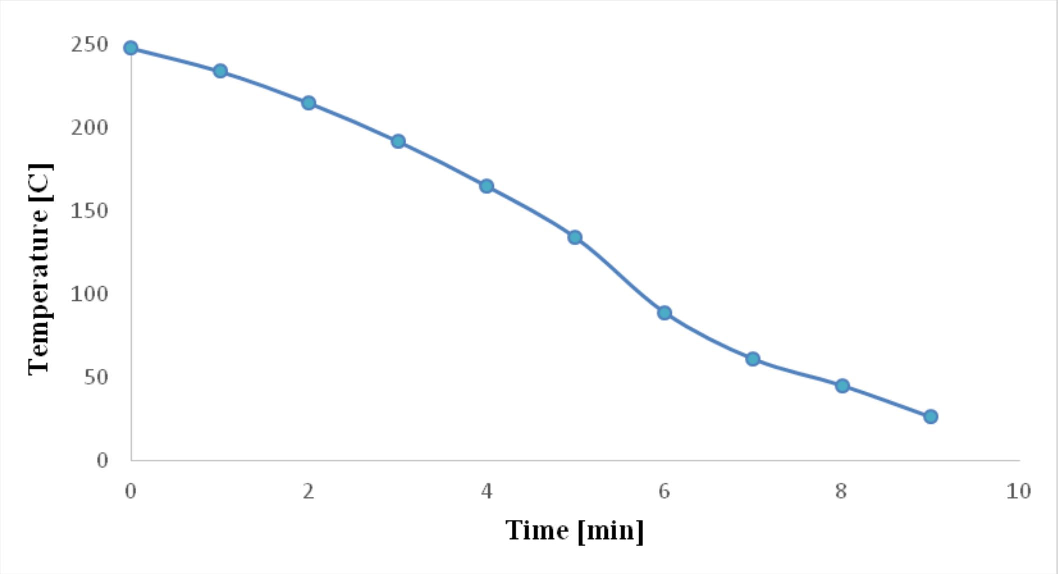

Figure C.4 Temperature time profile for cooling period of reactor after reaction.

Appendix C.2 Calibration curves for the quantitative analysis of α-methylstyrene and cumene

Quantification of the components was performed by using the biphenyl as internal standard throughout all analysis for higher accuracy. The calibration curves consist of three levels with concentrations up to 5 mg/ml for α-methylstyrene (0.5, 2 and 5mg/ml) and 0.2 mg/ml for a cumene (0.05, 0.1 and 0.2 mg/ml) with a known concentration of biphenyl (0.1 mg/ml). All samples were injected in triplicate and each point on the curve corresponds to average value. The ratio of the concentration of the sample and the standard are plotted against the ratio of area of the two compounds in the mixture. The details for both calibration curves were presented in Table C.6 and Table C.7 respectively for cumene and α-methylstyrene. The relationship between the ratio of areas ($A_{cumene}/A_{biphenyl}$, $A_{\alpha\text{-methylstyrene}}/A_{biphenyl}$) and ratio of corresponding concentrations ($C_{cumene}/C_{biphenyl}$, $C_{\alpha\text{-methylstyrene}}/C_{biphenyl}$) are given for both calibration curves. Calibration curves showed regression line coefficients R^2>0.96 (Figure C.5 and Figure C.6).

Table C.6 Details for the calibration curve of cumene.

C_{cumene} [mg/mL]	$C_{biphenyl}$ [mg/mL]	Average (Ab*s) A_{cumene}	$A_{biphenyl}$	$C_{cumene}/C_{biphenyl}$	$A_{cumene}/A_{biphenyl}$
0.05	1	2.55E7	4.38E8	0.05	0.06
0.1	1	4.35E7	4.43E8	0.1	0.10
0.2	1	9.05E7	4.74E8	0.2	0.19

Table C.7 Details for the calibration curve of α-methylstyrene.

		Average (Ab*s)			
$C_{\alpha\text{-methylstyrene}}$ [mg/mL]	C_{biphenyl} [mg/mL]	$A_{\alpha\text{-methylstyrene}}$	A_{biphenyl}	$C_{\alpha\text{-methylstyrene}}/C_{\text{biphenyl}}$	$A_{\alpha\text{-methylstyrene}}/A_{\text{biphenyl}}$
0.5	1	5.16E82	7.05E8	0.5	0.73
2	1	1.26E9	6.83E8	2	1.84
5	1	1.72E9	6.39E8	5	2.69

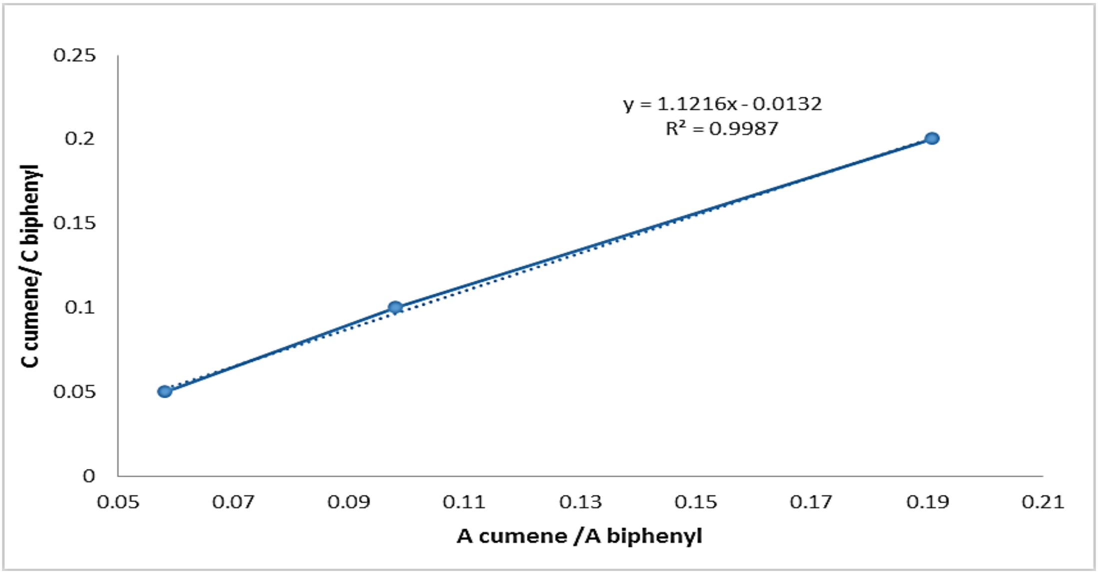

Figure C.5 Calibration curve for cumene obtained via GC-MS by using the biphenyl as an internal standard. Regression coefficient and polynomial equation are presented on the figure (A_i – integrated area under the curve of i, C_i- concentration of i).

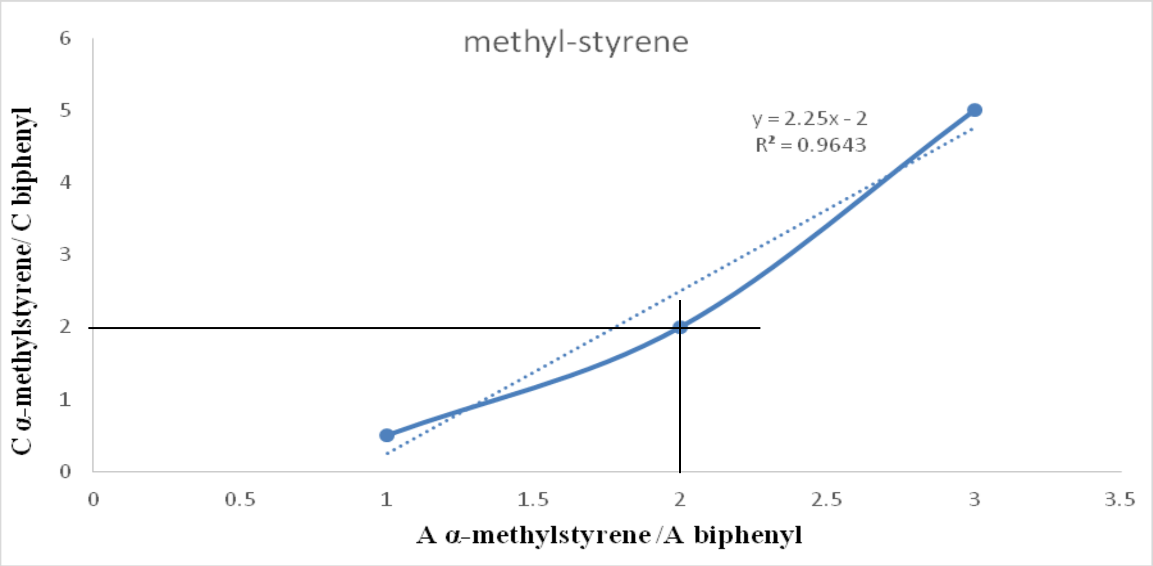

Figure C.6 Calibration curve for α-methylstyrene obtained via GC-MS by using the biphenyl as an internal standard. Regression coefficient and polynomial equation are presented on the figure (A_i – integrated area under the curve of i, C_i- concentration of i).

Appendix C.3 The extraction efficiency and error of quantification

Accuracy of quantification method was tested further by performing control experiments which involved the methanol extraction of cumene and α-methylstyrene without any heating. Same procedure was applied for recovery as shown in the section of 5.2.3.2 in Chapter 5. Comparison of added concentration with measured values were reported for α-methylstyrene and cumene in Table C.8 and Table C.9 respectively. Based on the relative error between values, quantification of compounds is to be trusted, but only for concentrations of 0.4 mg/mL or higher. At concentration of 0.2 mg/mL, error percent was as high as 20 %.

Table C.8 Results for the control experiments for recovery of α-methylstyrene without heating

Added [mg/mL][a]	A-methylstyrene /A biphenyl	C α-methylstyrene/ C biphenyl	Measured [mg/mL]	Relative Error [%]
5	3.18	5.15	5.15	3
3	2.26	3.08	3.08	3

[a]Error value (increments) of pipette is ±5 μL

Table C.9 Results for the control experiments for recovery of cumene without heating.

Added [mg/mL][a]	A cumene /A biphenyl	C cumene/ C biphenyl	Measured [mg/mL]	Relative Error [%]
0.2	0.23	0.24	0.24	20
0.4	0.35	0.38	0.38	-5

[a]Error value (increments) of pipette is ±5 μL

Appendix C.4 Calculation of conversion

Conversion was calculated based on the mass basis. Measured concentration of methylstyrene was converted to mass by a simple calculation which involved multiplication of it to amount of methanol. By using following equation, conversion was calculated:

$$conversion\,(\%\,) = \frac{m_i\ - m_f}{m_i}\ x\ 100$$

where m$_i$ initial mass of of α-methylstyrene and m is final mass of of α-methylstyrene measured after the reaction. Mass of α-methylstyrene for the reactions, volume of solvents for the extraction is given in Table C.10.

Table C.10 Details of α-methylstyrene used for corresponding reactions.[a]

Reactions	Initial volume [μL]	Initial Mass [mg]	Volume of Solvent for extraction [mL]
1-4	659.72	570	100
5	173.61	150	50

[a] See Table 5.2 for experimental details of reactions.

Sample calculation:

Asphaltene + methystyrene	1:1	250 °C	60 minutes

1) Measured concentration of α-methylstyrene after the reaction shown above was 4.78 mg/mL (Table 5.6) which can be converted to the mass of of α-methylstyrene remained after the reaction. Final mass of of α-methylstyrene:

$$m_{final} = \left[c_{\ \alpha\mathrm{-methylstyrene}}\ x\, V_{solvent}\right] = \ 4.78\frac{\mathrm{mg}}{\mathrm{mL}} x 100mL = 478\,mg$$

2) Conversion (%):

$$conversion\,(\%\,) = \frac{m_i\ - m_f}{m_i}\ x\ 100 = \frac{570 - 478}{570} = 16.15\ \%$$

Appendix C.5 Calculation of selectivity and mass balance for the reactions

For the reaction shown in Table 5.7:

It was demonstrated that extractive recovery of reagents from asphaltenes are complete. However, same cannot be said about byproducts. So it is particularly important to report both mass of product recovered and mass of unrecovered products. Otherwise, it assumes that all products have been fully extracted during solvent recovery. Calculation was performed by following steps.

1) Mass of α-methylstyrene and cumene measured can be calculated based on the available concentation data.

$$m_{cumene} = [c_{cumene} \ x \ V_{solvent}] =$$

m – mass, c – concentration, V – solvent, i - component

2) Mass of recovered byproduct was defined semi-quantitatively by following equation:

$$c_{byproduct} = \left[\frac{A_{byproduct}}{A_{internal\ standard}}\right] x \ c_{internal\ standard}$$

$$m_{byproduct} = c_{byproduct} x \ V_{solvent}$$

A – Integrated area under the peak of corresponding compounds

3) Mass of unrecovered product can be calculated by difference in mass between the reagent consumed and product mass.

$$m_{unrecovered\ product} = m_{\alpha-methylstyrene\ consumed} - m_{product}$$

$$m_{\alpha-methylstyrene\ consumed} = m_{initial\ mass} - m_{measured}$$

$$m_{product} = m_{cumene} + m_{byproduct\ recovered}$$

4) Equation for the selectivity:

$$Selectivity\ (\%) = \frac{m_i}{m_{\alpha-methylstyrene\ consumed}}$$

i – cumene , byproducts recovered, unrecovered products.

Sample calculation for following reaction:

Asphaltene + methystyrene	1:1	250 °C	60 minutes

1) From Table 5.4, c $_{\text{cumene}}$ = 0.28 mg/mL and , c $_{\alpha\text{-methylstyrene}}$ = 4.78 mg/mL

$$m_{cumene} = [c_{\ cumene}\ x\ V_{solvent}] = \ 0.2802\frac{mg}{mL}\ x\ 100\ mL = 28.02\ mg$$

$$m_{\alpha-\text{methylstyrenes}} = \left[c_{\ \alpha-\text{methylstyrene}}\ x\ V_{solvent}\right] = \ 4.7795\ \frac{mg}{mL}\ x\ 100\ mL = 477.95\ mg$$

2) Mass of recovered byproduct:

$$c_{byproduct} = \left[\frac{A_{\ byproduct}}{A_{internal\ standard}}\right]\ x\ c_{internal\ standard} = 0.5737$$

$$m_{byproduct} = c_{byproduct} x\ V_{solvent} = 57.37 \text{ mg}$$

3) Mass of unrecovered product:

$$m_{\alpha-methylstyrene\ consumed} = m_{initial\ mass} - m_{measured} = 570\ mg - 477.95\ mg$$
$$= 93.05\ mg$$

$$m_{unrecovered\ product} = m_{\alpha-methylstyrene\ consumed} - m_{product}$$
$$= \ 93.05 - [\ 57.37 + 28.02] = 7.65\ mg$$

4) Selectivity:

$$Selectivity\ (cumene) = \frac{m_i}{m_{\alpha-\text{methylstyrene consumed}}} = \frac{28.02}{93.05}\ x\ 100 = 30.12\ \%$$

$$Selectivity\ (recovered\ byproduct) = \frac{57.37}{92.05}\ x\ 100 = 61.66\ \%$$

$$Selectivity\ (unrecovered\ product) = \frac{7.65}{92.05}\ x\ 100 = 8.22\ \%$$

Similarly, mass of recovered and unrecovered products was calculated for the experiments of 1:1 asphaltenes to α-methylstyrene and results were presented in Table C.11. Also selectivity of each product class was estimated based on the calculated values.

Table C.11 Material balance for the experiments of the 1:1 asphaltenes to α-methylstyrene in the temperatures range of 150 and 250 °C for 1 h.

	Mass [mg]				Selectivity [%]		
Temperature [°C]	α-methylstyrene converted	Cumene	Recovered byproducts	Unrecovered byproducts	Cumene	Recovered byproducts	Unrecovered byroducts
150	0.99	0.00	0.00	0.99	0.00	-	-
180	2.53	2.06	0.00	0.47	81.36	0.00	18.63
200	8.82	7.61	0.00	1.21	86.29	0.00	13.71
220	22.76	18.47	1.35	2.94	81.17	5.93	12.90
250	93.05	28.02	57.37	7.65	30.11	61.66	8.22

[a] For measured concentration of cumene and methylstyrene, see Table 5.4.

Material balance was also performed for the experiments which is shown in Table 5.8, and reported in Table C.12.

Table C.12 Material balance for estimation of unrecovered products.

Reactants[a]	Time (min)	cumene [mg/ml]	Average mass [mg]			
			α-methylstyrene converted	Cumene recovered	Recovered byproducts	Unrecovered products
Asphaltene+ α-methylstyrene (1:1)[b]	60	0.28	93.05	28.02	57.37	7.65
Asphaltene + α-methylstyrene (1:1) [b]	240	0.65	188.61	65.24	99.41	23.96
Asphaltene + methylstyrene (3:1) [c]	60	0.61	141.3	61.06	17.43	63.04
Asphaltene + α-methylstyrene + 9,10-dihydroanthracene (1:2:1) [c]	60	0.84	101.25	83.86	16.43	0.96
9,10-dihydroanthracene+ α-methylstyrene (1:1) [c]	60	0.09	59.76	9.20	x	x

[a] Reaction temperature for all experiments were 250 °C.

x – material balance could not be performed due to unknown product (a dimerization product of α-methylstyrene and 9, 10-dihydroanthracene)

[b] Repeated from Table B.7.

[c] For measured values (concentration, conversion of reagent), see Table 5.7 and Table 5.8.

Appendix C.6 Identification of products from the reaction of 9, 10-dihydroanthracene and α-methylstyrene

The chromatogram of the products from the reaction of α-methylstyrene and 1,9-dihydroantracene at 250 °C is given in Figure C.7. All extracted products are listed in Table C.13.

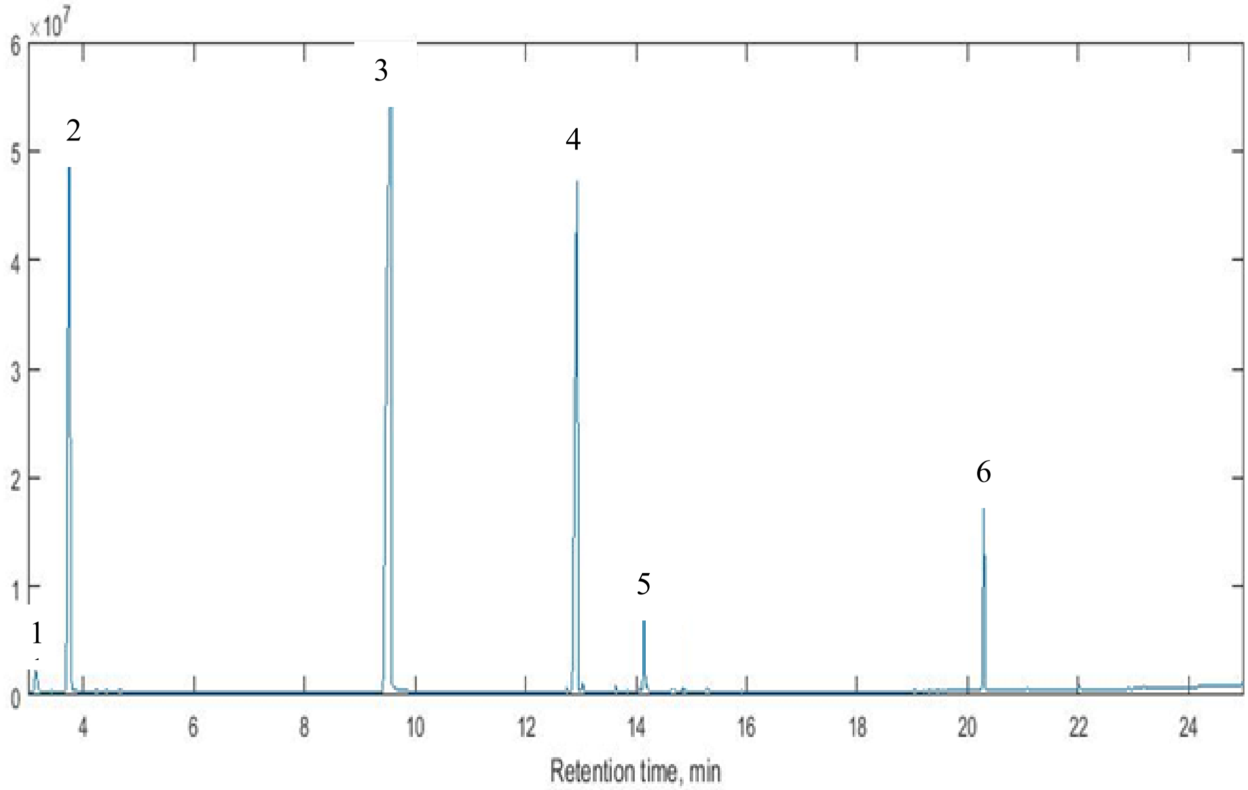

Figure C.7 Chromotogram of reaction products of 1,9-dihydroantracene and α-methylstyrene at 250 °C (Details are presented in Table C.13)

Table C.13 The list of the products was identified by GC-MS from the reaction of α-methylstyrene with asphaltene.

Number	Name	Retention time [min]	Formula
1	cumene	3.12	C_9H_{12}
2	α-methylstyrene	3.75	C_9H_{10}
3	diphenylether	9.51	$C_{12}H_{10}O$
4	9, 10-dihydroanthracene	12.89	$C_{14}H_{12}$
5	anthracene	14.16	C_9H_{10}
6	Not identified[a]	20.31	Not identified

[a] mass spectrum of product 6 is given in Figure C.21.

Mass ionization spectrum of peak, which numbered with 6 in Figure C.7 and Figure C.9, is given in Figure C.8. The molecular ion, M^+ at m/z = 298, and a base peak of m/z 179 can be considered as combination of two following fragments: m/z = 119 (M^++1 of α-methylstyrene) and m/z 179 (M^+-1 of 9,10-dihydroanthracene).

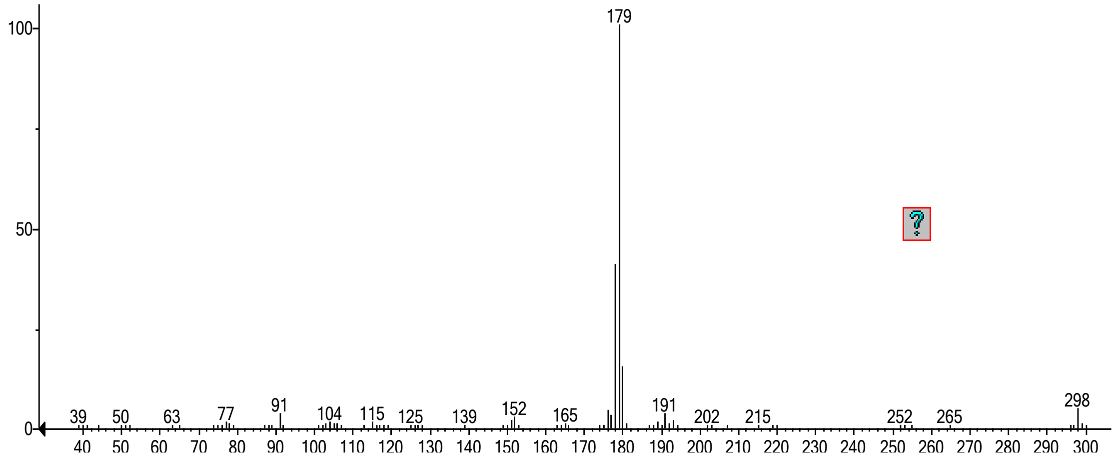

Figure C.8 Mass ionization spectrum of product 6 formed in the reaction of asphaltene and methylstyrene

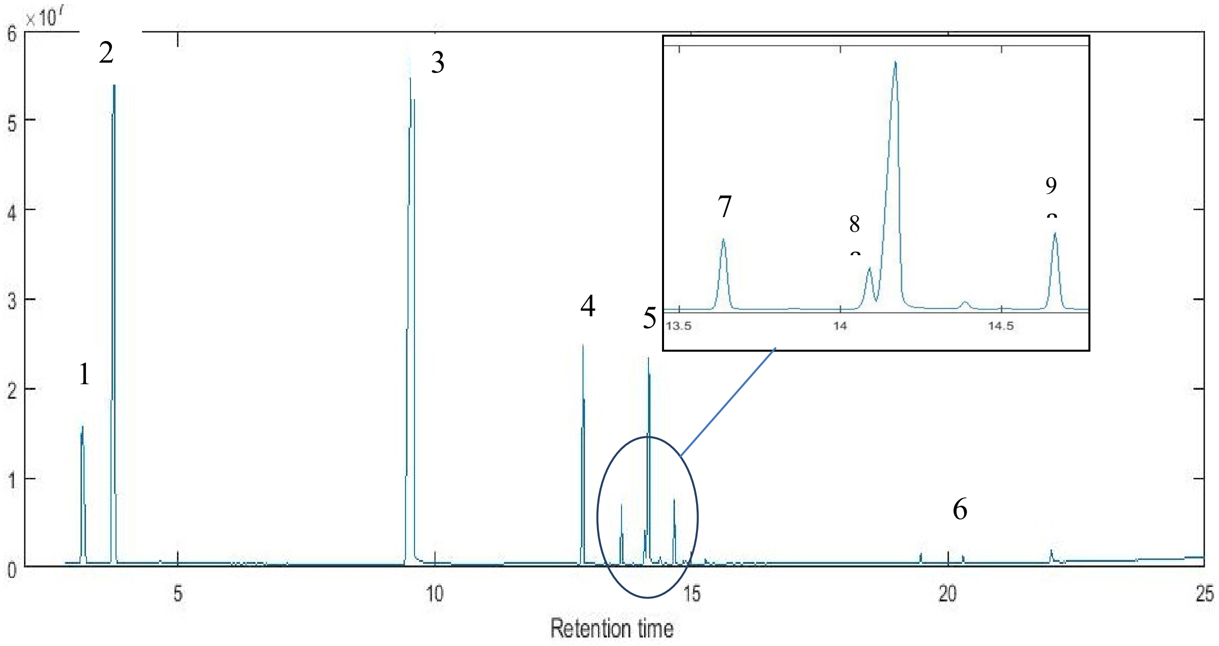

Figure C.9 Chromotogram of reaction products of α-methylstyrene with asphaltenes and 9, 10-dihydroanthracene at 250 °C (Details are presented in Table C.14)

Table C.14 The list of the products was identified by GC-MS (Figure C.9) from the reaction of α-methylstyrene with asphaltenes and 9, 10-dihydroanthracene .

Number[a]	Name	Retention time [min]	Formula
7[b]	Benzene, 1,1'-(1,1,2,2-tetramethyl-1,2-ethanediyl)bis-	13.64	$C_{14}H_{22}$
8[b]	2,4-Diphenyl-4-methyl-1-pentene	14.09	$C_{14}H_{20}$
9[b]	Hex-1-ene,2,5-diphenyl	14.67	$C_{14}H_{20}$

[a] The rest of the products are given in previous table (Table C.13)

[b] Structure of compounds are given in Table 5.3. Mass spectra are shown in Figure C.14, Figure C.15 and Figure C.16 respectively.

In Table C.15, anthracene and 9,10-dihydroanthracene was quantified as area % in the experiment of α-methylstyrene + asphaltene + 9,10-dihydroanthracene and α-methylstyrene + 9,10-dihydroanthracene. Assuming that relative response factor of both compounds is identical, relative concentration might still provide some important information. Relative peak area of 9,10-dihydroanthracene to anthracene greatly reduced after addition of asphaltenes to the reaction α-methylstyrene and 9,10-dihydroanthracene, indicating higher conversion of 9,10-

dihydroanthracene in the presence of asphaltenes. This can be attributed to free radical content of asphaltene which easily forming bond with transferred hydrogen atom from 9,10-dihydroanthracene. It was also observed that dimerization product of α-methylstyrene and 9,10-dihydroanthracene was significantly suppressed in the presence of asphaltenes.

Table C.15 Integrated peak areas of products from the following experiments: α-methylstyrene + asphaltene + 9,10-dihydroanthracene and α-methylstyrene + 9,10-dihydroanthracene at 250 °C (1 h).

Reactions at 250 °C	Area		
	9,10-dihydroanthracene	Anthracene	Byproduct[a]
α-methylstyrene + asphaltene + 9,10-dihydroanthracene	5.04E8	6.30E8	1.89E7
α-methylstyrene + 9,10-dihydroanthracene	1.59E9	1.72E8	3.21E8

[a] dimerization product of 9,10-dehydroanthracene and α-methylstyrene.

Appendix C.7 Mass spectra of the products from the reaction of asphaltene and α-methylstyrene

Electron ionization mass spectrum was used as a tool to deduce the structure of dimers formed in the reaction of asphaltene and α-methylstyrene. The mass spectra of cumene and α-methylstyrene are given in Figure C.10 and Figure C.11 respectively which confirmed with commercial products and can be assisted for the interpretations of the additional products. As seen from spectrums, both cumene and α-methylstyrene can lose either a hydrogen or methyl radical. The high intensity of the peak at m/z 105 indicates that loss of a methyl radical is favoured over hydrogen loss probably due to the greater stability of methyl radicals than hydrogen radical. In a similar fashion, the peak at m/z 103 can be related to the loss of methyl radical. However, from a statistical standpoint the loss of hydrogen radical is very likely to occur in α-methylstyrene which might be attributed to presence of a double bond.

Identification of two dimer compounds was discussed more elaborately in Discussion section 5.4.2. Mass spectra of the dimers are given in Figure C.12 - Figure C.18. Similar fragmentation technique can be applied efficiently for the interpretation of the cumyl radicals. Identities of compounds were also supported by their corresponding spectra in NIST library.

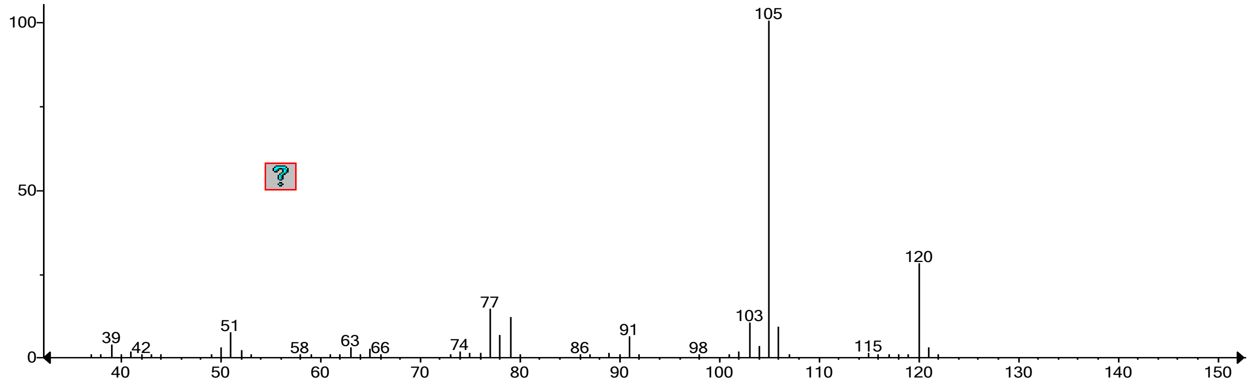

Figure C.10 Mass ionization spectrum of cumene.

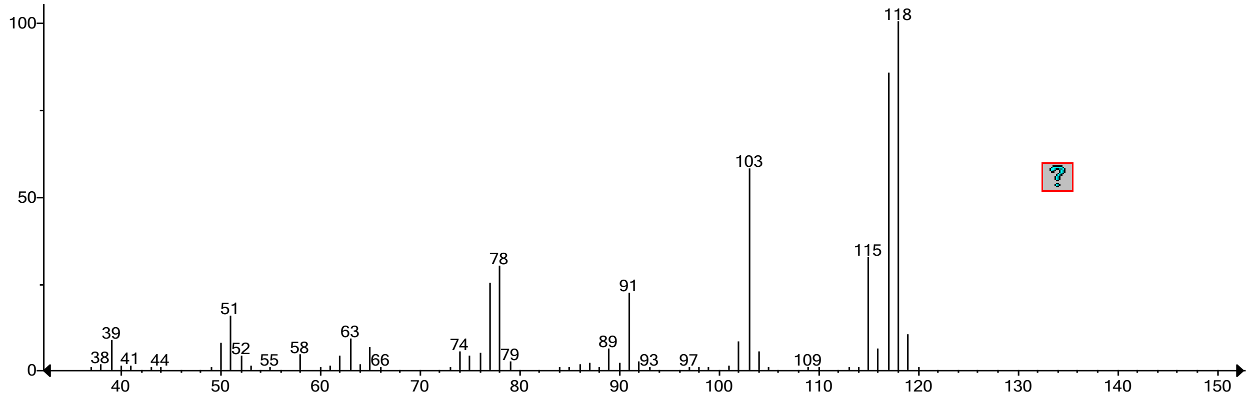

Figure C.11 Mass ionization spectrum of α-methylstyrene

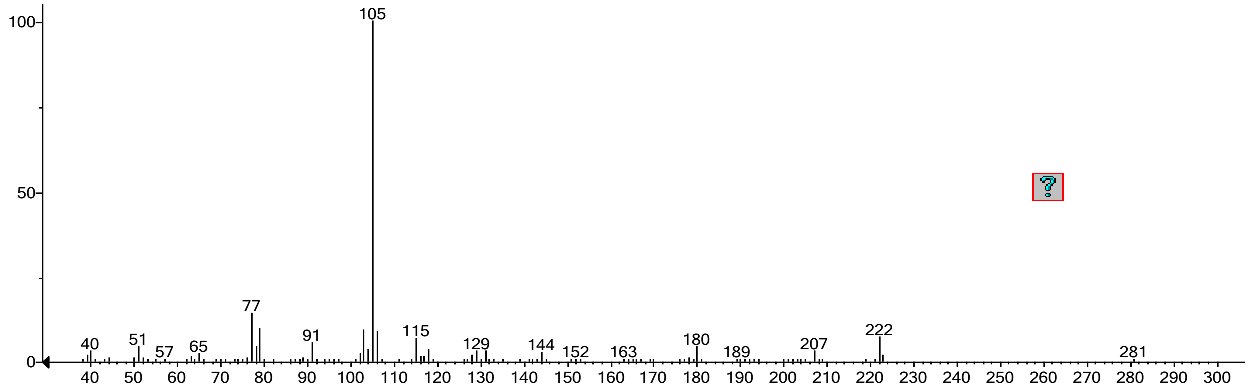

Figure C.12 Mass ionization spectrum of Product 4 formed in the reaction of asphaltene and methylstyrene

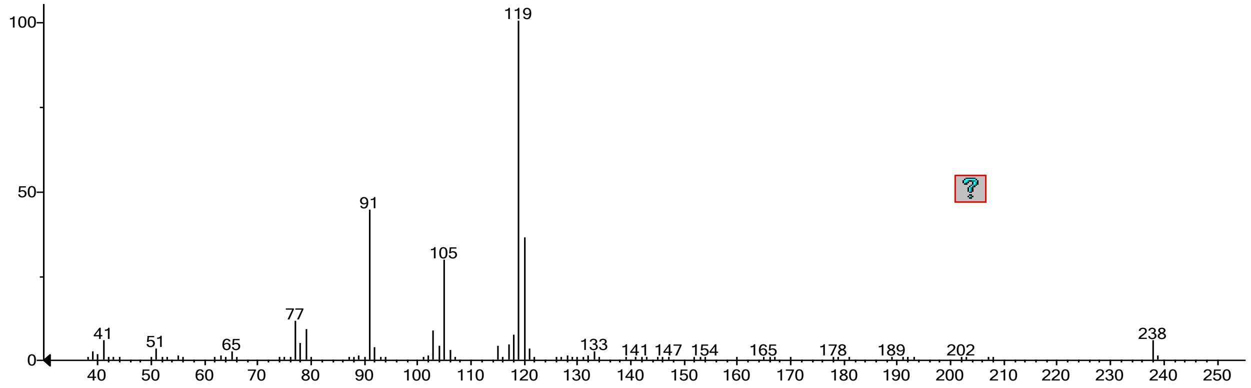

Figure C.13 Mass ionization spectrum of Benzene, 1,1'-(1,1,2,2-tetramethyl-1,2-ethanediyl)bis- (Product 5) formed in the reaction of asphaltene and α-methylstyrene.

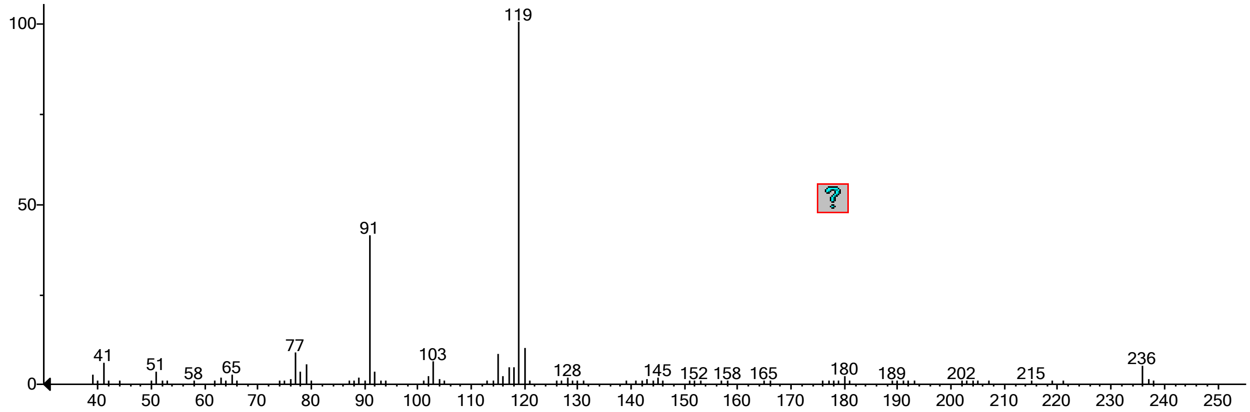

Figure C.14 Mass ionization spectrum of Benzene, 1,1'-(1,1,2,2-tetramethyl-1,2-ethanediyl)bis- (Product 6) formed in the reaction of asphaltene and α-methylstyrene.

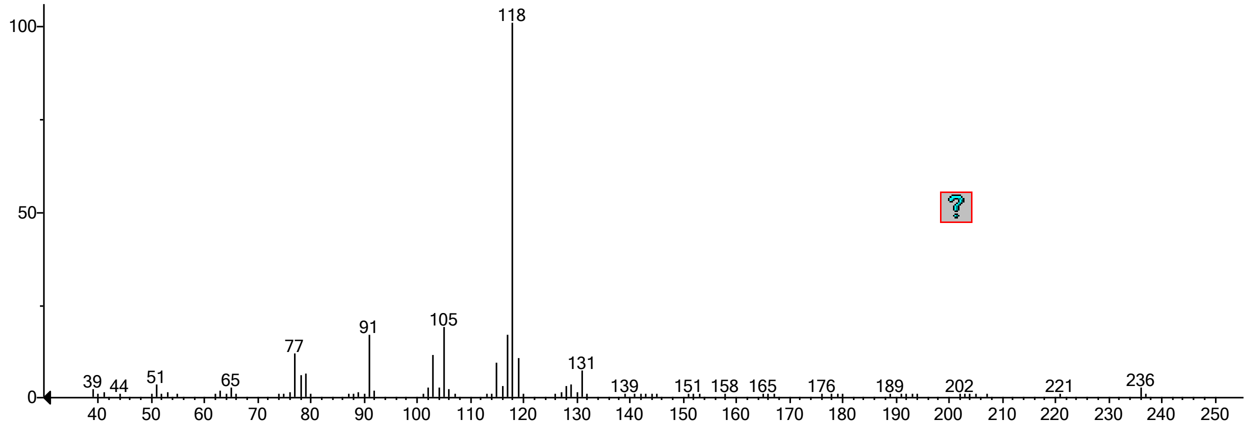

(Text File) Scan 1778 (14.667 min): R_20.D\ data.ms

Figure C.15 Mass ionization spectrum of Hex-1-ene,2,5-diphenyl- (Product 7) formed in the reaction of asphaltene and α-methylstyrene.

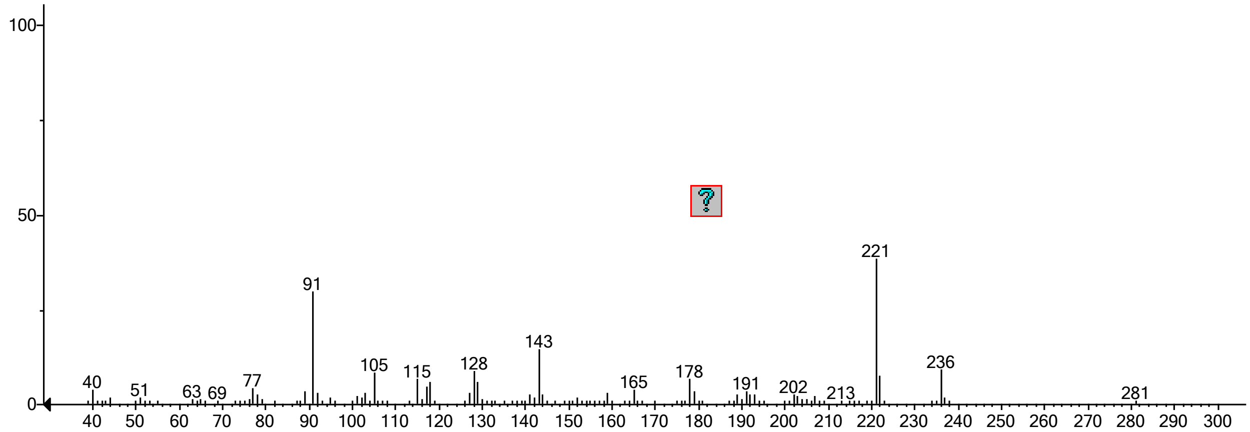

Figure C.16 Mass ionization spectrum of 1-phenyl-1,3,3-trimethylindane (Product 8) formed in the reaction of asphaltene and α-methylstyrene.

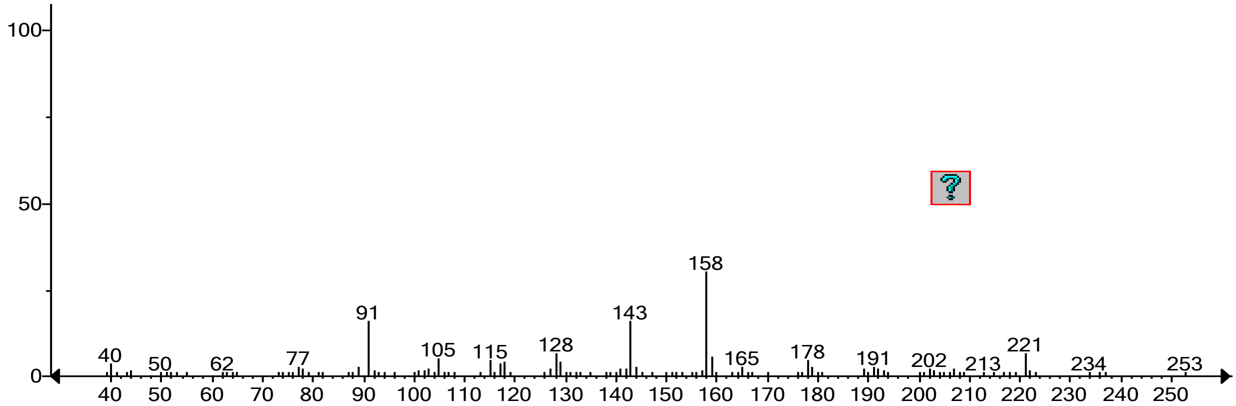

Figure C.17 Mass ionization spectrum of 2,4-Diphenyl-4-methyl-2(E)-pentene (Product 9) formed in the reaction of asphaltene and α-methylstyrene.

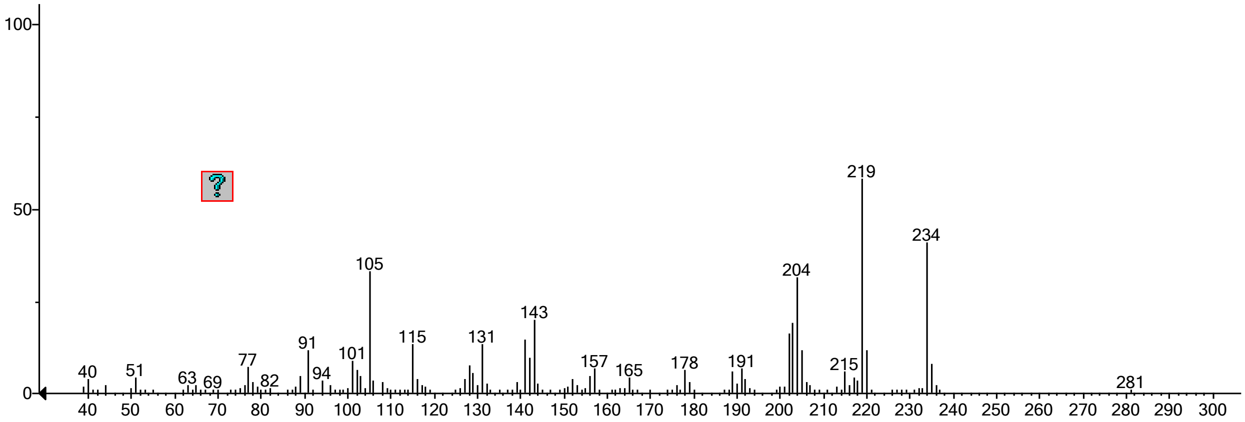

Figure C.18 Mass ionization spectrum of 2.5-Diphenyl-2,4-hexadiene (Product 10) formed in the reaction of asphaltene and α-methylstyrene.

Appendix C.8 Identification of products from the reaction of indene and α-methylstyrene.

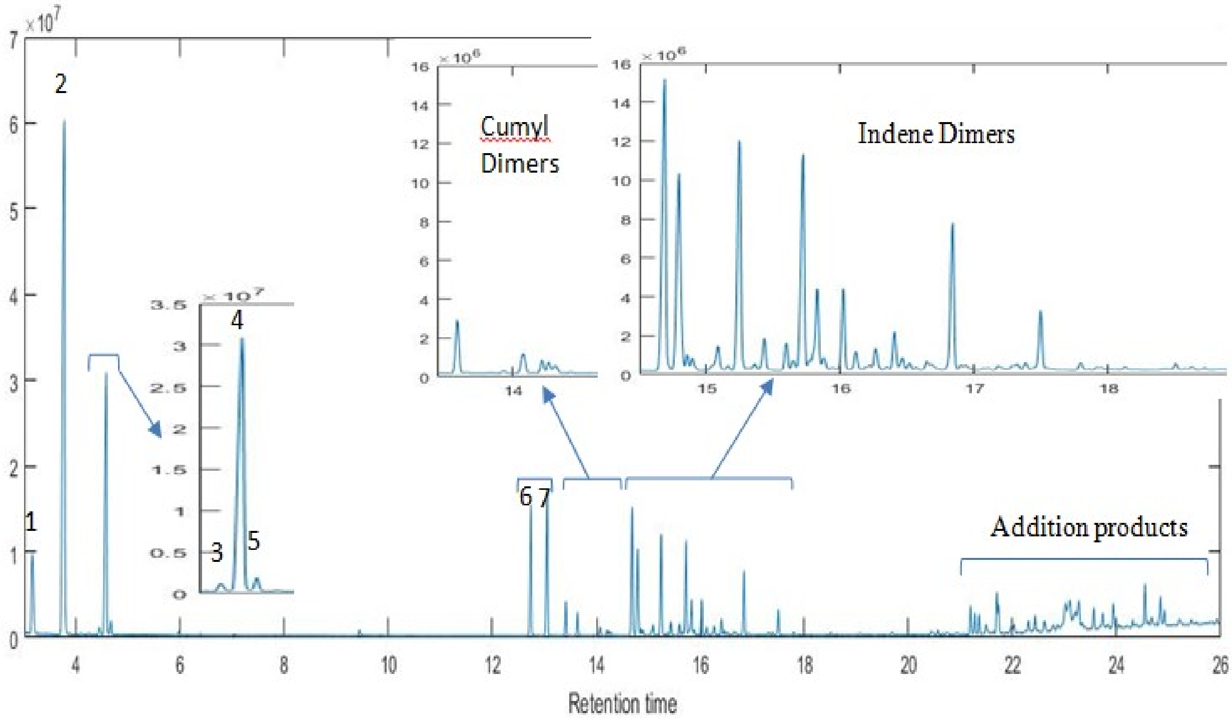

Figure C.19 Chromatogram of reaction products of indene and α-methylstyrene at 250 °C. Details are given in Table C.16.

The reaction of indene with α-methylstyrene formed variety of products including cumene due to hydrogenation of α-methylstyrene. The products were listed in Table C.16. The products were primarily dimers of cumyl and indenyl radicals. The mass spectra of by-products 6 and 7, which were also identified in the reaction of α-methylstyrene and asphaltenes, has molecular ion, M^+ at m/z = 224, and a base peak of m/z 105. Exact molecular structure of those compounds was not able to be found.

Addition of 9,10-dehydroanthracene caused a quantitative difference in the reaction products of α-methylstyrene and indene. Relative conversion of indene was estimated based on integrated peak areas of products which presented in Table C.17. Although addition of the hydrogen donor did not suppress recombination of indenyl radicals, conversion of indene reduced from 80 % to 51 %. This reduction can be attributed to quenching of the indenyl radicals via hydrogen transfer from donor compound (9,10-dehydroanthracene).

Table C.16 The list of the products was identified by GC-MS from the reaction of α-methylstyrene with indene.

Number	Name	Retention time [min]	Formula
1[a]	cumene	3.16	C_9H_{12}
2[a]	α-methylstyrene	3.77	C_9H_{10}
3[b]	indane	4.44	$C_{12}H_{10}O$
4[b]	indene	4.57	$C_{14}H_{12}$
5[c]	Not identified	4.66	
6[d]	Not identified	12.74	
7[d]	Not identified	13.05	

[a,b] Structures are given in Table 5.3and Table 5.14 respectively.
[c] Mass spectrum of compound 5 is shown in Figure C.20.
[c] Mass spectra of compounds (6) and (7) are given in Figure C.21.

Table C.17 Integrated peak areas of the reaction products of α-methylstyrene and indene in the presence of 9,10-dihydroanthracene.

Compounds	Area
cumene	1.41E8
α-methylstyrene	2.01E9
cumyl dimers	3.57E8
indane	1.75E7
indene	1.07E9
indene dimer	6.34E8
addition product	4.84E8
9,10-dihydroanthracene	1.76E9
anthracene	2.38E8
Dimerization product of 9,10-dihydroanthracene and α-methylstyrene	1.14E9

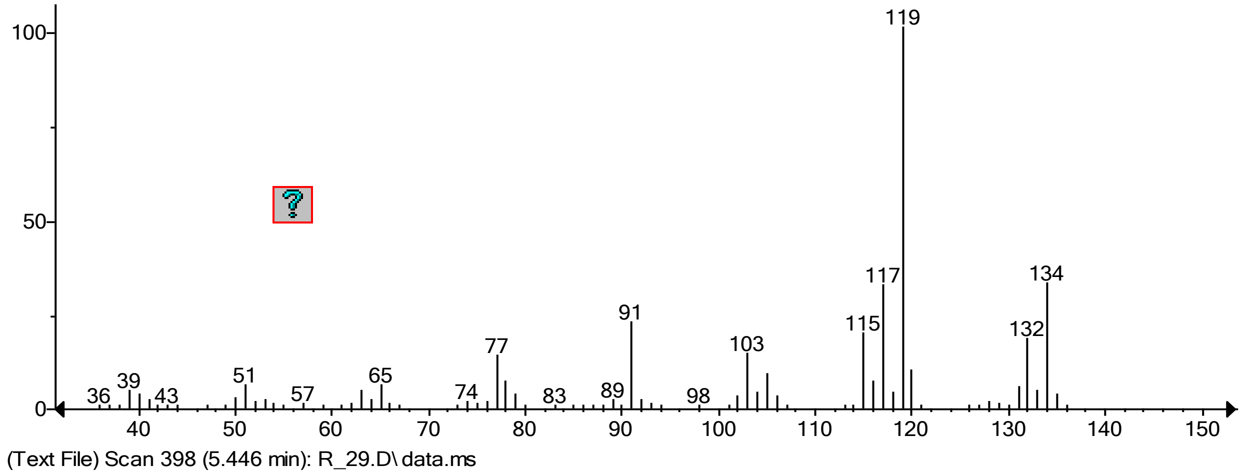

Figure C.20 Mass ionization spectrum of compound (5) which was in the indene feed as an impurity.

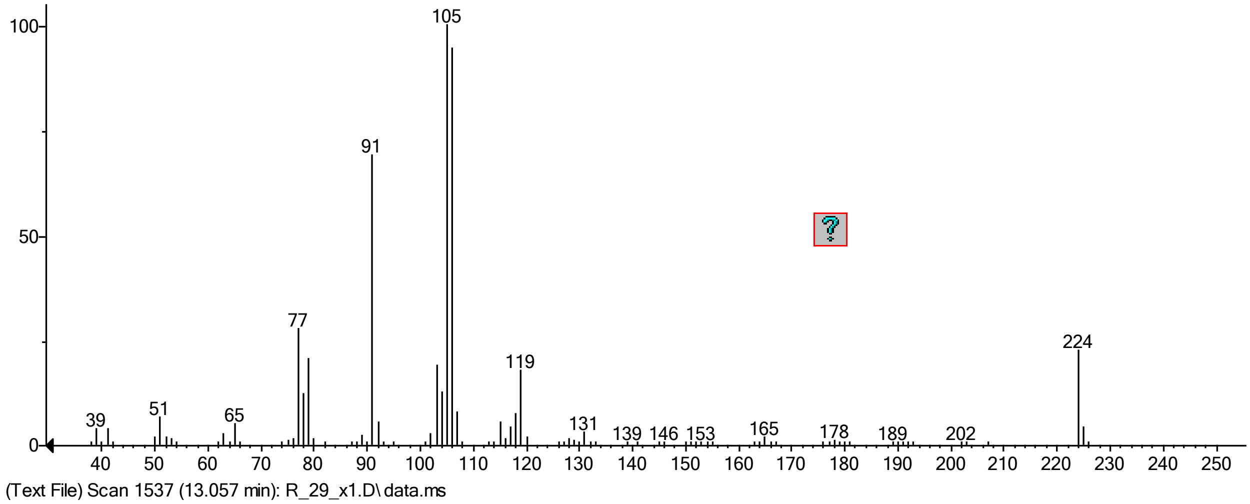

Figure C.21 Mass ionization spectrum of compound (6) and (7) which are isomers.

Appendix C.9 Identification of the products from indene conversion 250 °C.

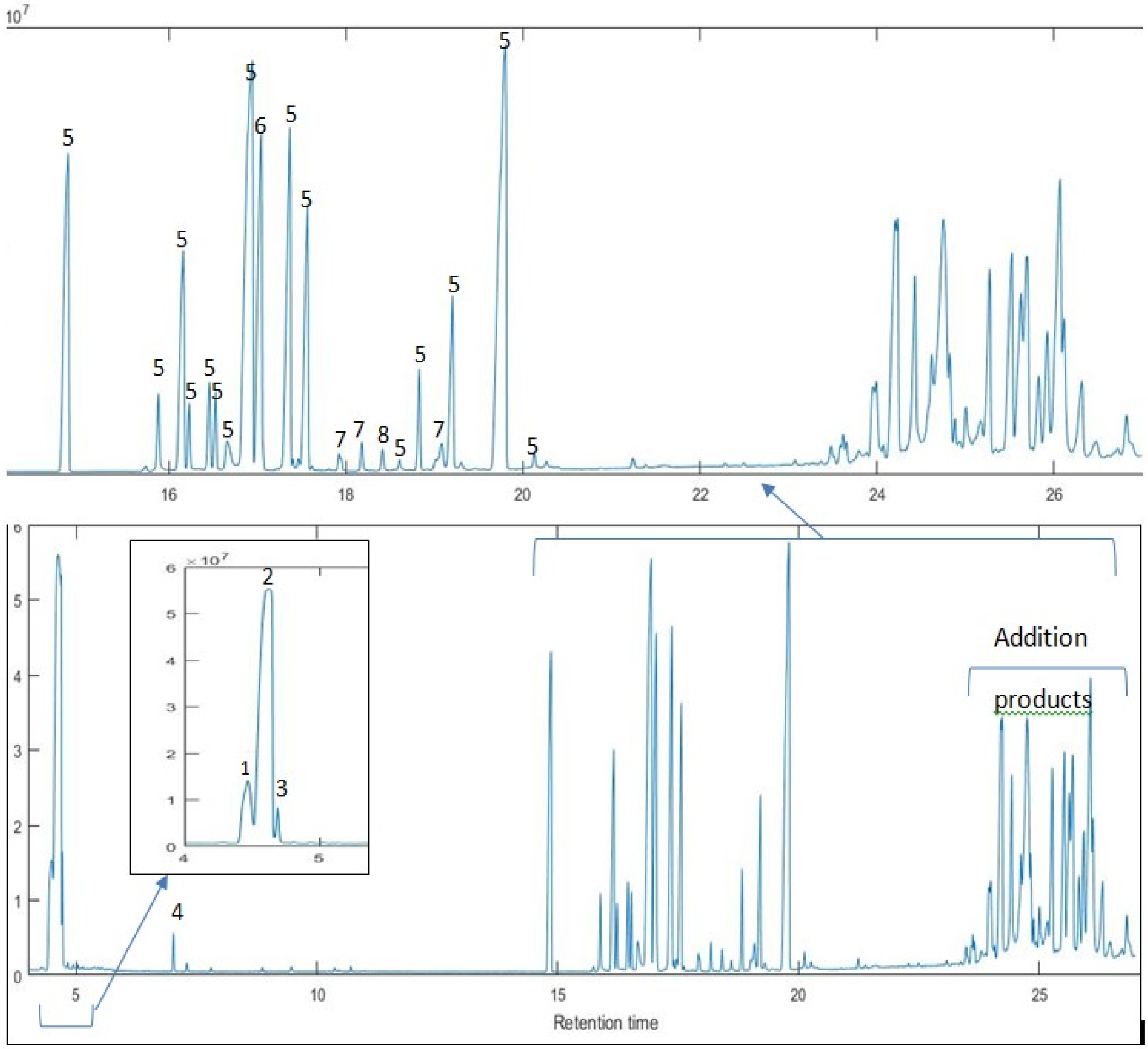

Figure C.22 GC MS chromatogram of the reaction products of indene conversion at 250 °C for 1 h period.

GC MS chromatogram of the reaction products of indene conversion is given in Figure C.22**.** Due to very diverse range of isomers of additional products, they were classified according to their molecular mass. Products can be grouped into two main categories: dimers and addition product which were mainly higher molecular weight compounds. $C_{18}H_{16}$ is found to be major additional product obtained from indene conversion at 250 °C. Chromatogram has been dominated by different isomers of $C_{18}H_{16}$. Due to limitations of electron ionization mass spectrum, position of double bond or the carbon which are linked through double bond were not determined. Mass spectrum of indene (M^+ at m/z = 116, M^+ - 1 at m/z =115) can be assisted to interpret the other peaks in chromatogram. All mass spectra of isomers exhibited a base peak of m/z 117 or m/z 116 and major fragment of m/z 232 which were considered as possible isomers of $C_{18}H_{16}$ (Figure C.26).

Another significant type of dimer was identified as isomers of $C_{18}H_{14}$ based on the overall mass spectra. The molecular ion, M^+ at m/z = 230, can be explained as dimer of m/z = 115, which might represent an indenyl radical, formed through a loss of hydrogen atom radical from indene (Figure C.28). $C_{18}H_{18}$ isomer was also identified which can be supported by the molecular ion, M^+ at m/z = 234, and a base peak m/z =117, indicating combination of two indane radical (formed due to loss of an hydrogen atom) (Figure C.27).

One compound (M^+ at m/z = 216 with higher abundance, relatively small base peak at m/z =108) which detected among the products differs in the type from the rest of the dimers (Figure C.29). Identification of 11-H-Benzo[b]fluorene ($C_{17}H_{12}$) suggested that instead of indenyl-indenyl dimerization products, additional product can also possibly form by combination of indenyl radical and indene, which later undergo cyclization by intermolecular addition reactions.

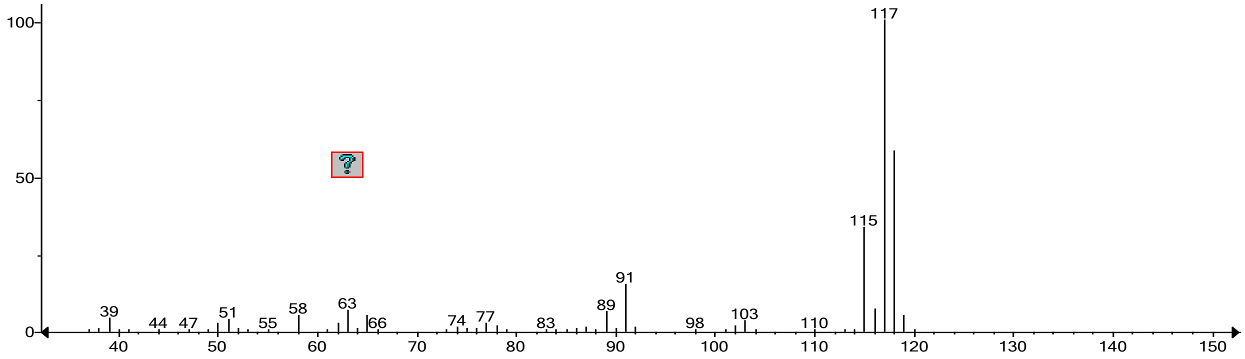

Figure C.23 Mass ionization spectrum of indane (C_9H_{10})

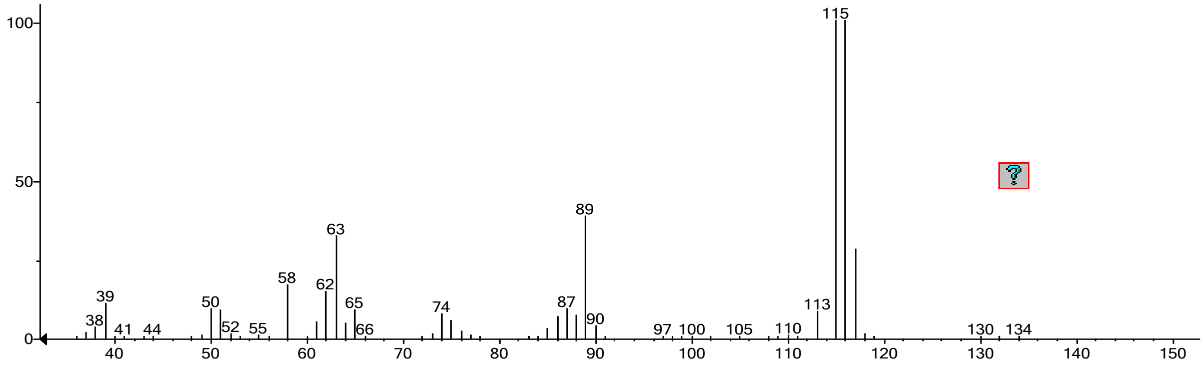

Figure C.24 Mass ionization spectrum of indene.

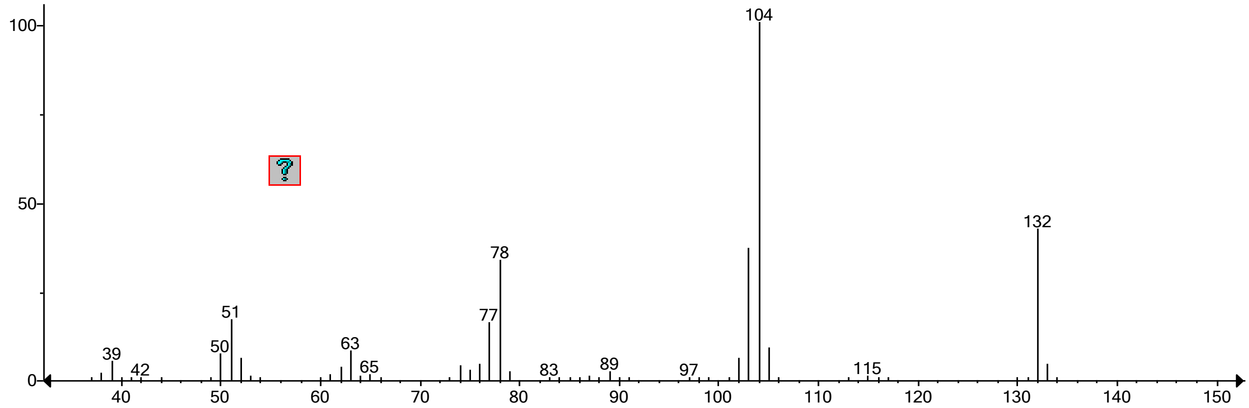

(Text File) Scan 633 (7.017 min): R_32.D\ data.ms

Figure C.25 Mass ionization spectrum of 2-indanone (Compound 4).

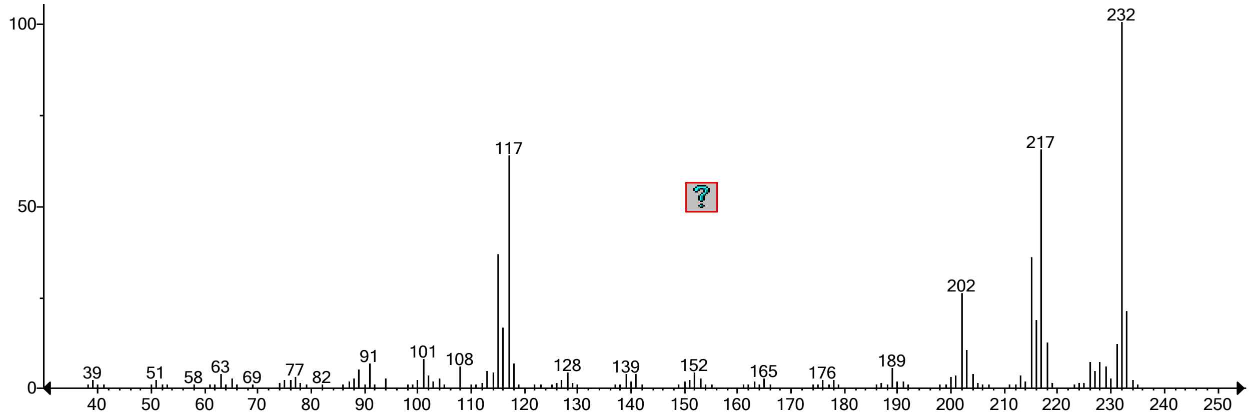

Figure C.26 Mass ionization spectrum given for one of the isomers of $C_{18}H_{16}$ (Compound 5).

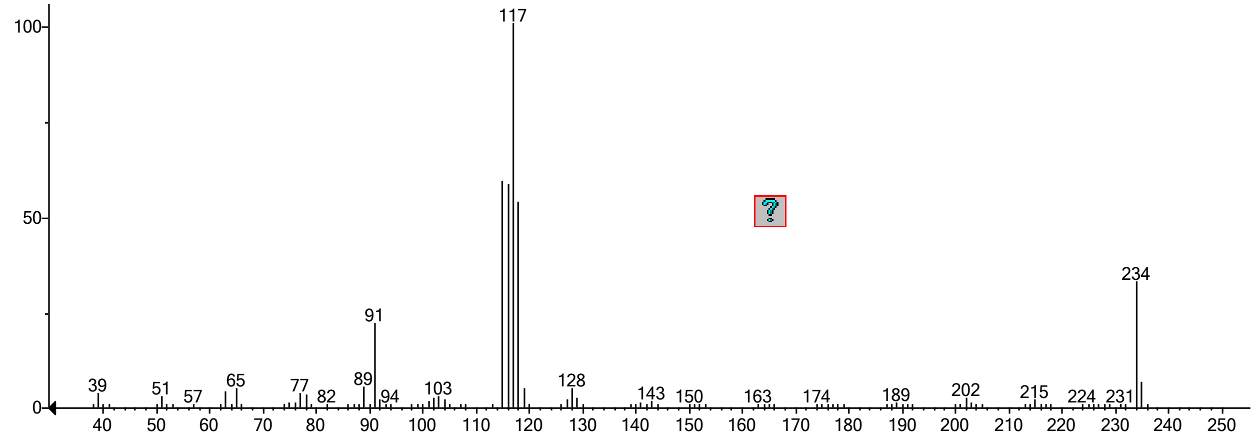

(Text File) Scan 2131 (17.026 min): R_32.D\ data.ms

Figure C.27 Mass ionization spectrum given for one of the isomers of $C_{18}H_{18}$ (Compound 6).

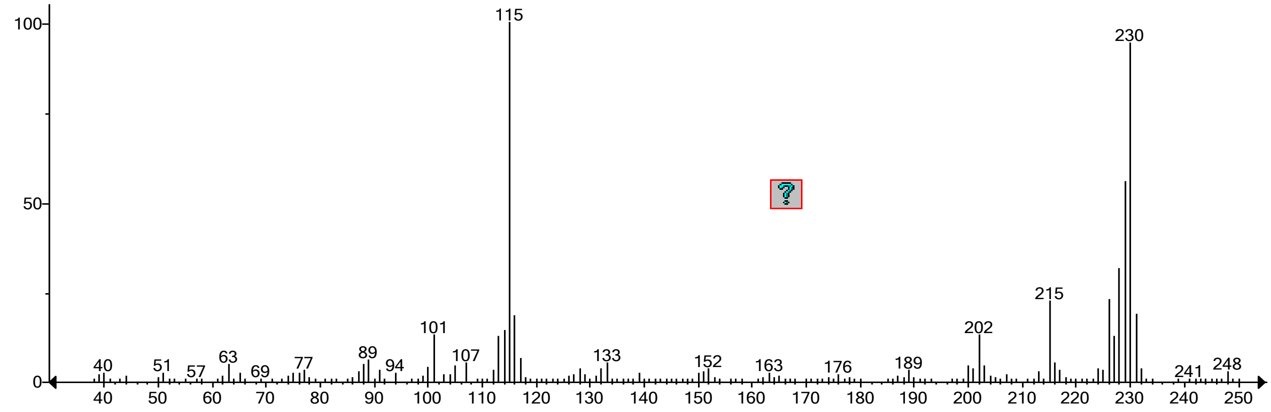

Figure C.28 Mass ionization spectrum for one of the isomers of $C_{18}H_{14}$ (Compound 7).

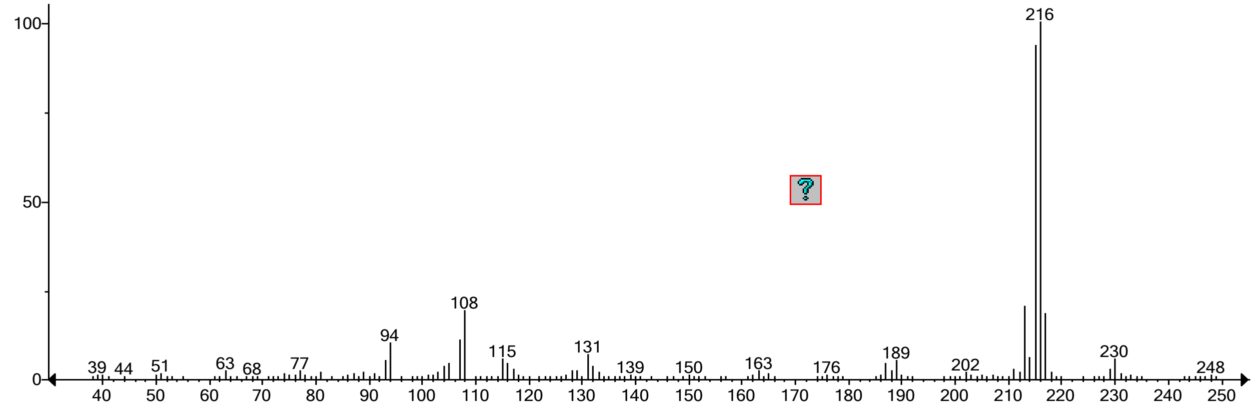

Figure C.29 Mass ionization spectrum of 11-H-Benzo[b]fluorene ($C_{17}H_{12}$).

Appendix C.10 Reaction of asphaltenes with 9, 10-dihydroanthracene and anthracene.

GC MS chromatogram of the reaction products from conversion of anthracene and 9,10-dihydroanthracene is given in Figure C.30 and Figure C.31.

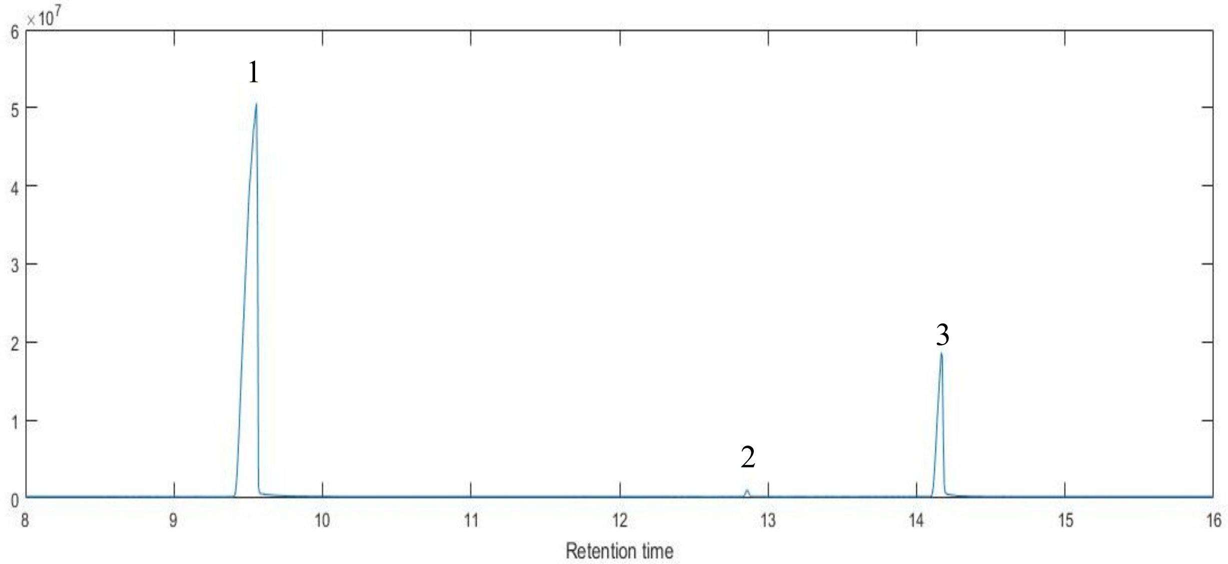

Figure C.30 GC MS chromatogram of the reaction products of anthracene conversion at 250 °C for 1 h period.

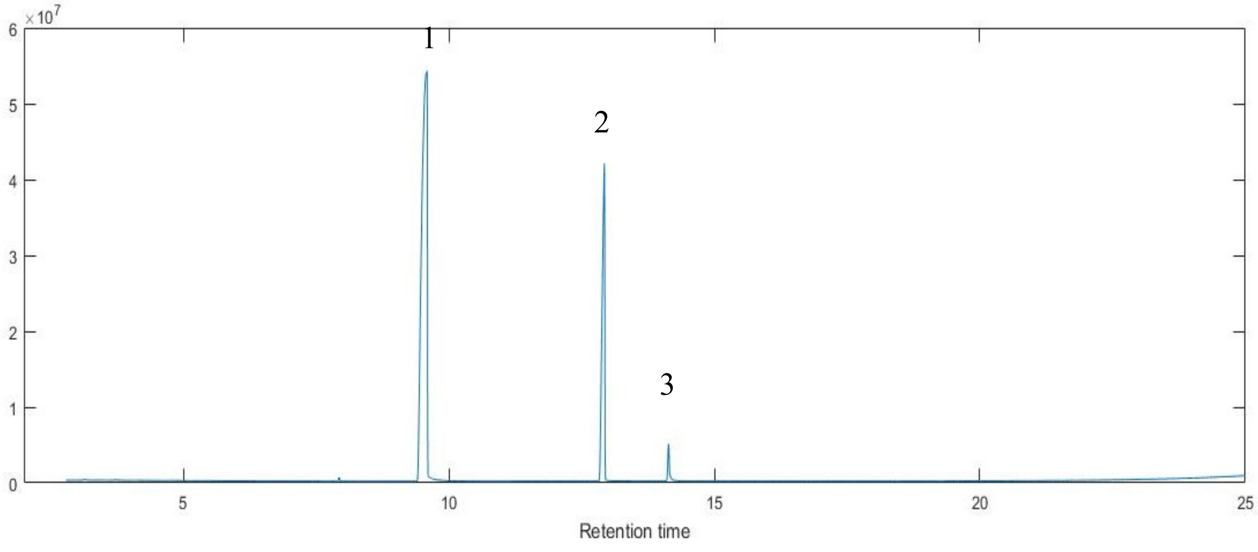

Figure C.31 GC MS chromatogram of the reaction products of 9, 10-dihydroanthracene and asphaltenes at 250 °C for 1 h period.